

Ministry of Higher Education and  
Scientific Research  
University of Diyala  
College of Science  
Department of Chemistry



# **Adsorption of Water Pollutant Toxic Ions on Dual -Oxide Nano Catalysts**

A Thesis Submitted to the  
Council of the College of Science, University of Diyala  
In Partial Fulfillment of the Requirements for the Degree  
Of Master of Science in Chemistry

By

**Nawras Adnan Jawad**

**B.Sc. In Chemistry Science 2014  
College of Science – University of Tikrit**

Supervised by

**Prof. Dr. Karim Henikish Hassan**

**2021 AD**

**IRAQ**

**1443 AH**

بِسْمِ اللّٰهِ الرَّحْمٰنِ الرَّحِیْمِ

(( یرفع اللّٰه الذین امنوا منکم والذین

اوتوا العلم ورجت واللّٰه بما

تعملون خیرا ))

صدق اللّٰه العظیم

سورة المجاولة ، آية (11)



To My greater teacher, prophet Mohammed (May ALLAH bless and grant him) who taught us the purpose of life.....

To My homeland Iraq.....

To My title of authenticity and science, who I proudly carry his name, my father.....

To the symbol of emotion who her prayed was the secret of my successful my mother.....

To my dear forgiven my sister, Raghad.....

To those I see my Life in their eyes, my sisters ( Esraa and Anfal ).....

To my second father and my first friend, my brother (Yasser).....

To my supervisor for his efforts and advices during my study (prof.dr.karim).....

To those who honor me by my study my profs teachers.....

To all my friends, especially my best friend (Hiba) many thanks.....

NAWRAS



## *Acknowledgment*

First and foremost , I am deeply grateful to the almighty ALLAH who help me to complete this thesis.

While I am in the final steps of my writing my thesis I should give my sincere gratitude to everyone who has any contribution even a simple way to my work .It is also my pleasure to extend my sincere thanks to my supervisor prof .Dr. Karim Henikish Hassan who has the credited next to that of ALLAH in the guidance of my research line through his instruction and direction,may ALLAH reward him for that efforts. My thanks are also extended to all staff member of my department.

Unlimited gratitude extends to all my friends for their assistance ,encouragement and support .

Finally, I would like to thank everybody who was important to the successful realization of this thesis as well as expressing my apology that may forget to mention some of them personally one by one.

**NAWRAS**

## ***Supervisor Certification***

We certify that this thesis ( *Adsorption of Water Pollutant Toxic Ions on Dual-Oxide Nano Catalysts* )was carried out under our supervision in Chemistry Department, College of Science, Diyala University in partial fulfilment of the requirement for the degree of master of science in chemistry by the student (**NAWRAS ADNAN JAWAD**).

**(Supervisor)**

Signature:

Name: Dr. Karim Henikish Hassan

Title: Professor

Date:    /    / 2021

## **Head of the Department of Chemistry**

In view of the available recommendation, I forwarded this thesis for debate by the examination committee.

Signature:

Name: Dr. Ahmed Najem Abd

Title: Professor

Date:    /    / 2021

## *Scientific Certification*

I certify that the thesis entitled (*Adsorption of Water Pollutant Toxic Ions on Dual-Oxide Nano Catalysts*) presented by (NAWRAS ADNAN JAWAD) has been evaluated scientifically; therefore, it is suitable for debate by examining committee.

Signature:

Name: Dr Entisar Eliwi Al-abodi

Title: professor

Date: / / 2021

## *Linguistic Certification*

I certify that the thesis entitled (*Adsorption of Water Pollutant Toxic Ions on Dual-Oxide Nano Catalysts*) presented by (**NAWRAS ADNAN JAWAD**) has been corrected linguistically; therefore, it is suitable for debate by examining committee.

Signature:

Name: Dr. Ziad Tariq Ibrahim

Title: Assistant professor

Date:    /    / 2021

## ***Examination Committee Certificate***

We certify, that we have read the thesis entitled (*Adsorption of Water Pollutant Toxic Ions on Dual-Oxide Nano Catalysts*), presented by (NAWRAS ADNAN JAWAD), and as an examining committee, we examined the student on its contents, and in what is related to it and our opinion it meets the standard for the degree of Master in Chemistry Science.

**(Chairman)**

Signature:

Name: Dr. Ahmed Najem Abd

Title: professor

Date:    /    / 2021

**(Member)**

Signature:

Name: Dr.Dhia H.Hussain

Title: Assistant professor

Date:    /    / 2021

**(Member)**

Signature:

Name: Dr.Abdulqadier Hussien  
Alkhazraji

Title: Assistant professor

Date:    /    / 2021

**(Member / Supervisor)**

:

Name: Dr. Karim Henikish Hassan

Title: professor

Date:    /    / 2021

Approved by The Council of College of the Science, University of  
Diyala.

**(The Dean)**

Signature:

Name: Dr. Tahseen Hussein Mubarak

Title: professor

Date:    /    / 2021





## ABSTRACT

In this study, nano **NiO** was prepared by using Arundo Donaxi Leaves Extract and from Nickel chloride hexahydrate (source of nickel), and nano  $\gamma$ -**Al<sub>2</sub>O<sub>3</sub>** was prepared by co-precipitation method from aluminum chloride hexahydrate (source of aluminum) with calcination at temperature of 550 °C. The nano NiO/  $\gamma$ -Al<sub>2</sub>O<sub>3</sub> catalyst was prepared by mixing a certain ratio of nano oxide of 20% Nickel oxide and 80% Alumina by ultrasonicification.

They are characterized by X-ray diffraction, FTIR spectroscopy, and atomic force microscope techniques. XRD spectra reveals that particle size obtained is about (12.83) nm for NiO nanoparticle, (6.46) nm for  $\gamma$ -Al<sub>2</sub>O<sub>3</sub> and (5.04) nm for NiO/  $\gamma$ -Al<sub>2</sub>O<sub>3</sub> nano catalyst.

Water pollution with many heavy metals is a major damage for environment ,therefore the NiO/  $\gamma$ -Al<sub>2</sub>O<sub>3</sub> nano catalysts are prepared to remove Copper and Cobalt ions from dilute aqueous solution .In this field ,a number of factors have been studied for effect the percentage removal of metals .The time required to remove (Cu<sup>+2</sup> and Co<sup>+2</sup>) ions to reach equilibrium was (50) min .The removal of Copper and Cobalt ions was found to be slightly reduced by increasing the concentration of adsorbate and increase by increasing the weight of surface .The effect of temperature on Copper and Cobalt ions removal showed that the percentage removal was reduced by increasing the temperature ,which means that the process is exothermic .

Calculated values of the thermodynamic functions ( $\Delta G$ ,  $\Delta H$ , $\Delta S$  ) of the adsorption declare that it is spontaneous ,exothermic and less randomness at each metals on

nano NiO/  $\gamma$ -Al<sub>2</sub>O<sub>3</sub> catalyst .The experimental data were fitted into the following kinetic models :pseudo-first order , pseudo-second order ,Intraparticle diffusion and Elovich model. It was observed that pseud-second order describe the adsorption with high correlation factor ( $R^2$ ) better than any other kinetic models.

Finally temkin isotherm was found to be the best one which can describe removal of Cu<sup>+2</sup>, and freundlich isotherm was the best one which can describe removal Co<sup>+2</sup>, all these were noted from the correlation coefficients values.

## *List of Contents*

<i>Subject number</i>	<i>Subject</i>	<i>Page</i>
<i>Dedication</i>		
<i>Acknowledgement</i>		
	<i>Abstract</i>	<i>I</i>
	<i>List of contents</i>	<i>III</i>
	<i>List of Tables</i>	<i>VIII</i>
	<i>List of Figures</i>	<i>XI</i>
	<i>List of Symboles and Abbreviation</i>	<i>XV</i>
<i>Chapter One (Introduction)</i>		
<b>1.1</b>	<b>General introduction</b>	<b>1</b>
<b>1.2</b>	<b>Literature review</b>	<b>3</b>
<b>1.3</b>	<b>Aim of study</b>	<b>9</b>
<i>Chapter Two (Theoretical part)</i>		
<b>2.1</b>	<b>Pollution</b>	<b>10</b>
<b>2.2</b>	<b>Heavy metals</b>	<b>12</b>
<b>2.2.1</b>	<b>Definition of heavy metals</b>	<b>12</b>
<b>2.2.2</b>	<b>Industrial Wastwater source of heavy metals</b>	<b>13</b>
<b>2.2.3</b>	<b>Heavy metal wastewater treatment teqniques</b>	<b>14</b>
<b>2.2.3.1</b>	<b>Chemical precipitation</b>	<b>15</b>
<b>2.2.3.2</b>	<b>Ion exchange</b>	<b>15</b>
<b>2.2.3.3</b>	<b>Member filtration</b>	<b>15</b>

<b>2.2.3.4</b>	<b>Electrochemical treatment</b>	<b>16</b>
<b>2.2.3.5</b>	<b>Adsorption processes</b>	<b>16</b>
<b>2.3</b>	<b>Force of the adsorption</b>	<b>18</b>
<b>2.4</b>	<b>Types of adsorption</b>	<b>18</b>
<b>2.5</b>	<b>Adsorption mechanism from solution</b>	<b>21</b>
<b>2.6</b>	<b>Factor influencing adsorption processes</b>	<b>21</b>
<b>2.7</b>	<b>Theories of adsorption</b>	<b>25</b>
<b>2.7.1</b>	<b>Langmuir isotherm</b>	<b>25</b>
<b>2.7.2</b>	<b>Freundlich isotherm</b>	<b>26</b>
<b>2.7.3</b>	<b>Temkin isotherm</b>	<b>28</b>
<b>2.8</b>	<b>Nanomaterial</b>	<b>29</b>
<b>2.9</b>	<b>Adsorption kinetic</b>	<b>30</b>
<b>2.9.1</b>	<b>Pseudo-first order model</b>	<b>31</b>
<b>2.9.2</b>	<b>Pseudo-second order model</b>	<b>32</b>
<b>2.9.3</b>	<b>Intra-particle Diffusion model</b>	<b>32</b>
<b>2.9.4</b>	<b>Elovich model</b>	<b>33</b>
<b>2.10</b>	<b>Catalysts</b>	<b>33</b>
<b>2.10.1</b>	<b>Definition of catalyst</b>	<b>33</b>
<b>2.10.2</b>	<b>Catalysts classification according to phase</b>	<b>35</b>
<b>2.10.2.1</b>	<b>Homogeneous catalysis</b>	<b>35</b>
<b>2.10.2.2</b>	<b>Heterogeneous catalysis</b>	<b>35</b>
<b>2.10.2.3</b>	<b>Enzyme catalysis</b>	<b>36</b>
<b>2.10.2</b>	<b>Catalyst components</b>	<b>37</b>

<b>2.10.3</b>	<b>Key factors for FTS catalyst design</b>	<b>38</b>
<b>2.11</b>	<b>Oxide catalyst preparation</b>	<b>39</b>
<i><b>Chapter Three (Experimental part)</b></i>		
<b>3.1</b>	<b>Instruments and Apparatus</b>	<b>41</b>
<b>3.1.1</b>	<b>The instrument and tools used</b>	<b>41</b>
<b>3.1.2</b>	<b>Apparatus used</b>	<b>42</b>
<b>3.2</b>	<b>Materials</b>	<b>43</b>
<b>3.2.1</b>	<b>The chemical materials</b>	<b>43</b>
<b>3.2.2</b>	<b>Adsorbate used in this study</b>	<b>43</b>
<b>3.2.3</b>	<b>Prepared nanoparticles used in this study</b>	<b>44</b>
<b>3.3</b>	<b>Preparation of adsorbent catalyst</b>	<b>44</b>
<b>3.3.1</b>	<b>Preparation of alumina using co-precipitation method</b>	<b>44</b>
<b>3.3.2</b>	<b>Preparation of nickel oxide nanoparticle using Arundo donaxi leaves extract</b>	<b>45</b>
<b>3.3.3</b>	<b>Preparation of nano NiO/ <math>\gamma</math>-Al<sub>2</sub>O<sub>3</sub> catalyst</b>	<b>47</b>
<b>3.4</b>	<b>Preparation of solutions used in adsorption processes</b>	<b>47</b>
<b>3.4.1</b>	<b>Sodium hydroxide</b>	<b>47</b>
<b>3.4.2</b>	<b>Standard stock solution of Cu (II) ions</b>	<b>47</b>
<b>3.4.3</b>	<b>Standard stock solution of Co (II) ions</b>	<b>47</b>
<b>3.5</b>	<b>Studing the factors affecting adsorption method</b>	<b>48</b>
<b>3.5.1</b>	<b>The Effect of contact time on Cu (II) and Co (II) ions adsorption</b>	<b>48</b>
<b>3.5.2</b>	<b>Effect of quantity of NiO/<math>\gamma</math>-Al<sub>2</sub>O<sub>3</sub> adsorbent</b>	<b>48</b>

<b>3.5.3</b>	<b>Effect of initial concentration of Cu (II) and Co (II) ions</b>	<b>48</b>
<b>3.5.4</b>	<b>Effect of temperature</b>	<b>49</b>
<b>3.6</b>	<b>Calculation of metal Removal</b>	<b>49</b>
<b>3.7</b>	<b>Kinetic of adsorption of Cu (II) and Co (II) ions</b>	<b>49</b>
<b><i>Chapter Four(Results &amp; Discussion)</i></b>		
<b>4.1</b>	<b>Characterization of the nanomaterials</b>	<b>50</b>
<b>4.1.1</b>	<b>X-ray diffraction analysis</b>	<b>50</b>
<b>4.1.1.1</b>	<b>X-ray diffraction of NiO nanoparticles</b>	<b>50</b>
<b>4.1.1.2</b>	<b>X-ray diffraction of <math>\gamma</math>-Al<sub>2</sub>O<sub>3</sub></b>	<b>51</b>
<b>4.1.1.3</b>	<b>X-ray diffraction of NiO/ <math>\gamma</math>-Al<sub>2</sub>O<sub>3</sub> nanocatalyst</b>	<b>52</b>
<b>4.1.2</b>	<b>Atomic force microscope</b>	<b>53</b>
<b>4.1.2.1</b>	<b>AFM of NiO nanoparticle</b>	<b>53</b>
<b>4.1.2.2</b>	<b>AFM of <math>\gamma</math>-Al<sub>2</sub>O<sub>3</sub> nanoparticle</b>	<b>55</b>
<b>4.1.2.3</b>	<b>AFM of NiO/<math>\gamma</math>-Al<sub>2</sub>O<sub>3</sub> nano catalyst</b>	<b>56</b>
<b>4.1.3</b>	<b>Fourier Transform Infrared ( FTIR ) Spectra Analysis</b>	<b>58</b>
<b>4.1.3.1</b>	<b>FTIR spectrum of NiO nanoparticle</b>	<b>58</b>
<b>4.1.3.2</b>	<b>FTIR spectrum of <math>\gamma</math>-Al<sub>2</sub>O<sub>3</sub> nanoparticle</b>	<b>60</b>
<b>4.1.3.3</b>	<b>FTIR spectrum of NiO/ <math>\gamma</math>-Al<sub>2</sub>O<sub>3</sub> Nano catalyst</b>	<b>60</b>

<b>4.2</b>	<b>Adsorption of Cu(II) and Co(II) ions on NiO/ <math>\gamma</math>-Al<sub>2</sub>O<sub>3</sub></b>	<b>61</b>
<b>4.2.1</b>	<b>Effect of contact time on adsorption</b>	<b>61</b>
<b>4.2.2</b>	<b>Effect of adsorbent quantity on adsorption</b>	<b>64</b>
<b>4.2.3</b>	<b>Effect of initial adsorbate concentration on adsorption</b>	<b>67</b>
<b>4.2.4</b>	<b>Effect of temperature on adsorption</b>	<b>69</b>
<b>4.3</b>	<b>Kinetics Studies for Adsorption Process of Cu<sup>+2</sup> and Co<sup>+2</sup> ions</b>	<b>71</b>
<b>4.4</b>	<b>Thermodynamic study of adsorption of NiO/<math>\gamma</math>-Al<sub>2</sub>O<sub>3</sub> nanocatalyst</b>	<b>81</b>
<b>4.5</b>	<b>The adsorption isotherm</b>	<b>85</b>
<b>4.5.1</b>	<b>Langmuir adsorption isotherm</b>	<b>87</b>
<b>4.5.2</b>	<b>Freundlich adsorption isotherm</b>	<b>88</b>
<b>4.5.3</b>	<b>Temkin adsorption isotherm</b>	<b>89</b>
<b>4.6</b>	<b>Conclusions</b>	<b>92</b>
<b>4.7</b>	<b>Future works</b>	<b>93</b>
<b><i>References</i></b>		<b>94</b>

## *List of Tables*

<i>Table number</i>	<i>Subject</i>	<i>page</i>
<i>Chapter two (Theoretical part)</i>		
(2.1)	Type of pollutants	11
(2.2)	Comparison between physical and chemical adsorption	20
<i>Chapter three(Experimental part)</i>		
(3.1)	The instrumentation used in this study	41
(3.2)	Apparatus used in Characterization	42
( 3.3)	The chemicals used	43
<i>Chapter four (Results &amp; Discussion)</i>		
(4.1)	The strongest three peaks in the XRD spectrum of prepared NiO nanoparticle	51
(4.2)	The strongest three peaks in the XRD spectrum of prepared $\gamma$ -Al <sub>2</sub> O <sub>3</sub> nanoparticle	52
(4.3)	The strongest three peaks in the XRD spectrum of NiO/ $\gamma$ -Al <sub>2</sub> O <sub>3</sub> nano catalyst	53
(4.4)	Granularity cumulating distribution and average diameter NiO nanoparticle	54
(4.5)	Granularity cumulating distribution and average diameter of $\gamma$ -Al <sub>2</sub> O <sub>3</sub> nanoparticle	56
(4.6)	Granularity cumulating distribution and average diameter of NiO/ $\gamma$ -Al <sub>2</sub> O <sub>3</sub> nano catalyst	57
(4.7)	Effect of contact time on the adsorption of Cu (II) ion by NiO/ $\gamma$ -Al <sub>2</sub> O <sub>3</sub> nano catalyst at 298 K	62
(4.8)	Effect of contact time on the adsorption of Co (II) ion by NiO/ $\gamma$ -Al <sub>2</sub> O <sub>3</sub> nano catalyst at 298 K	63
(4.9)	Effect of adsorbent quantity on the adsorption of Cu(II) ion by NiO/ $\gamma$ -Al <sub>2</sub> O <sub>3</sub> nano catalyst at 298 K	65
(4.10)	Effect of adsorbent quantity on the adsorption of Co(II)	66



	ion by NiO/ $\gamma$ -Al <sub>2</sub> O <sub>3</sub> nano catalyst at 298 K	
(4.11)	Effect of initial concentration on the adsorption of Cu(II) ions by NiO/ $\gamma$ -Al <sub>2</sub> O <sub>3</sub> nano catalyst at 298 K	67
(4.12)	Effect of initial concentration on the adsorption of Co(II) ions by NiO/ $\gamma$ -Al <sub>2</sub> O <sub>3</sub> nano catalyst at 298 K	68
(4.13)	Effect of temperature on the adsorption of Cu (II)ion by NiO/ $\gamma$ -Al <sub>2</sub> O <sub>3</sub> nano catalyst	70
(4.14)	Effect of temperature on the adsorption of Co (II)ion by NiO/ $\gamma$ -Al <sub>2</sub> O <sub>3</sub> nano catalyst	71
(4.15)	The adsorption data for Cu(II) ions on removal with NiO/ $\gamma$ -Al <sub>2</sub> O <sub>3</sub> nanocatalyst at 308 K	72
(4.16)	The adsorption data for Cu(II) ions on removal with NiO/ $\gamma$ -Al <sub>2</sub> O <sub>3</sub> nanocatalyst at 313 K	73
(4.17)	The adsorption data for Cu(II) ions on removal with NiO/ $\gamma$ -Al <sub>2</sub> O <sub>3</sub> nanocatalyst at 318 K	73
(4.18)	The adsorption data for Cu(II) ions on removal with NiO/ $\gamma$ -Al <sub>2</sub> O <sub>3</sub> nanocatalyst at 323 K	74
(4.19)	The adsorption data for Co(II) ions on removal with NiO/ $\gamma$ -Al <sub>2</sub> O <sub>3</sub> nanocatalyst at 308 K	76
(4.20)	The adsorption data for Co(II) ions on removal with NiO/ $\gamma$ -Al <sub>2</sub> O <sub>3</sub> nanocatalyst at 313 K	77
(4.21)	The adsorption data for Co(II) ions on removal with NiO/ $\gamma$ -Al <sub>2</sub> O <sub>3</sub> nanocatalyst at 318 K	77
(4.22)	The adsorption data for Co(II) ions on removal with NiO/ $\gamma$ -Al <sub>2</sub> O <sub>3</sub> nanocatalyst at 323 K	78
(4.23)	Adsorption Kinetics Constants for Cu(II) ions adsorption on NiO/ $\gamma$ -Al <sub>2</sub> O <sub>3</sub> nano catalyst	81
(4.24)	Adsorption Kinetics Constants for Co(II) ions adsorption on NiO/ $\gamma$ -Al <sub>2</sub> O <sub>3</sub> nano catalyst	81
(4.25)	Effect of temperature on equilibrium constant for the adsorption of Cu (II) ions on NiO/ $\gamma$ -Al <sub>2</sub> O <sub>3</sub> nano catalyst	83
(4.26)	Effect of temperature on equilibrium constant for the	84

	<b>adsorption of Co (II) ions on NiO/<math>\gamma</math>-Al<sub>2</sub>O<sub>3</sub> nano catalyst</b>	
<b>(4.27)</b>	<b>Values of thermodynamic function for the adsorption of Cu (II) and Co(II) on NiO/<math>\gamma</math>-Al<sub>2</sub>O<sub>3</sub> nano catalyst at different temperature</b>	<b>86</b>
<b>(4.28)</b>	<b>The ideal condition of the adsorption of Cu (II) and Co(II) on NiO/<math>\gamma</math>-Al<sub>2</sub>O<sub>3</sub> nano catalyst</b>	<b>86</b>
<b>(4.29)</b>	<b>Adsorption parameters value of Cu (II) on NiO/<math>\gamma</math>-Al<sub>2</sub>O<sub>3</sub> nano catalyst at ideal condition</b>	<b>87</b>
<b>(4.30)</b>	<b>Adsorption parameters value of Co (II) on NiO/<math>\gamma</math>-Al<sub>2</sub>O<sub>3</sub> nano catalyst at ideal condition</b>	<b>88</b>
<b>(4.31)</b>	<b>Langmiur, Freundlich and Temkin constants and the correlation coefficients for the adsorption of of Cu (II) and Co(II) ions in presence of variable initial ions concentration</b>	<b>92</b>

## *List of Figures*

<i>Figure number</i>	<i>Subject</i>	<i>Page</i>
<i>Chapter Two (Theoretical part)</i>		
(2.1)	The major source of water pollution	12
(2.2)	Summarization of techniques used in industrial waste water	14
(2.3)	Adsorption versus adsorption (processes)	17
(2.4)	Physical and chemical adsorption	19
(2.5)	The linear form of Langmuir isotherm	26
(2.6)	The linear relationship of Freundlich isotherm	28
(2.7)	Potential energy diagram for a heterogeneous catalytic reaction (solid line)	34
(2.8)	The mutual dependencies of the catalyst components	37
(2.9)	Concept of triangle of catalyst design	38
<i>Chapter Three (Experimental)</i>		
(3.1)	Steps of the preparation of $\gamma\text{-Al}_2\text{O}_3$ using co-precipitation method	44
(3.2)	Steps of the preparation of NiO nanoparticles using Arundo Donaxi Leaves Extract	46
(3.3)	Flow diagram showing the steps used in preparing Nickel (II) oxide nanoparticles using Arundo donaxi Leaves Extract	46
<i>Chapter Four (Results &amp; Discussion)</i>		
(4.1)	X-ray diffraction of prepared (NiO)	51
(4.2)	X-ray diffraction of prepared $\gamma\text{-Al}_2\text{O}_3$	52
(4.3)	X-ray diffraction of prepared NiO/ $\gamma\text{-Al}_2\text{O}_3$	53

<b>(4.4)</b>	<b>AFM images of the NiO nano catalyst</b>	<b>54</b>
<b>(4.5)</b>	<b>Granularity cumulating distribution of NiO nano particle</b>	<b>55</b>
<b>(4.6)</b>	<b>AFM images of the <math>\gamma</math>-Al<sub>2</sub>O<sub>3</sub> nano particle</b>	<b>55</b>
<b>(4.7)</b>	<b>Granularity cumulating distribution of <math>\gamma</math>-Al<sub>2</sub>O<sub>3</sub> nano particle</b>	<b>56</b>
<b>(4.8)</b>	<b>AFM images of the NiO/<math>\gamma</math>-Al<sub>2</sub>O<sub>3</sub> nano catalyst</b>	<b>57</b>
<b>(4.9)</b>	<b>Granularity cumulating distribution of NiO/<math>\gamma</math>-Al<sub>2</sub>O<sub>3</sub> nano catalyst</b>	<b>58</b>
<b>(4.10)</b>	<b>FTIR spectrum of prepared Nickel (II)oxide nanoparticle</b>	<b>59</b>
<b>(4.11)</b>	<b>FTIR spectrum of prepared nanoparticle <math>\gamma</math>-Al<sub>2</sub>O<sub>3</sub> nanoparticle</b>	<b>60</b>
<b>(4.12)</b>	<b>FTIR spectrum of prepared NiO/<math>\gamma</math>-Al<sub>2</sub>O<sub>3</sub> nano catalyst</b>	<b>61</b>
<b>(4.13)</b>	<b>Effect of contact time on the removal (%) of Cu (II) ion on NiO/<math>\gamma</math>-Al<sub>2</sub>O<sub>3</sub> nano catalyst at 298 K</b>	<b>63</b>
<b>4.14)</b>	<b>Effect of contact time on the removal (%) of Co (II) ion on NiO/<math>\gamma</math>-Al<sub>2</sub>O<sub>3</sub> nano catalyst at 298 K</b>	<b>64</b>
<b>(4.15)</b>	<b>Effect of adsorbent quantity on the removal (%) of Cu(II) ions NiO/<math>\gamma</math>Al<sub>2</sub>O<sub>3</sub>nano catalyst at 298 K</b>	<b>65</b>
<b>(4.16)</b>	<b>Effect of adsorbent quantity on the removal (%) of Co(II) ions NiO/<math>\gamma</math>Al<sub>2</sub>O<sub>3</sub>nano catalyst at 298 K</b>	<b>66</b>
<b>(4.17)</b>	<b>Effect of initial concentration on the removal (%) of Cu (II)ion on NiO/<math>\gamma</math>-Al<sub>2</sub>O<sub>3</sub> nano catalyst</b>	<b>68</b>
<b>(4.18)</b>	<b>Effect of initial concentration on the removal (%) of Co (II)ion on NiO/<math>\gamma</math>-Al<sub>2</sub>O<sub>3</sub> nano catalyst</b>	<b>69</b>
<b>(4.19)</b>	<b>Effect of temperature on the removal (%) of Cu (II)ion on NiO/<math>\gamma</math>-Al<sub>2</sub>O<sub>3</sub> nano catalyst</b>	<b>70</b>

(4.20)	Effect of temperature on the removal (%) of Co (II)ion on NiO/ $\gamma$ -Al <sub>2</sub> O <sub>3</sub> nano catalyst	71
(4.21)	The Pseudo First – Order Kinetic Model for Cu(II) ions adsorption on NiO/ $\gamma$ -Al <sub>2</sub> O <sub>3</sub> nano catalyst	74
(4.22)	The Pseudo- Second Order Kinetic Model for Cu(II) ions adsorption on NiO/ $\gamma$ -Al <sub>2</sub> O <sub>3</sub> nano catalyst	75
(4.23)	The Intraparticle Diffusion Model for Cu(II) ions adsorption on NiO/ $\gamma$ -Al <sub>2</sub> O <sub>3</sub> nano catalyst	75
(4.24)	The Elovich Model for Cu(II) ions adsorption on NiO/ $\gamma$ -Al <sub>2</sub> O <sub>3</sub> nano catalyst	76
(4.25)	The Pseudo First – Order Kinetic Model for Co(II) ions adsorption on NiO/ $\gamma$ -Al <sub>2</sub> O <sub>3</sub> nano catalyst	78
(4.26)	The Pseudo- Second Order Kinetic Model for Co(II) ions adsorption on NiO/ $\gamma$ -Al <sub>2</sub> O <sub>3</sub> nano catalyst	79
(4.27)	The Intraparticle Diffusion Model for Co(II) ions adsorption on NiO/ $\gamma$ -Al <sub>2</sub> O <sub>3</sub> nano catalyst	79
(4.28)	The Elovich Model for Co(II) ions adsorption on NiO/ $\gamma$ -Al <sub>2</sub> O <sub>3</sub> nano catalyst	80
(4.29)	The Van't Hoff plot for adsorption of Cu(II) ions on NiO/ $\gamma$ -Al <sub>2</sub> O <sub>3</sub> nano catalyst	84
(4.30)	The Van't Hoff plot for adsorption of Co(II) ions on NiO/ $\gamma$ -Al <sub>2</sub> O <sub>3</sub> nano catalyst	85
(4.31)	Linear Langmiur isotherm of Cu(II) ion removal on NiO/ $\gamma$ -Al <sub>2</sub> O <sub>3</sub> nano catalyst at various initial concentration	88
(4.32)	Linear Langmiur isotherm of Co(II) ion removal on NiO/ $\gamma$ -Al <sub>2</sub> O <sub>3</sub> nano catalyst at various initial concentration	89
(4.33)	Linear Freundlich isotherm of Cu(II) ion removal on NiO/ $\gamma$ -Al <sub>2</sub> O <sub>3</sub> nano catalyst at various initial concentration	89

<b>(4.34)</b>	<b>Linear Freundlich isotherm of Co(II) ion removal on NiO/<math>\gamma</math>-Al<sub>2</sub>O<sub>3</sub> nano catalyst at various initial concentration</b>	<b>90</b>
<b>(4.35)</b>	<b>Linear Temkin isotherm of Cu(II) ion removal on NiO/<math>\gamma</math>-Al<sub>2</sub>O<sub>3</sub> nano catalyst at various initial concentration</b>	<b>91</b>
<b>(4.36)</b>	<b>Linear Temkin isotherm of Co(II) ion removal on NiO/<math>\gamma</math>-Al<sub>2</sub>O<sub>3</sub> nano catalyst at various initial concentration</b>	<b>91</b>

## *List of Symbols and Abbreviations*

<i>Symbol or Abbreviation</i>	<i>Definition</i>
<b>AAS</b>	<b>Atomic absorption spectrophotometer</b>
<b>AFM</b>	<b>Atomic force microscope</b>
<b>Avg</b>	<b>Average</b>
<b>ADLE</b>	<b>Arundo Donaxi Leaves Extract</b>
$C_e$	<b>Equilibrium concentration of adsorbate</b>
$C_t$	<b>Concentration of adsorbate after any time</b>
$C_0$	<b>Initial concentration of adsorbate</b>
<b>D</b>	<b>Crystallite size</b>
<b>FTIR</b>	<b>Fourier transform infrared spectroscopy</b>
<b>FWHM</b>	<b>Full width at half maximum</b>
<b>IR</b>	<b>Infrared spectroscopy</b>
<b>K</b>	<b>Thermodynamic equilibrium constant</b>
<b>K</b>	<b>Equilibrium Constant</b>
$k_1$	<b>Pseudo-First Order Constant</b>
$k_2$	<b>Pseudo-Second Order Constant</b>
$k_D$	<b>Diffusion Constant</b>
$K_{\text{elovich}}$	<b>Elovich model constant</b>
<b>M</b>	<b>Weight of adsorbent</b>
<b>min</b>	<b>Minute</b>
$Q_e$	<b>Adsorption capacity of the adsorbent at equilibrium time</b>
$q_e$	<b>Quantity of adsorbate at equilibrium</b>
$q_t$	<b>Quantity of adsorbate at any time</b>
<b>R</b>	<b>Gas constant</b>
$R^2$	<b>Correlation coefficient</b>
<b>R%</b>	<b>Percentage removal of adsorbate</b>
<b>RMS</b>	<b>Root mean square</b>
<b>Rpm</b>	<b>Revolution per minute</b>
<b>T</b>	<b>Temperature</b>

$t^{1/2}$	square root of the time
V	Volume of solution
wt%	Weight percentage
K <sub>f</sub>	Freundlich constant related with adsorption capacity
n	Freundlich constant related with adsorption intensity
A	Langmuir constant related with adsorption capacity
B	Langmuir constant related with energy of adsorption
B <sub>T</sub>	Temkin isotherm constant
b <sub>T</sub>	Related to heat of adsorption
A <sub>T</sub>	Equilibrium binding constant
XRD	X-ray diffraction
$\Theta$	Bragg's angle
$\Delta G$	Gibbs free energy
$\Delta H$	Enthalpy
$\Delta S$	Entropy



# **Chapter One**

## **(Introduction)**

## 1.1. General introduction

"Environment" means the sum total of all surroundings of a living organism, including natural forces and other living things, which provide conditions for development and growth as well as of danger and damage <sup>(1)</sup>.

It also means surrounding and everything that affects on organism during its lifetime or it is sum total of water, air and land and also their relationship with the human being. It involves all the physical and biological surrounding and their interactions <sup>(2)</sup>. So, pollutants entrance to a natural environment leads to disorder, instability, damage or discomfort of the ecosystem i.e. physical systems or living organisms known as the environmental pollution<sup>(3)</sup>.

There are many types of environmental pollution such as water pollution, light pollution, air pollution, noise pollution, soil pollution, thermal pollution, radiation pollution, and the agents which cause environmental pollution are known as pollutants <sup>(4)</sup>. Water pollution, known as the water bodies pollution (for example rivers, lakes, oceans and ground water) is one of the most serious environmental problems. It is caused by a variety of human activities such as industrial, agricultural and domestic takes place when contaminates are happened in direct way or indirectly into water bodies without enough remediation to remove harmful compounds <sup>(5)</sup>.

Water pollutants include those that are biodegradable, such as sewage effluent, which cause no permanent harm if adequately treated and dispersed, as well as those which are non-biodegradable, such as chlorinated hydrocarbon pesticides, certain industrial dyes, organic compounds and heavy metals in some industrial effluents <sup>(6)</sup>.

Heavy metal toxicity could result, for instance, from drinking-water, raised the concentration of the metal in air at source of emission and intake by food chain <sup>(6, 7)</sup>. Many methods have been used to remove heavy metals from water and wastewater, mainly chemical precipitation, ion-exchange, membrane separation, classical adsorption processes, electrolysis, etc... <sup>(8)</sup>.

The presence of heavy metals is one of the major concerns and that used target pollutants in research studies of the well- documented human health problems associated to these compounds and also their high toxicity <sup>(9,10)</sup>.

Green chemistry focuses on the production of desired products without generation of hazardous intermediate by products in chemical reaction processes. Integrating green chemistry principles into nanotechnology has led to the identification of environmentally friendly reagents that are multifunctional, which they can serve as a reducing agent and a capping agent <sup>(11, 12)</sup>.

Adsorption is one of the effective treatment processes as compared to other technologies for the remediation of different contaminates from aqueous environment due to the low-cost factor, moreover it can separate small number of toxic elements from the large volume solutions. Different kind of adsorbents have been commercialized or developed for the treatment of waste water <sup>(13, 14)</sup>.

Metal oxides nanoparticles are classified as the promising adsorbent for removal of heavy metals from aquatic systems due to their large surface areas and high activities; therefore, increasing attention has been focused on metal oxide such as iron, aluminum, titanium, and manganese, zirconium, and nickel oxides <sup>(15)</sup>.

The present study is focused on the synthesis of nickel and aluminum oxides nanoparticles which were used in the synthesis of NiO/ $\gamma$ -Al<sub>2</sub>O<sub>3</sub> nano catalyst. This catalyst was applied to remove different concentration of (cobalt and copper) from aqueous solution. The parameter effect on metal removal studied were contact time, nature of adsorbent, nature of adsorbate, effect of temperature from which the adsorption isotherms and kinetic study were investigated.

## 1.2. Literature Review

(P. Vijaya Kumar, et.al, 2019) reports on the main physical properties of nickel oxide nanoparticles (NiO NPs) synthesized by a completely green process using *Gymnema sylvestere* plant extract and sodium hydroxide as an effective reducing agent for co-precipitation method. The synthesized nanoparticles were characterized by XRD, HRTEM, EDS, FTIR, UV-visible, XPS, EPR and zeta potential analysis methods. The synthesized NiO NPs toxicity were evaluated in vitro using microbial and MCF-7 cancer cell line models. Further cytotoxicity studies and acridine orange and ethidium bromide staining confirmed that green synthesized NiO NPs possess low toxicity as compared to the chemically synthesized NiO NP<sup>(16)</sup>.

(Karim, et.al, 2018) In their study, copper oxide nanoparticles (CuO) were prepared by a simple method from the corresponding salt using Fig leaves extracts. The particles were characterized using XRD, SEM, TEM, and AFM techniques. XRD spectra revealed that the particle size obtained was around (7.31 nm), which agreed fairly well with those estimated from SEM and TEM. Surface morphology of the nanoparticles was studied by SEM, TEM and AFM<sup>(17)</sup>.

(Jagpreet Singh, et.al, 2018) In this review summarized the fundamental processes and mechanisms of “green” synthesis approaches, especially for metal and metal oxide [e.g., gold (Au), silver (Ag), copper oxide (CuO), and zinc oxide (ZnO)] nanoparticles using natural extracts. Importantly, they explored the role of biological components, essential phytochemicals (e.g., flavonoids, alkaloids, terpenoids, amides, and aldehydes) as reducing agents and solvent systems. The stability/toxicity of nanoparticles and the associated surface engineering techniques for achieving biocompatibility are discussed and also covered the applications of such synthesized products to environmental remediation in terms of antimicrobial activity, catalytic activity, removal of pollutants dyes, and heavy metal ion sensing<sup>(18)</sup>.

(Zafar, et.al, 2018), studied the adsorption of cobalt (II) ion using alumina from aqueous medium. The optimum conditions for removal of Co (II) ions were found at pH (7.5-8.5), adsorbent dose of solution is 20 g/L<sup>-1</sup>, equilibrium time (90 minutes) and initial concentration range (5-50) mg/L<sup>-1</sup>. The pseudo-second-order kinetics was observed for adsorption of Co<sup>+2</sup>. (cobalt removal adsorption isotherm intra-particle diffusion, Langmuir, Freundlich and Dubnin- Radushkevich were applied to analyze the equilibrium isotherms for adsorption of Co(II) ions onto Al<sub>2</sub>O<sub>3</sub>. The experimental results indicated that equilibrium data follows the Langmuir model within used concentration range<sup>(19)</sup>.

(H.RajaNaika, et.al, 2018) investigation aims at the synthesis of copper oxide nanoparticles (CuO Nps) using *Gloriosa superba* L. plant extract as fuel by solution combustion synthesis. X-ray diffraction studies showed that the particles are monoclinic in nature. The UV–visible absorption spectrum of CuO Nps indicates the blue shift with increase of concentration of plant extract. SEM images reveal that the particles are spherical in nature. TEM

image indicates that as-formed CuO Nps are spherical in shape, and the size is found to be in the range 5–10 nm<sup>(20)</sup>.

(**Tabesh, et.al, 2017**), prepared  $\gamma$ -Al<sub>2</sub>O<sub>3</sub> by using modified sol–gel method, aluminum nitrate, ethylene glycol (EG), citric acid (CA) and triethanolamine (TEA) were used as an Al<sup>3+</sup> source, gel, chelating and surfactant agents, respectively. They were structurally characterized using X-ray diffraction (XRD), scanning electron microscopy (SEM), thermo-gravimetric analysis (TGA) and infrared spectroscopy (IR). Then, the removal efficiency of heavy metal ions (lead and cadmium) in the adsorption process by the as-synthesized alumina nanoparticle has been investigated in PH (5), contact time is (20 and 30) min for Pb<sup>+2</sup> and Cd<sup>+2</sup> respectively<sup>(21)</sup>.

(**Xiaodong Yi, et.al, 2017**), in their research study they have prepared NiMo/Al<sub>2</sub>O<sub>3</sub> hydrodesulfurization (HDS) catalyst by using Ni (NO<sub>3</sub>)<sub>2</sub>.6H<sub>2</sub>O, (NH<sub>4</sub>)<sub>6</sub>Mo<sub>7</sub>O<sub>24</sub> and AlCl<sub>3</sub>.6H<sub>2</sub>O as a solid raw materials and polyethylene glycol (PEG) as additive on the precursor. Thermal decomposition catalytic properties and dibenzothiophene HDS activity were investigated. The powder prepared catalysts were characterized using nitrogen adsorption-desorption measurements, X-ray diffraction (XRD), thermogravimetric analysis /differential scanning calorimetry (TGA/DSC)<sup>(22)</sup>.

(**Jbara, et.al , 2017**), prepared  $\gamma$ -Al<sub>2</sub>O<sub>3</sub> by co-precipitation under annealing temperature effect, the structural characterization using XRD analysis indicates that the particle diameter ranging from 6 to 24 nm of gamma phase alumina .The surface area of the prepared nano powders is in the range of (109 to 367) m<sup>2</sup>/g. The morphology analysis indicates that  $\gamma$ -Al<sub>2</sub>O<sub>3</sub> nano-powders are consisted of grains almost spherical in shape<sup>(23)</sup>.

(Mohamed & Atta, 2016), prepared nano  $\gamma$ - $\text{Al}_2\text{O}_3$  support by co-precipitation method using different calcination temperatures (550,650, and 750) °C and prepared nano NiMo/  $\gamma$ - $\text{Al}_2\text{O}_3$  catalyst by impregnation method with nickel carbonate and ammonium paramolybdate with nano  $\gamma$ - $\text{Al}_2\text{O}_3$  support at calcination temperature of 550 °C. It was characterized by X-ray diffraction, X-ray fluorescent, AFM, SEM, BET surface area, and pore volume <sup>(24)</sup>.

(Wang, et.al, 2016), have studied the synthesized of  $\text{Al}_2\text{O}_3$  from the boehmite sol. A series of  $\text{Al}_2\text{O}_3$  materials were used as supports for sulfided NiMo catalysts used in the hydrodesulfurization (HDS) of dibenzothiophene (DBT) and 4,6-dimethyldibenzothiophene (4,6-DMDBT). The as-synthesized  $\text{Al}_2\text{O}_3$  materials with different crystal forms and the conforming NiMo catalysts were characterized by using XRD, nitrogen physisorption, FTIR, UV–Vis, Raman,  $\text{H}_2$  TPR, XPS, and HRTEM characterization techniques. The NiMo/ $\gamma$ - $\text{Al}_2\text{O}_3$  catalyst showed the highest DBT and 4,6-DMDBT change at all the weight hourly space velocities (WHSVs).

(A. Rahdar, et.al, 2015) In this paper, nanostructured nickel oxide (NiO) was synthesized by co-precipitation method using Nickel (II) Chloride Hexahydrate ( $\text{NiCl}_2 \cdot 6\text{H}_2\text{O}$ ) and sodium hydroxide (NaOH) as starting material. Structural, optical and magnetic properties of nanostructures were characterized by X-ray diffraction (XRD), scanning electron microscopy (SEM), Atomic force microscope (AFM), UV–Vis absorption; Fourier transformed infrared (FTIR) and vibrating sample magnetometer (VSM) technique. The X-ray diffraction pattern studies revealed that the NiO have a face-centered cubic (FCC) structure and confirmed the presence of high degree of crystallinity with nanoparticles average size found to be 26 nm <sup>(26)</sup>.

(**R. yuvakkumar, et.al, 2014**) report sustainable novel simple green synthetic strategy to synthesize NiO nanocrystals. This is first report on sustainable biosynthesis of NiO nanocrystals employing *Nephelium lappaceum* L., peel extract as a natural ligation agent. Green synthesis of NiO nanocrystals was carried out via nickel–ellagate complex formation using rambutan wastes. Successful formation of NiO nanocrystals was confirmed. Possible mechanism of NiO nanocrystals formation using rambutan extract was proposed. Prepared NiO nanocrystals were coated on cotton fabric and their antibacterial activity was analyzed<sup>(27)</sup>.

(**Gabriella Garbarino, et.al, 2014**) have investigated the hydrogenation of carbon dioxide producing methane and CO over Ni/Al<sub>2</sub>O<sub>3</sub> catalysts. prepared catalyst have been characterized by XRD and Temperature Programmed Reduction(TPR). Spent catalysts have been characterized by XRD and Field Emission SEM<sup>(28)</sup>.

(**Jiajian gao, et.al, 2013**) studied the correlation between phase structures and surface acidity of Al<sub>2</sub>O<sub>3</sub> supports calcined at different temperatures and the catalytic performance of Ni/Al<sub>2</sub> O<sub>3</sub> catalysts in the production of synthetic natural gas (SNG) via CO methanation. A series of 10 wt% NiO/Al<sub>2</sub>O<sub>3</sub> catalysts were prepared by the conventional impregnation method, and the phase structures and surface acidity of supports were adjusted by calcining the commercial  $\gamma$ -Al<sub>2</sub>O<sub>3</sub> at different temperatures (600–1200 °C)<sup>(29)</sup>.

(**Rahman pour, et.al, 2012**), reported a new method for synthesis of nano size ( $\gamma$ - Al<sub>2</sub>O<sub>3</sub>) by precipitation method under ultrasonic vibration mixing. The formed alumina was characterized by using SEM, XRD, BET, and TPD techniques. The materials in nano-scale show different characteristics in comparison with their bulk state<sup>(30)</sup>.



(Karim, et.al, 2011), studied the preparation of alumina by sol-gel technique and using urea in aqueous media. The resulting sol composed of Al (OH)<sub>3</sub> particles was heated at 280°C to obtain alumina particles. The γ-Alumina powder is characterized by (FTIR, XRD and BET) techniques. Electron micrograph shows that the particles are nano-sized having non-spherical shape<sup>(31)</sup>.

(Maia, et.al, 2006) Nanoparticles of FCC NiO phase were obtained by heating the dried resin result of a mixture of gelatin and NiCl<sub>2</sub> · 6H<sub>2</sub>O in aqueous solution. The average particle size and micro-strain were calculated from the line broadening of X-ray powder diffraction peaks, and these values were between 15 nm and 78 nm, and 0.056% and 0.172%, respectively<sup>(32)</sup>.

### 1.3. Aim of study

1. preparation of nano nickel (II) Oxide nano particles using Arundo donax leaf extract (ADLE) method and characterization it by X-ray diffraction , FTIR and Atomic force microscope.
2. Preparation and characterization of nano  $\gamma$ -Al<sub>2</sub>O<sub>3</sub> using co-precipitation method.
3. Preparation of nano NiO/  $\gamma$ -Al<sub>2</sub>O<sub>3</sub> using impregnation method and characterize it.
4. Determining the ideal condition for the adsorption of Cu<sup>+2</sup> and Co<sup>+2</sup> ions such as (contact time, quantity of adsorbent, temperature, and initial adsorbate concentration).
5. Thermodynamic studies of adsorption processes of Cu<sup>+2</sup> and Co<sup>+2</sup> ions on these adsorbents.
6. Investigate the kinetic studies of adsorption process.

# **Chapter Two**

## **(Theoretical Part)**

## 2.1. Pollution

Pollution is defined as any harmful or bad change in the environment that resulted from the physical, chemical, or biological side-effects of human industrial or social activities. The atmosphere, rivers, seas, and the soil are affected by pollution <sup>(33)</sup>.

The pollution of wastewater with heavy metals is currently attracting global attention because of the harmful effects on the environment, especially on human health <sup>(34)</sup>.

Water is an important commodity for life on earth and is something which is needed daily activities <sup>(35)</sup>. So; it is very suitable to say that water is vital, both as universal solvent and being an important component of metabolic process within the human body. Fresh and clean water is a major for the existence of life <sup>(36)</sup>. Pollution is any unpleasant or harmful change in the environment that results from the chemical, physical or biological impacts of social activities or human industrial <sup>(33)</sup>. Any substance causing nuisance or harmful effects or uneasiness to the organisms then that particular substance may be called as the pollutant <sup>(37)</sup>.

Also, the agents which cause environmental pollution is known as pollutants <sup>(38)</sup> with being shown in table (2.1). There are several types of environmental pollution such as; (water pollution, air pollution, light pollution, radiation pollution, noise pollution & soil pollution).

Table (2.1) Type of Pollutants <sup>(33)</sup>

Category	Examples
Organic chemicals	Poly chlorinated biphenyls (PCBs), oil, many pesticides, dyes
Inorganic chemicals	Salts, nitrate, metals and their salts
Organo metallic Chemicals	Methyl mercury, tri butyl tin, tetra ethyl lead
Acids	Nitric, hydrochloric, acetic , sulfuric,
Physical	Eroded soil, trash
Radioactive materials	Radon, radium, uranium
Biological organisms	Microorganisms, pollens

Nowadays, lack of clean water is an important problem around the world because the quick development of different industries, a huge quantity of wastewater has been generated from industrial processes and it has been discharged in water and soils systems <sup>(39)</sup>.

A water pollutant can be defined as a chemical or biological factor causing aesthetic or detrimental effects on aquatic life and on those who consume water. Majority of the water pollutants are, however, in the form of chemical which remain dissolved or suspended in water and give an environment response which is often objectionable .Sometimes physical and biological factor also act as pollutants .Among the physical factors, heat and radiations are important factors which have marked effects on organisms .Certain microorganisms present in water ,especially pathogenic species cause diseases to men and animals and can be referred as bio pollutants<sup>(40)</sup>.Figure (2.1) indicate the major source of water pollution.



**Figure ( 2.1):** The major sources of water pollution <sup>(41)</sup>.

Water pollutants may be classified in to organic and inorganic water pollutants:

1. Organic water pollutants: They comprise of insecticides and herbicides, organ halides and other forms of chemicals; bacteria from sewage and livestock's farming; food processing wastes; pathogens; volatile organic compounds etc.
2. Inorganic water pollutants: They may arise from heavy metals of acid mine drainage, silt from surface run-off, logging, and land filling; fertilizers from agricultural run-off which include nitrates and phosphates etc. and chemical waste from industrial effluents <sup>(41)</sup>.

## 2.2. Heavy metals

### 2.2.1. Definition of heavy metals

Heavy metals are generally referred to as those metals which possess a specific density of more than  $5 \text{ g/cm}^3$  and adversely affect the environment and living organisms <sup>(42)</sup>. These metals are quintessential to maintain various biochemical and physiological functions in living organisms when in very low concentrations; however they become noxious when they exceed certain threshold concentrations. Although it is acknowledged that those heavy metals have many adverse health effects and last for a long period of time, heavy metal exposure continues and is

increasing in many parts of the world. Heavy metals are significant environmental pollutants and their toxicity is a problem of increasing significance for ecological, evolutionary, nutritional and environmental reasons <sup>(43,44)</sup>. The most commonly found heavy metals in wastewater are arsenic, cadmium, chromium, cobalt, copper, lead, nickel, and zinc, all of which cause risks for human health and the environment <sup>(45)</sup>. Heavy metals enter the surroundings by natural means and through human activities. Various sources of heavy metals include soil erosion, natural weathering of the earth's crust, mining, industrial effluents, urban runoff, sewage discharge, insect or disease control agents applied to crops, and many others <sup>(46)</sup>.

Heavy metal pollution of water is dangerous environmental disturbances which impact the fineness of water <sup>(47,48)</sup>. The toxicity of heavy metals is related to the formation of complexes with proteins, in which carboxylic acid (-COOH), amine (-NH<sub>2</sub>), and thiol (-SH) groups are involved. When metals bind to these complexes, important enzyme and protein structures are affected <sup>(49)</sup>.

### **2.2.2. Industrial Wastewater Sources of heavy metals:**

The definition of industrial wastewater is any wastewater generated from any manufacturing, processing, institutional, commercial, or agricultural operation, or any operation that discharges other than domestic or sanitary wastewater <sup>(50)</sup>. Chemical pollutants in wastewater are either organic or inorganic. Organic consists mainly of protein, fats and carbohydrates. Inorganic pollutants of wastewater are free ammonia, organic nitrogen, nitrites, nitrates and trace element such as heavy metals <sup>(51)</sup>. Increased use of metals and chemicals in process industries has resulted in generation of large quantities of effluent that contains high level of toxic heavy metals and their presence poses environmental-disposal problems due to their non-degradable and persistence nature. In addition, mining, mineral processing and extractive-metallurgical operations also generate toxic liquid wastes <sup>(52)</sup>. With rapid development of industries such as metals wastewaters are directly or indirectly discharged into the environment increasingly <sup>(53)</sup>. Many processes such as smelting

activities, battery industrial, plating and mining discharge of municipal sewage and industrial wastewater include heavy metals such as, chromium, copper, cadmium, lead, nickel, cobalt, mercury, and zinc <sup>(54)</sup>.

### 2.2.3. Heavy metal wastewater treatment techniques:

Heavy metals are the environmental priority pollutants and it has become one of the most serious environmental problems today. So these toxic heavy metals should be removed from the wastewater to protect the people and the environment. Many methods that are being used to remove heavy metal ions include chemical precipitation, ion-exchange, adsorption, membrane filtration, electrochemical treatment technologies, etc <sup>(53)</sup> some of which are presented in Figure (2.2).

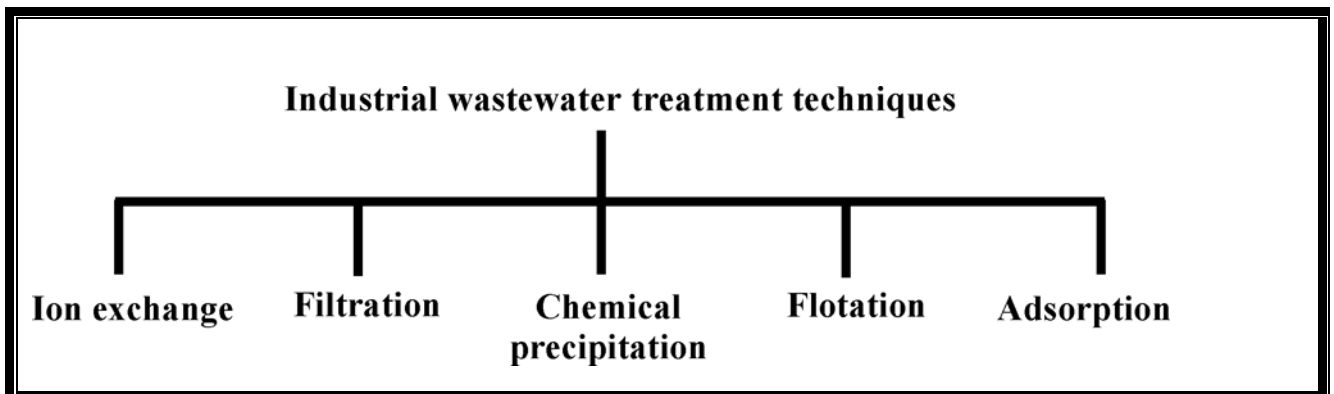


**Figure (2.2): Summarization of techniques used in industrial wastewater treatment.**



### 2.2.3.1 Chemical precipitation

Chemical precipitation is effective and by far the most widely used process in industry because it's relatively simple and inexpensive to operate. In precipitation processes, chemicals react with heavy metal ions to form insoluble precipitates. The forming precipitates can be separated from water by sedimentation or filtration and the treated water is then decanted and appropriately discharged or reused. The conventional chemical precipitation processes include hydroxide and sulfide precipitation <sup>(55, 56)</sup>.

### 2.2.3.2 Ion exchange

Ion-exchange is the type of processes has been widely used to remove heavy metals from wastewater because of their many advantages, such as high treatment capacity, high removal efficiency and fast kinetics <sup>(57)</sup> Ion-exchange resin, either synthetic or natural solid resin, has the specific ability to exchange its cations with the metals in the wastewater. Among the materials used in ion-exchange processes, synthetic resins are commonly preferred as they are effective to nearly remove the heavy metals from the solution <sup>(58)</sup>. Exchange resins are rather affected by certain variables such as pH, temperature, initial metal concentration and contact time <sup>(59)</sup>.

### 2.2.3.3 Membrane filtration

Membrane filtration is one of the type treatments which used to remove heavy metals by different types of membranes .Membrane filtration has been widely utilized in separation process of heavy metal due to its high separation efficiency simple and continuous operation, and no requirement of chemicals in the process and it include ultrafiltration reverse osmosis, Nano filtration and electro dialysis <sup>(53)</sup>.

### 2.2.3.4 Electrochemical treatment

Electrochemical methods involve the plating-out of metal ions on a cathode surface and can recover metals in the elemental metal state. Electrochemical wastewater technologies involve relatively large capital investment and the expensive electricity supply, so they haven't been widely applied. However, with the stringent environmental regulations regarding the wastewater discharge, electrochemical technologies have regained their importance worldwide during the past two decades <sup>(60)</sup> Electro deposition has been usually applied for the recovery of metals from wastewater. It is a clean technology with no presence of the permanent residues for the separation of heavy metals <sup>(61)</sup>.

### 2.2.3.5 Adsorption processes

The term adsorption is an important surface phenomenon usually describes the part of particles (ions, atoms, and molecules) both from the gas phase and from the solution on the surface of a solid material. The term (adsorbate) substance that is adsorbed and the term (adsorbent) the surface that adsorb this substance e.g. silica gel, porous clays, resins, and active charcoal <sup>(62)</sup>. One can be defined adsorption as the increase in concentration of reactant on the surface of the catalyst, due to increased concentration of the reactants the reactions proceed rapidly or overlap between two phases, liquid-liquid, liquid - solid, gas - liquid, and gas – solid. The links within the surface layer are cluttered because there is no overlay structure. The surface layer is therefore at a higher energy level and is described as surface active. Good adsorbents must have a large surface area containing many active sites and a porous structure <sup>(63)</sup>.

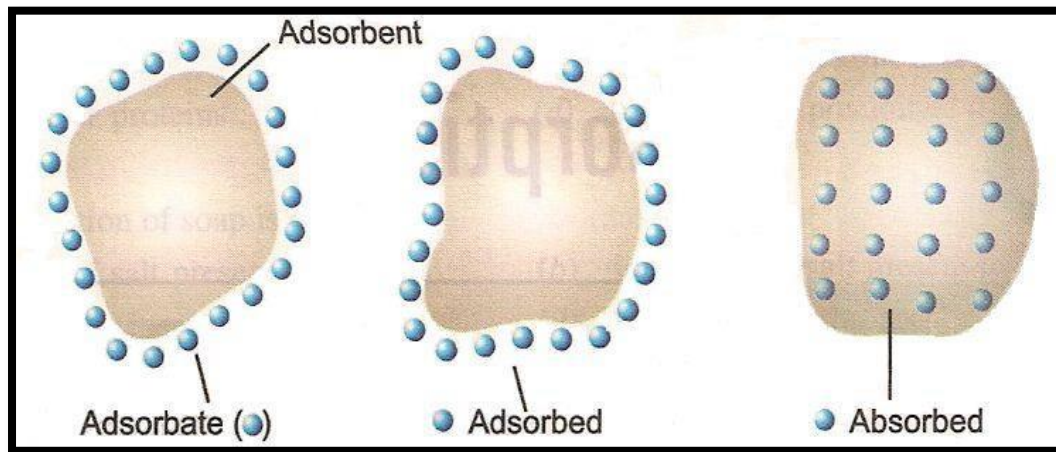


Figure (2.3) the adsorption versus absorption <sup>(6)</sup>.

Adsorption is considered as a method of high efficiency for water treatment due to its ease of operation and low cost <sup>(53)</sup>. It includes the up taking and immobilizing of pollutants on an adsorbent with related mechanisms, like surface adsorption, partition, surface precipitation, and structural adsorption <sup>(64,65)</sup>.

The reason for adsorption phenomenon is the existence of some unsaturated forces on the adsorbent due to the complete in coordination or insufficient material surface particles, like the liquid or solid phase adsorption which leads to saturate those forces on the adsorbent surface. Decreasing in surface free energy ( $\Delta G$ ) is occurred during the adsorption process, and decreasing in entropy ( $\Delta S$ ) at the surface that the adsorption take place, due to losing the degree of freedom possessed before adsorption. The decreasing of free energy ( $\Delta G$ ) and the entropy ( $\Delta S$ ) in the same time will cause decreasing in Heat content ( $\Delta H$ ) according to the thermodynamic relation <sup>(66, 67)</sup>.

$$\Delta G = \Delta H - T\Delta S \dots \dots \dots (2-1)$$

### 2.3. Forces of the adsorption

The forces of the adsorption process in solution are usually considered as follows <sup>(9, 68)</sup>:

1. Ion-exchange: replacement of counter ions of the double layer by similarly charged solute ions.
2. Ion pairing: electrostatic interactions between counter ions.
3. Acid-base interaction: hydrogen-bond formation between adsorbent and solute.
4. Adsorption by polarization of  $\pi$ -electrons: interaction between aromatic molecule groups and positive charges at the adsorbent surface.
5. Adsorption by dispersive forces.
6. Hydrophobic bonding: attractive interaction between hydrophobic groups of solute molecules and hydrophobic groups of adsorbents.

### 2.4. Types of adsorption

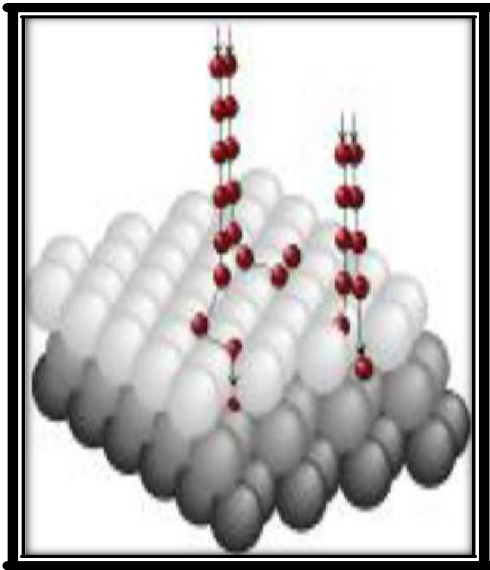
Forces of attraction exist between adsorbate and adsorbent. These forces of attraction can be due to Vander Waals forces of attraction which are weak forces or due to chemical bond which are strong forces of attraction. On the basis of type of forces of attraction existing between adsorbate and adsorbent, adsorption can be classified into two types: physical adsorption and chemical adsorption <sup>(69)</sup>.

#### 1. Physical adsorption:

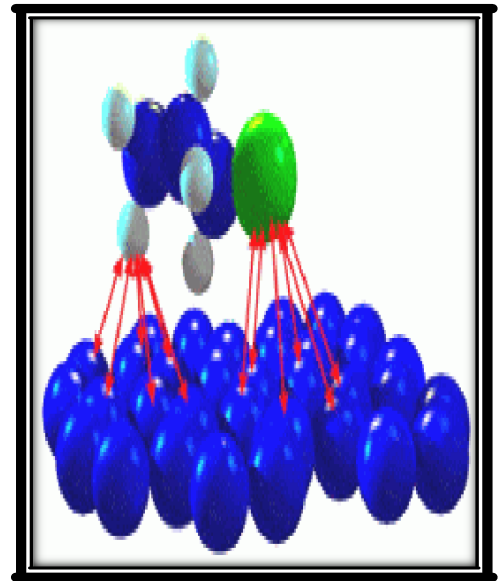
When there are weak forces such as forces Vander walls which connecting adsorbate and adsorbent, the process is called (physical adsorption) or (physisorption) as shown in figure (2.4) <sup>(70)</sup>.

#### 2. Chemical adsorption:

When there are chemical forces of attraction or chemical bond, which connect between adsorbate and adsorbent, the process is called (chemical adsorption) or (chemisorption) as show in figure (2.4) <sup>(71)</sup>.



(a) Physical adsorption

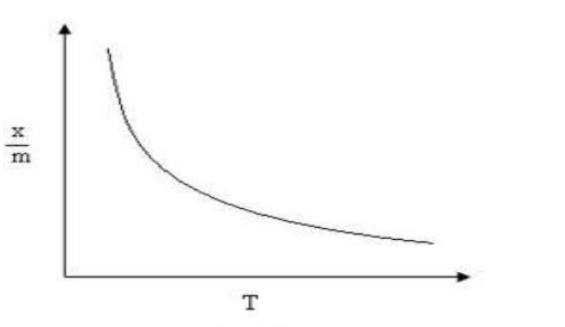
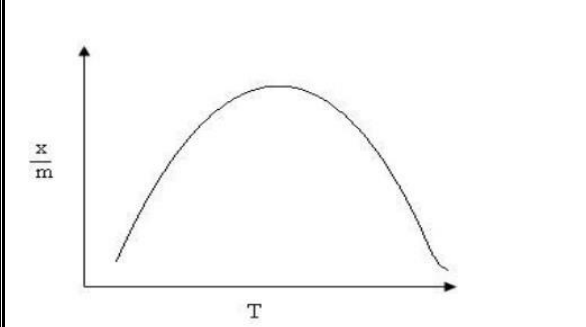


(b) Chemical adsorption

**Figure (2.4): Physical and chemical adsorption**

There are many differences between physisorption and chemisorption<sup>(72, 73)</sup> which is explained in, Table (2.2).

Table (2.2): Comparison between physical and chemical adsorption.

Physical adsorption	Chemical adsorption
It is due to the weak Vander Waals forces when adsorbate molecules accumulated onto adsorbent surface	It is due to the formation of chemical bond (covalent or ionic) when adsorbate molecules accumulated onto adsorbent surface
The adsorption processes decrease with increases in the temperature. So, the heat of adsorption is low (20-40) KJ/mole	The adsorption processes increase with increases in the temperature. So, the heat of adsorption is high (40-400) KJ/mole
The physical adsorption processes are reversible	The chemical adsorption processes are irreversible.
Adsorption is non-specific	Adsorption is highly specific
It is multilayer	It is monolayer
No reactions on the surface.	Reactions on the surface may take place; dissociation, catalyst, reconstruction.
No electron transfer although polarization of adsorbent may occur.	Electron transfer leading to bond formation between adsorbate and surface.
The physical adsorption does not require activation energy.	The chemical adsorption is required activation energy.
 <p><math>x</math> = amount of adsorbate <math>m</math> = amount of adsorbent</p>	 <p><math>x</math> = amount of adsorbate <math>m</math> = amount of adsorbent</p>

## 2.5. Adsorption mechanism from solution

The adsorption processes of solute onto solid surface is even more difficult to be treated theoretically than the corresponding of gas on solid processes cause the role of a solvent becomes more explicit<sup>(71)</sup>. The processes also depended on the nature of interactions between the solute and solvent in the solution phase and in the interfacial region, as well as on their interactions with the sorbent<sup>(74)</sup>. This process is relatively a complex phenomenon. It varies from adsorption of individual (gases, vapors, and pure liquids) in that solution contains at least two components forming a closely packed layer on the surface.

Adsorption from solution by porous surface may take place basically in the following steps<sup>(63)</sup>:

- 1- Transport of solute molecules from the bulk of solution to the exterior surface of the adsorbent material.
- 2- Movement of solute molecules across the interface and adsorption onto external surface sites occurs.
- 3- Migration of solute molecules within pores of the adsorbent.
- 4- Interaction of solute molecules with available sites on the interior surfaces, bounding the pore of the adsorbent and capillary spaces of the adsorbent.

One or more of the previous steps may control the rate by the amount of solute adsorbed onto the solid particle.

## 2.6. Factors influencing adsorption processes

The main factors that affect the percentage of adsorption are:

### 1. Contact time

Contact time can be defined as the longest time when the adsorption process complete and the balance or change is slight<sup>(72)</sup>. The time required for the

adsorption processes to reach equilibrium and depends on the surface nature and the available adsorption sites <sup>(75)</sup>.

## 2. Nature of the adsorbent

There are some factors affecting on adsorption energy of an adsorbent which are:

- **Surface Area:** Increase in the surface area of the adsorbent lead to increase the total amount of the adsorbate-adsorbed <sup>(76)</sup>.
- **Homogeneous Systems:** The work with clean metal surfaces have accentuated the complexities that certainly occur when metal powders, chemically deposited metal films, oxides of metals and non-metals are used as adsorbents <sup>(77)</sup>.
- **Heterogeneous Systems:** The non-homogeneity of a surface is characterized using the presence of adsorption sites with different adsorption energies <sup>(77)</sup>.
- **Polarity:** The polar surfaces tend to adsorb the more polar components in solution <sup>(69)</sup>.

### (3) Nature of the adsorbate

The interference between the adsorbent surface and the adsorbate particles affected by the nature of the adsorbate material shape, size, concentration and existence polar groups. The increase in molecular weight and solubility of polar group and charges affect the interference between the surface adsorbent and adsorbate particles which make the selective adsorption of one of the Components <sup>(69, 78, 79)</sup>.



**(4) Effect of the temperature and solubility**

The change in the temperature can influence the adsorption from solutions directly if the components of the solution are completely miscible, or with the nature and change of the solubility of the components if they are completely immiscible <sup>(80)</sup>.

The adsorption equilibrium constant,  $K$  is explained thermodynamically by using Van't Hoff equation as <sup>(81, 82)</sup>.

$$\ln K = -\frac{\Delta H}{R}\left(\frac{1}{T}\right) + \frac{\Delta S}{R} \dots\dots\dots(2.2)$$

Where:

**k:** The thermodynamic equilibrium constant

**$\Delta H$ :** The enthalpy change (kJ.mol<sup>-1</sup>).

**$\Delta S$ :** The change in entropy (kJ.mol<sup>-1</sup>.K<sup>-1</sup>).

**$R$ :** The gas constant (8.314 J.mol<sup>-1</sup>.K<sup>-1</sup>).

**$T$ :** The absolute temperature (K).

If  $\Delta H$  does not depend on the temperature with a known temperature interval, then  $\ln k$  is a linear function of the reciprocal of absolute temperature. The slope of the straight line of  $\ln k$  versus  $(1/T)$  is equal to  $-(\Delta H/R)$ , and the section on the axis of ordinates is equal to  $(\Delta S/R)$ . Thus, the temperature is depended on the equilibrium constant of the reaction,  $\Delta H$  and on the solubility. The effect of temperature on adsorption depends on the enthalpy change. Reaction in which heat is absorbed ( $\Delta H > 0$ ) is called endothermic ones, and a reaction in which heat is liberated ( $\Delta H < 0$ ) is exothermic ones. The entropy of a system is a function of a state of the system. Its change is equal to the sum of the reduced heats absorbed by the system in an equilibrium process. Entropy is a single-valued, continuous and finite function of state <sup>(80)</sup>.

### (5) Effect of the pH

The extent of adsorption may increase, decrease, or remain unchanged as a result of changing the pH. Many variables can take part in this process such as the nature of chemical state of the adsorbent, adsorbate, and solvent.

A competition is expected to take place as a consequence of  $H^+$  or  $OH^-$  ions interaction with the solute, surface or the solvent. Such an interaction can change the chemical state, which may lead to stronger or weaker extent of adsorption<sup>(83,84)</sup>.

## 2.7. Theories of adsorption

There are many types of adsorption isotherms and the most important ones are the following;

### 2.7.1. Langmuir isotherm

The American chemist Irving Langmuir who was awarded the Nobel Prize in chemistry in 1932 for “his discovers and researches in the realm of surface chemistry”, are developed the relationship between the amount of gas adsorbed on surface and the pressure of that gas in 1916<sup>(85)</sup>.

A model is set up that depends upon there being a fixed number of adsorption sites on adsorbent surface, each site capable of holding one molecule of adsorbate. All sites are equivalent in their affinity for adsorption of molecules, and the surface is uniform, however there will be no interaction between the adsorbed molecules.

Langmuir adsorption is monomolecular, it does not consider the case that further adsorption may take place on the adsorbate that is already present on the surface. The Langmuir isotherm can be expressed as follow<sup>(86-87)</sup>:

$$C_e/Q_e = 1/ab + C_e/a \dots \dots \dots (2.3)$$

Where:

$Q_e$ : The adsorption capacity at equilibrium per unit weight of adsorbent, (mg/g).

$C_e$ : The equilibrium concentration of adsorbate after adsorption, (mg /L).

$a$ : The Langmuir constant which is a measure of adsorption maximum capacity, (mg/g).

$b$ : The Langmuir constant which is a measure of energy of adsorption ,(L/mg).

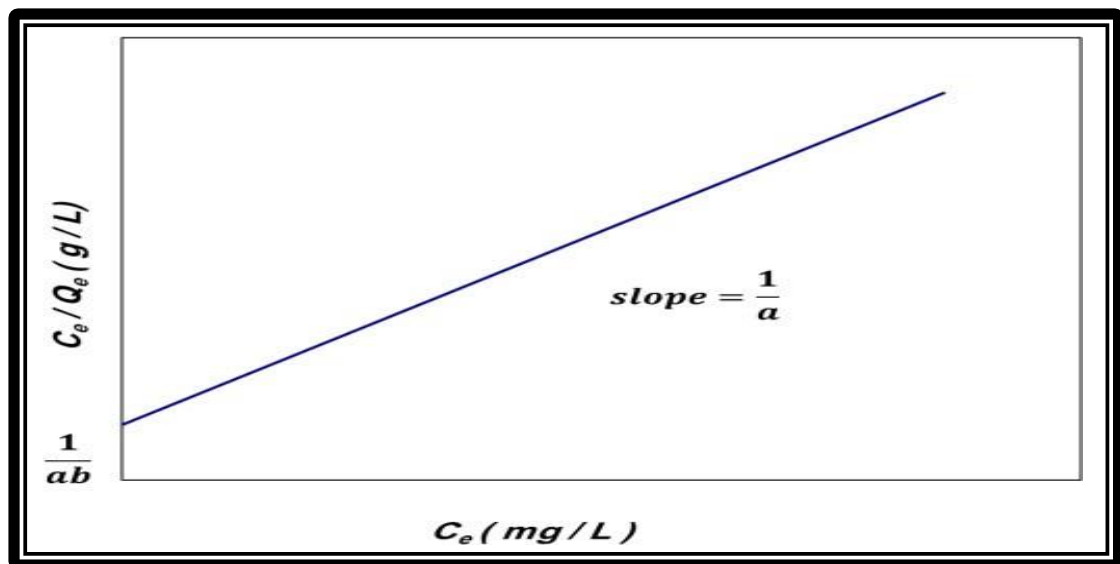


Figure (2.5): The linear form of Langmuir isotherm

This form can be used as a linearization of experimental data by plotting ( $C_e/Q_e$ ) against ( $C_e$ ) as shown in Figure (2.5). The Langmuir's constants ( $a$ ) and ( $b$ ) can be evaluated from the slope ( $1/a$ ) and intercept ( $1/ab$ ) of the linear equation<sup>(86)</sup>.

### 2.7.2. Freundlich isotherm

Herbert Max Finley Freundlich, a German physical Chemist, in 1926 presented an empirical adsorption isotherm for non-ideal system. In the derivation of Langmuir isotherm, it has been assumed that there is independence and

similarity in binding energy at each adsorption site. This linear relationship is obeyed by many but not all adsorbates at low concentration<sup>(85)</sup>.

His proposal was based on the experimental measurements. Freundlich adsorption isotherm equation may be derived assuming a heterogeneous surface with adsorption on each class of sites obeying the Langmuir equation.

The heterogeneous adsorption sites have different potential energies and different geometrical shapes on the surface, so the affinity from site to site toward the same molecule is different. The equation of Freundlich is as follows<sup>(87-88)</sup>:

$$Q_e = K_f C_e^{1/n} \dots \dots \dots (2.4)$$

Where:

$Q_e$  : quantity of adsorbate adsorbed per unit weight of adsorbent at equilibrium, (mg/g).

$C_e$  : equilibrium concentration of adsorbate in solution after adsorption, (mg/L).

$n$ : adsorption process extent.

$K_f$  : Freundlich constant, (mg/g).

The Freundlich constants can be obtained from the slope and intercept of the plot between the ( $\log Q_e$ ) versus ( $\log C_e$ ) after taking logarithms both side of equation (1.4) we get:

$$\log Q_e = \log K_f + 1/n \log C_e \dots \dots \dots (2.5)$$

If ( $\log Q_e$ ) is plotted against ( $\log C_e$ ) a straight line should be obtained as shown in Figure (2.6). The slope of the line will give the value of ( $1/n$ ) and the intercept on the Y-axis gives the value of ( $\log K_f$ )<sup>(86)</sup>.

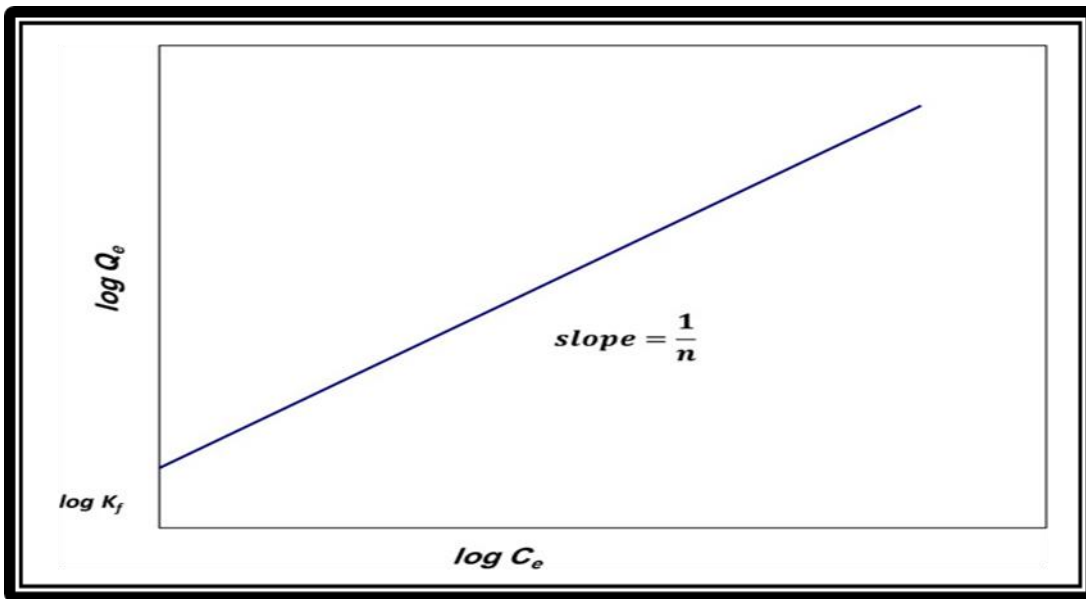


Figure (2.6): The Linear relationship Freundlich isotherm

### 2.7.3 Temkin isotherm

Temkin isotherm contains a factor that explicitly takes into account (adsorbing species- adsorbent interaction). This isotherm assumes that:

1. The heat of adsorption of all the molecules in the layer decreases linearly with coverage due to adsorbent –adsorbate interactions.
2. The adsorption is characterized by a uniform distribution, and that energy, up to some maximum binding energy. The Temkin isotherm is given by the following equation <sup>(85, 89)</sup>:

$$Q_e = B_T \ln (A_T \cdot C_e) \dots \dots \dots (2.6)$$

Where:

$A_T$ : is the equilibrium binding constant, (L/g).

$B_T$ : the Temkin isotherm constant which can be obtained as follow:

$$B_T = R_T / b_T \dots \dots \dots (2.7).$$

Where:

$b_T$ : is related to heat of adsorption, (J/mol).

$R$ : is the universal gas constant, (8.315 J/mol.K).

$T$ : is the absolute temperature, (K).

A linear form of Temkin isotherm was obtained by rearranging equation (2.6):

$$Q_e = B_T \ln A_T + B_T \ln C_e \dots \dots \dots (2.8).$$

The Temkin constants ( $A_T$ ) and ( $B_T$ ) were obtained from the slope and intercept of the plot between the  $Q_e$  and  $\ln C_e$ .

## 2.8. Nanomaterial

Nano material is defined as a physical substance with one dimension at the lowest between (1-100) nm, (1nm=10<sup>-9</sup>m) have received considerable interest because of the unique properties different from their bulk counterparts <sup>(90,91)</sup>. There are various applications for nanotechnology such as fuel cells, hydrogen storage, antibacterial activity, homogeneous and heterogeneous catalysis, electronics, and optics, magnetism, and material sciences, medical and biological sciences <sup>(92)</sup>. Modern advances in field nanotechnology have drove to the development of adsorbent nanoparticles for chromatographic uses. The morphology feature, high surface and small size made these materials to be utilized in removal technology.

The large surface area of the nanoparticles supplies more sites on the sorbent that increases the sorption capacity. Nanomaterial exhibit configuration of distinctive novel properties which can be used for separation of heavy metals from wastewater or water in the advance development of water treatment technologies.

Many nano-sized materials, such as metal oxide, zeolites, carbon-based nanoparticle, nano-clays, nano composites, have been used as adsorbent to remove heavy metal ions from water or wastewater <sup>(93)</sup>. Metals oxides nanoparticles are a highly valued material with various applications in optical, electrical and mechanical devices, catalysts, gas sensors, sunscreens and cosmetics <sup>(94)</sup>.

Many physical and chemical methods have been utilized for preparation of nanoparticles. However, a number of methods present disadvantages including use of high-energy consumption, hazardous products, toxic solvents.... etc., therefore there is an essential need to develop environment friendly methods for synthesis of metal nanoparticles.

The development of eco-friendly technologies in material synthesis is of considerable importance to expand their biological applications. Nowadays, varieties of green nanoparticles with well-defined chemical composition, size, and morphology have been synthesized by different methods and their applications in many innovative technological areas have been explored <sup>(95)</sup>. The renewable nature of plant extracts, eco-friendly aqueous medium and mild reaction conditions make the method advantageous over other hazardous methods. In the last years, different kind plants extract and their products have received attention due to its low cost, energy-efficient and nontoxic behavior in approach for synthesis of metal nanoparticles <sup>(96)</sup>.

## 2.9. Adsorption Kinetics

Chemical kinetics is concerned with understanding the rates of chemical reactions. It is to be contrasted with thermodynamics, which deals with the direction in which a process occurs but in itself tells nothing about its rate. Thermodynamics is time's arrow, while chemical kinetics is time's clock. The principles of chemical kinetics apply to purely physical processes as well as to chemical reactions. One reason for the importance of kinetics is that it provides

evidence for the mechanisms of chemical processes. Besides being of intrinsic scientific interest, knowledge of reaction mechanisms is of practical use in deciding what is the most effective way of causing a reaction to occur. Many commercial processes can take place by alternative reaction paths, and knowledge of the mechanisms makes it possible to choose reaction conditions that favor one path over others.

Kinetic is the study of chemical processes for description the adsorbate uptake rate. This rate helps to controls the time of adsorbate at the liquid – solid interface through using three main kinetic models:

1. Pseudo- first order model.
2. Pseudo-second order model.
3. Intraparticle Diffusion model.
4. Elovich model.

### 2.9.1 Pseudo-first order model

The first-order adsorption rate equation of solutes from a liquid solution on charcoal was the first kinetic equation of the adsorption of liquid/solid system based on solid capacity and was used extensively to describe the adsorption kinetics. In order to distinguish a kinetic equation based on the adsorption capacity of a solid and the one based on the concentration of a solution. Lagergren's first order rate equation and also called the pseudo-first order equation is represented by <sup>(97)</sup>.

$$dq/dt = k_1 (q_e - q_t) \dots \dots \dots (2.9)$$

In which :

$q_t$  is the amount adsorbed at any time, (mg/g)  $q_e$  is the amount adsorbed at equilibrium (mg/g)

$k_1$  is the pseudo- first order rate constant ( $\text{min}^{-1}$ )



The integrated form of the equation (2.9) for the boundary conditions of  $t=0$ ,  $q_t = 0$  and  $t = t$ ,  $q_t = q_t$ .

$$\ln(q_e - q_t) = \ln q_e - k_1 t \dots \dots \dots (2.10)$$

So the pseudo-first order constants can be obtained from the slope and intercept of plot between  $\ln (q_e - q_t)$  and time ( $t$  in min).

### 2.9.2 Pseudo-second order model

The second-order model, the rate-limiting step is the surface adsorption that involves chemisorption, so the physicochemical interactions between the two phases leads to remove from the solution. The equation of this model is given by <sup>(98-99)</sup>.

$$dq_t / dt = k_2 (q_e - q_t) \dots \dots \dots (2.11)$$

Where  $k_2$  is the pseudo-second order rate constant (g/mg.min). When  $t$  change from  $t = 0$  to  $t = t$  and  $q_t = 0$  to  $q_t = q_t$ , the **equation (2.11)** become:

$$1 / (q_e - q_t) = 1/q_e + k_2 t \dots \dots \dots (2.12)$$

Equation (2.12) can be rearranged to obtain the following linear form:

$$t/q_t = 1/(k_2 q_e^2) + 1/q_e t \dots \dots \dots (2.13)$$

The pseudo-second order constants can be obtained from the slope and intercept of the plot between the  $t/q_t$  against  $t$ .

### 2.9.3 Intra-Particle Diffusion Model

The intra-particle diffusion model describes the adsorption processes, where the rate of adsorption depends on the speed at which adsorbate diffuses towards adsorbent (i.e., the process is diffusion-controlled), which is gives by <sup>(100)</sup>.

$$q_t = k_D t^{1/2} + C \dots \dots \dots (2.14)$$

In which:

$q_t$  : the amount of adsorbed at any time (mg/g)

$k_D$  : the diffusion constant ( $\text{mg/g min}^{1/2}$ )

$t^{1/2}$ : the root of the time ( $\text{min}^{1/2}$ )

C: the thickness of boundary layer.

The diffusion constant was determined from the slope of the plot between  $qt$  and  $t^{1/2}$ .

### 2.9.4. Elovich Model

The Elovich or Roginsky –Zeldovich equation is generally expressed as follows <sup>(101)</sup>.

$$dq/dt = \alpha \exp(-\beta qt) \dots \dots \dots (2.15)$$

where

$qt$  : the amount of adsorbed at any time ( $\text{mg/g}$ )  $t$ ,

$\alpha$  : the initial adsorption rate ( $\text{mg.g}^{-1} .\text{s}^{-1}$ ),

$\beta$ : adsorption constant ( $\text{g/mg}^{-1}$ ) during any one experiment.

To simplify the Elovich equation, <sup>(102)</sup> assumed  $\alpha\beta t \gg 1$ , and on applying the boundary conditions  $qt = 0$  at  $t = 0$  and  $qt = qt$  at  $t = t$ , equation (2.15) then becomes <sup>(103)</sup>.

$$qt = \beta \ln(\alpha\beta) + \beta \ln t \dots \dots \dots (2.16)$$

Thus the constants can be obtained from the slope and intercept of the linear plot of  $qt$  versus  $\ln t$ . Equation (2.16) will be used to test the applicability of the Elovich equation to the kinetics of adsorption.

## 2.10. Catalysts

### 2.10.1 Definition of catalyst

A catalysts is a substance that increases the rate at which a chemical reaction approaches equilibrium without itself becoming permanently involved in the reaction .A catalysts is itself a chemical substance and as such becomes involved in the reaction , although not permanently . The chemical state of the catalysts is subject to all the rules of chemistry in its interaction with reactants but remains

unchanged at the end of reaction. In fact, we can describe the catalytic reaction as a cyclic event in which the catalyst participates and is recovered in its original form at the end of the cycle. A catalyst cannot alter the chemical equilibrium of a given reaction; it only creates a favorable reaction pathway. This is done by decreasing the activation barrier ( $E_{a,cat}$ ) compared to the gas phase reaction ( $E_{a,gas}$ ) and thus increasing the reaction rate see **Figure(2.7)**. Consequently, the reaction can take place at lower temperatures and pressures <sup>(104)</sup>.

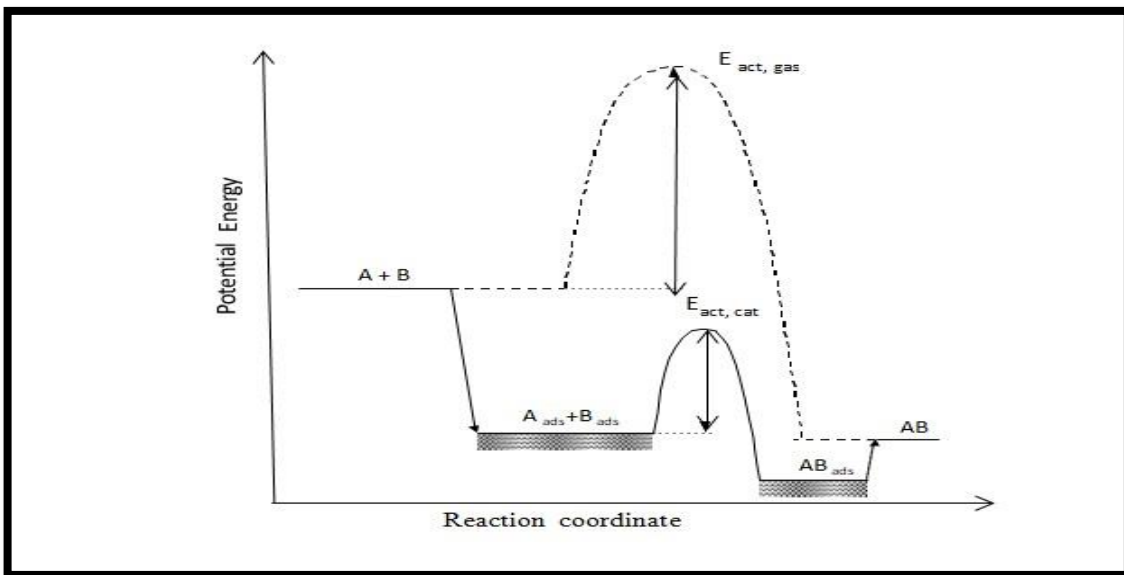


**(Figure 2.7) Potential energy diagram for a heterogeneous catalytic reaction (solid line)**

The solid catalysts are usually of none noble metal catalysts and noble types. None-noble metal catalysts include base metals and zeolites. Nobel metal catalyst includes a variety of precious metals from the platinum group. In many cases, catalytically active metals are combined with a solid support such as alumina, silica-alumina, zeolites, carbon, etc <sup>(105)</sup>.

## 2.10.2. Catalysts classification according to phase

### 2.10.2.1 Homogeneous catalysis

The catalysts are the same phase as the reactants and products. Example are hydrolysis of esters by acids (liquid-liquid), Oxidation of  $\text{SO}_2$  by  $\text{NO}_2$  (vapor-vapor), and decomposition of potassium chlorate by  $\text{MnO}_2$  (solid-solid). Usually, the liquid phase is most common, with both catalyst and reactants in the solution <sup>(106)</sup>.

Catalysis occurs through complexing and rearrangement between molecules and ligands of the catalyst. Reactions can be very specific, with high yields of desired products. Since the mechanisms involve readily identified species, these reactions are easily studied in the laboratory with the techniques of organometallic chemistry. However, they are difficult to operate commercially. Liquid phase operation places restrictions on temperature and pressure, so equipment is complicated. The catalyst must be separated from the products, imposing additional difficulties. For these reasons, homogeneous catalysis is found only in limited industrial use, appearing usually in the manufacture of specialty chemicals, drugs, and food. Exceptions are acetic acid production, olefin alkylation, and hydroformylation <sup>(106-107)</sup>.

### 2.10.2.2 Heterogeneous catalysis

The heterogeneous catalysis refers to the form of catalysis where the phase of the catalyst differs from that of the reactants. Phase here refers not only to solid, liquid, gas, but also immiscible liquids, e.g. oil and water. The great majority of practical heterogeneous catalysts are solids and the great majority of reactants are gases or liquids. Heterogeneous catalysis is of paramount importance in many areas of the chemical and energy industries, the heterogeneous catalysis is a surface phenomenon which involves the following steps <sup>(107-108)</sup>.

1. Diffusion of the reactants at the surface of the catalyst.
2. Adsorption of the molecules of the reactants at all active sites.
3. Occurrence of the chemical reaction on the surface of the catalyst.
4. Desorption of products molecules from the surface.
5. Diffusion of products away from the surface of the catalyst.

### 2.10.2.3. Enzyme catalysis

Enzymes are protein molecules of colloidal size, somewhere between the molecular homogeneous and the macroscopic heterogeneous and the macroscopic heterogeneous catalyst. Enzymes are the driving force for biochemical reactions, present in life processes, they are characterized by decomposes  $\text{H}_2\text{O}_2$   $10^9$  times faster than any inorganic catalyst. There is a great interest in harnessing enzyme catalysis for industrial use<sup>(106)</sup>.

### 2.10.2. Catalyst components:

Most catalysts have three type of easily distinguished components with their mutual dependencies presented in Figure (2.8) and they are:

1. Active component .
2. A support or carrier
3. Promoters

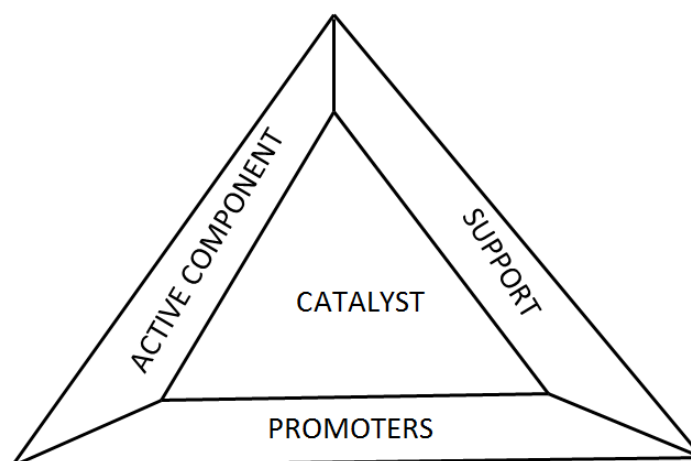


**Figure (2.8) The mutual dependencies of the catalyst components.**

Active components are responsible for the principal chemical reaction and the selection of the active component is the first step in catalyst design.

Supports, or carriers, perform many functions but the most important is maintenance of high surface area for the active component. Support function as stable surface over which the active component is dispersed in such a way that sintering is reduced. The support itself must be secured from thermal growth, which means high melting point which is least high than that of the active component. Mechanical strength and thermal stability of catalyst articles are always of concern to process designers<sup>(109)</sup>.

A promoter is a third agent when added often in small amounts, leads to desired activity, selectivity and stability effect. Promoters are designed to assist either the support or the activity component. One important example of support

promotion is control of the catalyst stability.

### 2.10.3. Key factors for FTS catalyst design

The design of heterogeneous catalysts with optimum performances for a given process requires a consideration of a combination of chemical, physical and mechanical properties. the “triangular concept” for catalyst design which has been adapted for FTS by Farrauto and Bartholomew, as illustrated in figure (2.9). In addition the physic-chemical properties of the active phase, specifically formulation shape, size and crystallinity of the nanoparticles are significant factors for optimization during catalyst design see figure (2.9) <sup>(110)</sup>.

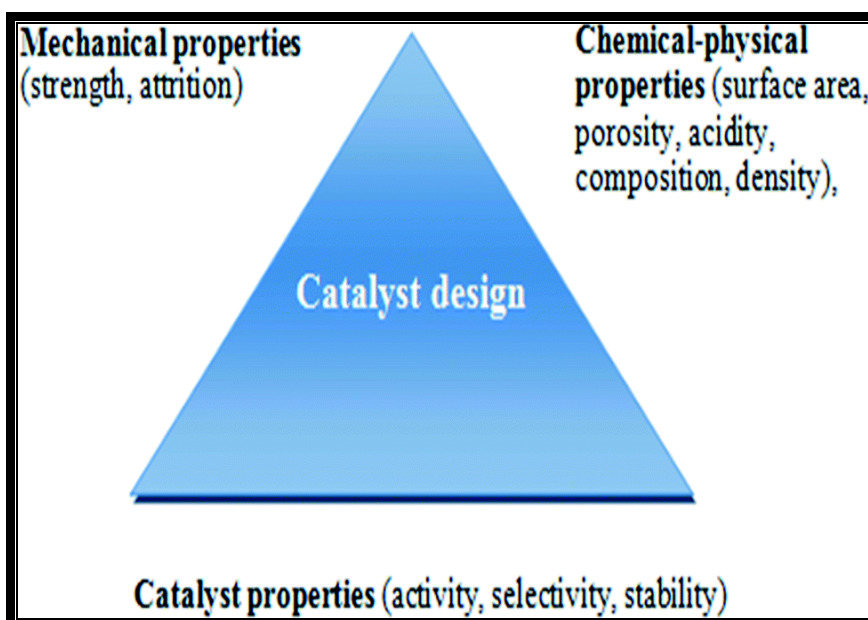


Figure (2.9) Concept of triangle of catalyst design

## 2.11. Oxide Catalyst Preparation

Oxides are used extensively in catalysis processes either as catalysts, supports, or precursors to active catalysts. For example, mixed oxides are readily transformed to supported high area metal catalysts on reduction in situ in the reactor, or can be transformed to sulfide by reaction with hydrogen sulfide or dimethyl disulfide in situ in the reactor. Hence, oxide preparation is a general starting point underpinning the origin of many commercial catalysts. In view of this diversity, this section will deal with only selected examples that are designed to emphasize key features<sup>(111)</sup>.

### 2.11.1. Single Oxides

Single oxides are not often used as catalysts, but they are often used as catalyst supports and, consequently, their preparation can be of crucial importance. However, some single oxides, e.g. NiO and  $\gamma$ -Al<sub>2</sub>O<sub>3</sub>, have been used as catalysts as well as supports. It should be recognized that oxides can be prepared by a variety of methods, e.g. oxidation of the metal or thermal decomposition of nitrates, carbonates, basic carbonates, hydroxides, and some of these precursors are prepared through precipitation techniques. Hence, it is important to consider single oxides as a starting point for oxide preparation<sup>(111)</sup>.

### 2.11.2. Mixed Oxides

Mixed oxides are the usual precursors to active catalysts commonly encountered in commercial operations. There are four general methodologies used for the synthesis of mixed oxides<sup>(112)</sup>.

- (a) Co-precipitation
- (b) Precipitation via chemical reaction between reactive precursors
- (c) Impregnation or adsorption onto a support
- (d) Fusion (high temperature treatment).



# **Chapter Three**

**(Experimental part)**

### 3.1. Instruments and Apparatus

#### 3.1.1. The instruments and tools used

The instruments and tools that are used in this study are tabulated with their details, origin, and location in **table (3.1)**.

**Table (3.1): The instruments used in this study.**

No.	Instruments name	Details & Origin	Location
1	Electric Balance	KERN ACJ/ACS,ACS 120-40, WB 12 AE 0308, max 120 g, d= 0.1 mg, (Germany)	The Laboratories of Chemistry Department, College of Science, University of Diyala, Iraq
2	Oven	BINDER,Hotline International (20-360°C), (Germany)	
3	Meter PH	PH/Ion Benchtop WTW inoLab PH Meters 7110 Benchtop Meters, (Germany)	
4	Hot Plate Magnetic Stirrer	MS-H280-pro ISO LAB Laboratory GmbH, (Germany)	
5	Water Bath with Shaker	SWB -802 11,220V/50HZ, (Korea)	
6	Centrifuge	HERMIE LABORTI CHINK Type Z200A, 6000 rpm, (Germany)	
7	Distillation device	LUZ DE AVISO AGUA INSUFICICENTE, (Germany)	
8	Electrical Furnace	Type -Nabertherm, Max Temperature 1300°C, 400V, 15.0 A, 50/60 Hz, (Germany)	
9	Ultrasonic device	Ningbo Runyes Medical Instrument Co. AC220V,F50Hz (China)	

### 3.1.2. Apparatus used

The apparatus used are shown in **table (3.2)** with their details, origin, and location.

**Table (3.2): Apparatus used in Characterization.**

No	Apparatus name	Details & Origin	Location
1	<b>X-ray Diffraction Spectrometer (XRD)</b>	XRD-6000 Cuk $\alpha$ ( $\lambda=1.5406 \text{ \AA}$ ), 220/50, HZ, SHIMADZU, (Japan)	Lab. of X-Ray Diffraction in Central Service laboratory, College of Education Ibn- AL-Haitham, University of Baghdad, Iraq
2	<b>Atomic Absorption Spectrometer (AAS)</b>	Shimadzu AA-7000, (Japan)	Lab. of Atomic Absorption Flame in Central Service laboratory, College of Science, Biological science department, University of Baghdad, Iraq
3	<b>Atomic Force Micrometer (AFM)</b>	Scanning Probe Microscope, AA 3000 SPM 220 V- Angstrom Advanced Inc, AFM contact mode, (USA)	The Special Laboratory of Dr. Abdulkareem M.A. AL-Sammarraie, College of Science, University of Baghdad, Iraq
4	<b>FTIR</b>	SHIMADZU (IR PRESTIGE21)	Chemistry department College of education for pure sciences /Diyala University

## 3.2. Materials

### 3.2.1. The chemical materials

The properties of the chemicals compounds which are used in this work are show in the table (3.3).

**Table (3.3): The chemicals used.**

No.	Chemicals	Formula	Purity (%)	Molecular mass	Source
1	Aluminium chloride hexahydrate	$\text{AlCl}_3 \cdot 6\text{H}_2\text{O}$	99	241.43	CDH
2	Nickel (II) chloride hexahydrate	$\text{NiCl}_2 \cdot 6\text{H}_2\text{O}$	99	238	Panreac Espana
3	Sodium hydroxide	$\text{NaOH}$	99	40	Alpha chemical
4	Ammonia solution	$\text{NH}_4(\text{OH})$	25	17.03	BDH
5	Absolute ethanol	$\text{C}_2\text{H}_5\text{OH}$	99.9	46.069	GCC
6	Cobalt(II) chloride hexahydrate	$\text{CoCl}_2 \cdot 6\text{H}_2\text{O}$	99.8	237.93	Sigma Aldrich
7	Copper (II) sulphate pentahydrate	$\text{CuSO}_4 \cdot 5 \text{H}_2\text{O}$	99.5	249.685	Western germany

### 3.2.2. Adsorbates used in this study

The heavy metals have used as adsorbates in this work were Cu (II) and Co(II) ions based on it is being strong pollutants need to be removed from wastewater.

### 3.2.3. Prepared nanoparticles used in this study

1. Nickel oxide nanoparticles were prepared by Arundo Donaxi Leaves Extract route denoted as: (ADLE.NiO.NP).
2. Alumina ( $\gamma\text{-Al}_2\text{O}_3$ ) prepared by co-precipitation method.

### 3.3. Preparation of adsorbent catalyst.

#### 3.3.1. Preparation of alumina ( $\gamma\text{-Al}_2\text{O}_3$ ) using co-precipitation method

Dissolved (47.0792g) of ( $\text{AlCl}_3 \cdot 6\text{H}_2\text{O}$ ) in (45ml) distilled water as show in Figure (3.1.A) and then 150 ml ethanol was added to get a transparent solution shown in (3.1.B), 60 ml of ammonium hydroxide was added drop by drop until the white precipitate as  $\text{Al}^{+3}$  gel hydroxides was formed as shown in Figure (3.1.C and D). The gel obtained is filtered, washed with deionized water several times to removed impurities and was dried at 80 °C for 10 hours in an oven, finally calcinated at 550 °C for 4 h as show in Figure (3.1.E) where a white fine of  $\gamma$ - alumina nano-powder was obtained see in Figure (3.1)

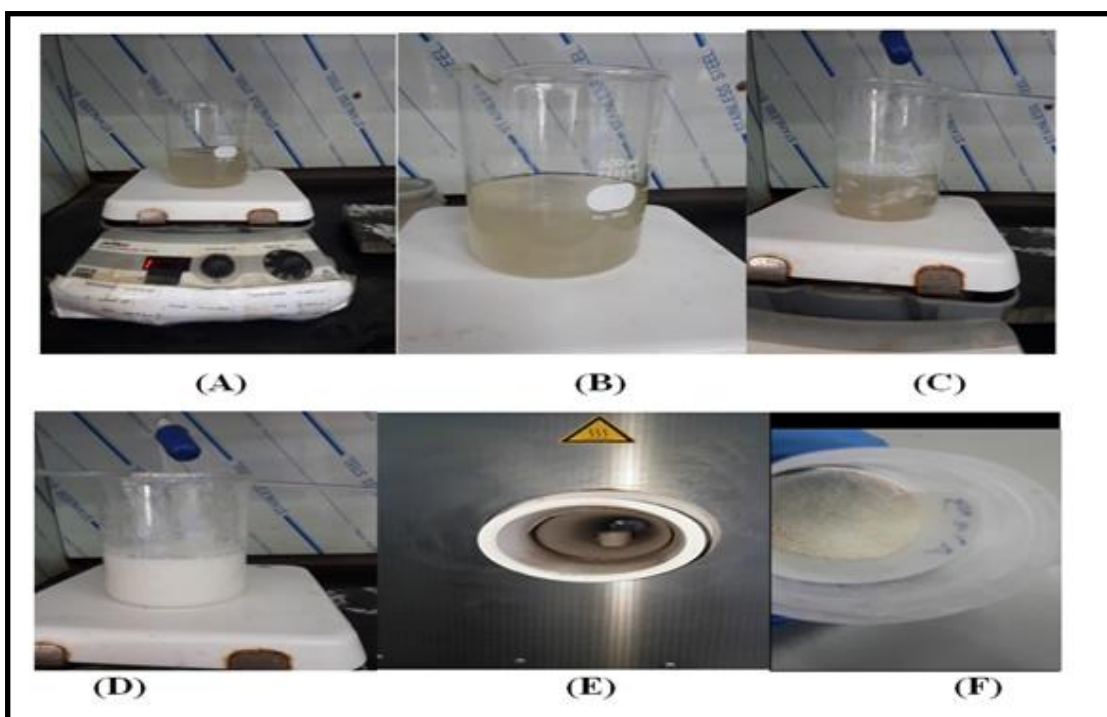


Figure (3.1) Steps of the preparation of  $\gamma\text{-Al}_2\text{O}_3$  using co-precipitation method.

### 3.3.2. Preparation of Nickel (II) oxide nanoparticles using Arundo donaxi Leaves Extract, (ADLE.NiO.NP)

#### 3.3.2.1. Preparation of ADLE

The Arundo Donaxi Leaves were collected from river side in Diyala government, then cleaned from the suspended dirt by tap water then washed with distilled water and dried in shade. They were grinded with electric grinder then sifting them and stored away from wet, as shown in Figure (3.2), (5) g of powder Arundo leaves was added to (400) ml of deionized water and boiled for (30) min until the solution color change and then cool the mixture to room temperature and filtered it, centrifuge the filtrate at (1200) rpm for (2) min to remove biomaterials and store the extract at room temperature for use in the preparation of the nickel oxide nanoparticles, as shown in Figure (3.2).

#### 3.3.2.2. Preparation of Nickel Oxide nanoparticle

Dissolve (0.5) g of nickel (II) chloride hexahydrate ( $\text{NiCl}_2 \cdot 6\text{H}_2\text{O}$ ) in (400) ml of deionized water with continuous stirring and then (10) ml of plant extract is added gradually with continuous stirring, raise temperature of solution to (80)  $^\circ\text{C}$  and then adjusts pH of the solution by adding sodium hydroxide (0.1) M approximately (10) ml where precipitate with a light green color formed, then this was filtered and washed with deionized water several times and then with absolute ethanol to remove impurities and dry in an oven at (70) $^\circ\text{C}$  for (2) hours. The steps are shown in Figure (3.2), Figure (3.3) is flow diagram showing the steps for preparing Nickel (II) oxide nanoparticles using Arundo donaxi Leaves extract.



Figure (3.2): Steps of the preparation of Nickel (II) oxide nanoparticles using Arundo donax Leaves Extract.

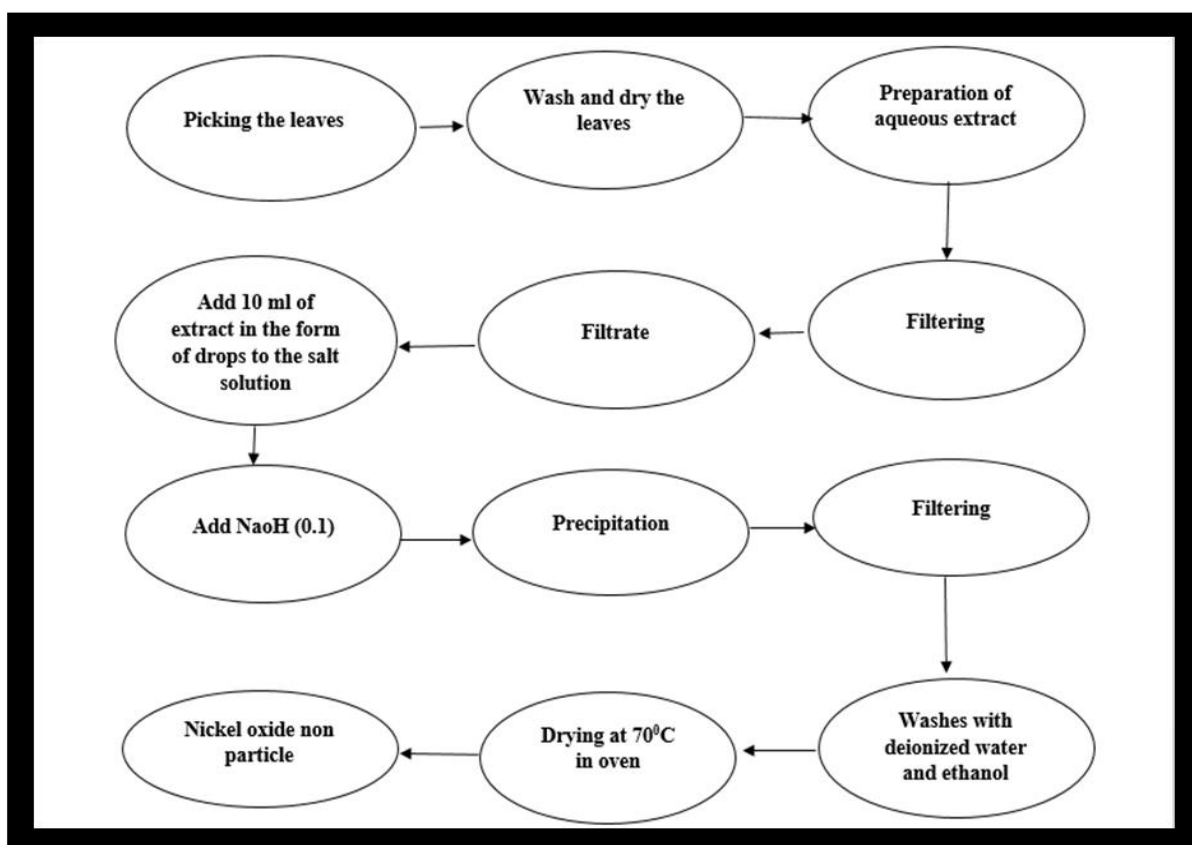


Figure (3.3): Flow diagram showing the steps used in preparing Nickel (II) oxide nanoparticles using Arundo donax Leaves Extract.

### 3.3.3. Preparation of Nano NiO/ $\gamma$ -Al<sub>2</sub>O<sub>3</sub> Catalyst

The NiO/ $\gamma$ -Al<sub>2</sub>O<sub>3</sub> catalyst composed of 20% wt NiO and 80% wt Al<sub>2</sub>O<sub>3</sub> was prepared by impregnation method. An impregnated aqueous solution was prepared by dissolving (1g) nickel oxide in (10ml) of distilled water and (4g) alumina in (20ml) of distilled water. These two solutions are mixed together at room temperature with constant stirring; the mixture was placed in ultrasonic apparatus for (1.5h). The impregnated nano NiO/ $\gamma$ -Al<sub>2</sub>O<sub>3</sub> was dried at 80 °C for 8 hours in an oven and finally NiO/ $\gamma$ -Al<sub>2</sub>O<sub>3</sub> nano-powder was obtained.

## 3.4. Preparation of solutions used in adsorption processes

### 3.4.1. Sodium hydroxide

(0.4) g of sodium hydroxide was weighed and transferred into (100) ml volumetric flask and the volume was completed to (100) ml with deionized water to produce the (0.1) M of NaOH solution.

### 3.4.2. Standard stock solution of Cu (II) ions

(1000 mg/L) stock solution of Cu (II) ion was prepared by weighing (3.9292gm) of (CuSO<sub>4</sub>.5H<sub>2</sub>O) and dissolve it in deionized water and then dilute it to 1000 ml with deionized water in volumetric flask. A series of solution with (50, 100, 150, 200, 250 mg/L) were prepared by adequate volumes dilution from the stock solution and deionized water

### 3.4.3. Standard stock solution of Co (II) ions

(1000 mg/L) stock solution of Co(II) ion was prepared by weighing (4.0372gm) of (CoCl<sub>2</sub>.6H<sub>2</sub>O) and dissolve it in deionized water and then dilute it to 1000 ml with deionized water in volumetric flask. A series of solution with (50, 100, 150, 200, 250 mg/L) were prepared by adequate volume dilution from the stock solution and deionized water.



### 3.5. Studying the factors affecting adsorption method

#### 3.5.1. Effect of contact time on Cu (II) and Co (II) ions Adsorption

The time that is required for the adsorption process to reach equilibrium at temperature of 298 K was determined by using five volumetric flasks with a volume of (100) ml and containing (50) ml of  $\text{Cu}^{+2}$  or  $\text{Co}^{+2}$  ions solution with initial concentration of (100) mg/L.

Adsorbent amount of (0.1) g of (prepared  $\text{NiO}/\gamma\text{-Al}_2\text{O}_3$ ) was added into each flask and covered them with glass stopper and placed in a water bath shaker at constant temperature of (298) K at speed of (150) rpm at various time intervals (10, 20, 30, 40, 50) min. Then filtered the solutions to prevent catalysts nanoparticles interference and finally measure the concentrations of  $\text{Cu}^{+2}$  or  $\text{Co}^{+2}$  ions in solutions to reach equilibrium using atomic absorption spectrophotometer at  $\lambda_{\text{max}}$  of (324.7) nm for Cu (II) and (240.7) nm for Co(II) ions.

#### 3.5.2. Effect of quantity of $\text{NiO}/\gamma\text{-Al}_2\text{O}_3$ catalysts adsorbent

The effect of adsorbent quantity was studied using (0.06, 0.08, 0.10, 0.12 and 0.15) g from (prepared  $\text{NiO}/\gamma\text{-Al}_2\text{O}_3$ ) for the removal of  $\text{Cu}^{+2}$  or  $\text{Co}^{+2}$  ions using a fixed (50) ml of (100) mg/L  $\text{Cu}^{+2}$  or  $\text{Co}^{+2}$  ions), temperature of (298) K at stirring speed of (150) rpm. The contact time for adsorption was (50) min in all cases.

#### 3.5.3. Effect of initial concentration of Cu (II) and Co (II) ions.

The effect of concentration was studied using solution that contain (50) mL of (50, 100, 150 and 250) mg /L Cu(II) or Co(II) of at the following conditions; (0.1) g of (prepared  $\text{NiO}/\gamma\text{-Al}_2\text{O}_3$ ), temperature of (298) K and stirring speed of (150) rpm . The contact time for Cu(II) and Co(II) ions adsorption used was (50) min on all experiments.

#### 3.5.4. Effect of temperature.

Adsorption experiments are carried out as mentioned in section (2.5.1-2.5.4) at different temperatures (293, 303, 313, 323 and 333) K to remove Cu(II) or Co(II) ion

from aqueous solutions in order to investigate the effect of temperature on adsorption.

### 3.6. Calculation of Metal Removal

The percentage removal of metal (R%) was calculated using the below equation<sup>(113-114)</sup>.

$$R \% = \frac{(C_o - C_e)}{C_o} \times 100 \quad \dots\dots\dots (3.1)$$

Where

R % : The percentage metal removal.

C<sub>o</sub> : The initial concentration of metal ion (mg /L) .

C<sub>e</sub>: The equilibrium concentration of metal ion after adsorption at any time (mg /L).

### 3.7. Kinetic of adsorption of Cu<sup>+2</sup> and Co<sup>+2</sup> ions

To study the kinetic of adsorption of copper and cobalt ions, five volumetric flasks (50 ml) of each ion with initial concentration of (100) mg/L were used. Weight (0.1) g of prepared NiO / $\gamma$ -Al<sub>2</sub>O<sub>3</sub> and added to each flask which is then placed in water path shaker at (150 rpm) and a temperature 298 K under continuous shaking. The samples were withdrawn from the shaker at a regular time interval of (5,15,25,35 and 45) min and was filtered to separate the adsorbent and then atomic absorption spectroscopy was used to measure the absorbance of the solutions to determine the concentration of each metal ion. The previous experiment was repeated using the adsorbent at a temperature (308 ,313 , 318, 323) K

The order of adsorbate – adsorbent interaction was investigated by using four kinetic models describe by (2.10) ,(2.13),(2.14),(2.16) .

# **Chapter Four**

## **(Results and Discussion)**

## 4.1. Characterization of the nanomaterials

### 4.1.1. X-ray diffraction analysis:

The XRD technique was used to determine and confirm the crystal structure of the nanoparticles as it is the best one to do.

#### 4.1.1.1. X-ray diffraction of NiO nanoparticles

XRD pattern of prepared nickel (II) oxide nanoparticles is shown in Figure (4.1) with the data of strongest three peaks shown in Table (4.1). The peaks position of the samples exhibit the monoclinic structure and single phase of NiO nanoparticles. The broadening of the diffraction peaks indicates that the crystal size is small.

The particle sizes were calculated from Deby-Sherrer formula given below <sup>(122)</sup>

$$D = 0.9\lambda/\beta \cos \theta \dots\dots\dots(4.1)$$

Where:

D is the crystallite size,

$\lambda$  is the wave length of radiation,

$\theta$  is the Bragg's angle,

$\beta$  is the full width at half maximum (FWHM).

The calculated crystal size is (12.83 nm) and the presence of sharp peaks in the XRD and crystal size being less than 100 nm refers to the Nano-crystalline nature.

**Table (4.1)** The strongest three peaks in XRD spectrum of prepared NiO nanoparticles.

No.	$2\theta$ (deg)	$d$ (Å)	FWHM (deg)	Intensity(counts)
1	33.18	2.6990	0.796	131
2	38.36	2.3591	3.66398	96
3	37.22	2.3819	14.96341	84

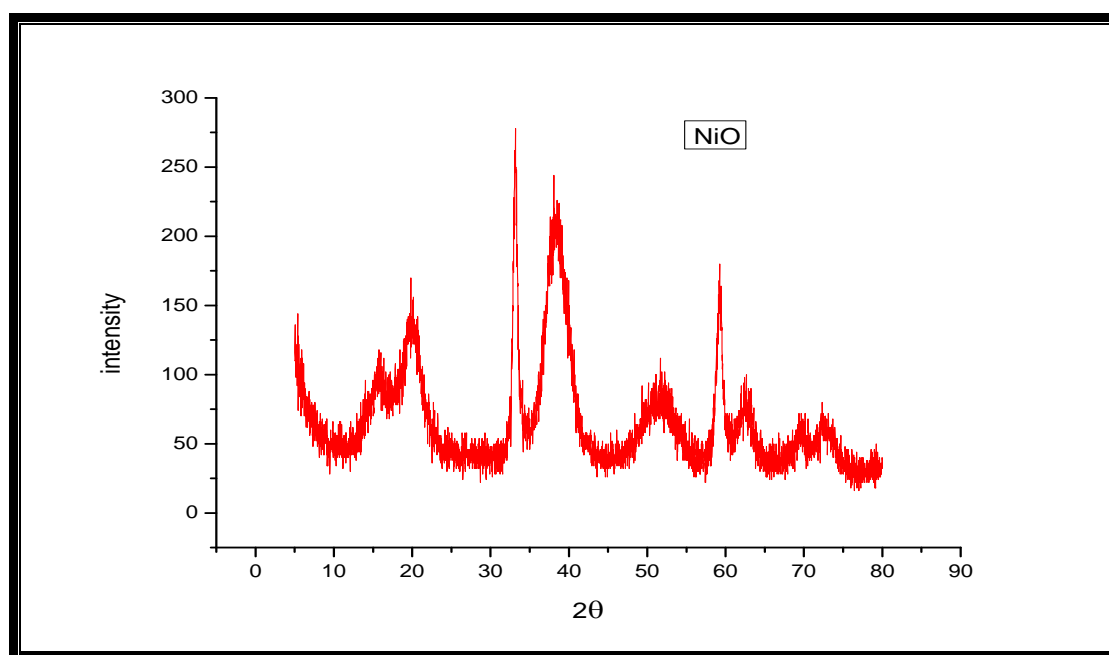


Figure (4.1) :X-ray diffraction of prepared (NiO) nanoparticle .

#### 4.1.1.2. X-ray diffraction of $\gamma$ - $\text{Al}_2\text{O}_3$

XRD pattern of the prepared alumina nanoparticles is shown in Figure (4.2) with the data of strongest three peaks shown in (Table 4.2) .The peaks position of the samples exhibit the monoclinic structure and single phase of  $\gamma$ - $\text{Al}_2\text{O}_3$  nanoparticles. The broadening of the diffraction peaks indicates that the crystal

size is small. The calculated crystal size is (6.46 nm) and the presence of sharp peaks in the XRD and particle size being less than 100 nm refers to the nano size nature.

**Table ( 4.2).** The strongest three peaks in XRD spectrum of prepared  $\gamma$ -  $\text{Al}_2\text{O}_3$  nanoparticles

No.	$2\theta$ (deg)	$d$ (Å)	FWHM (deg)	Intensity(counts)
1	66.7822	1.39965	1.48000	20
2	66.2024	1.41050	1.60000	18
3	46.0752	1.96839	1.17000	12

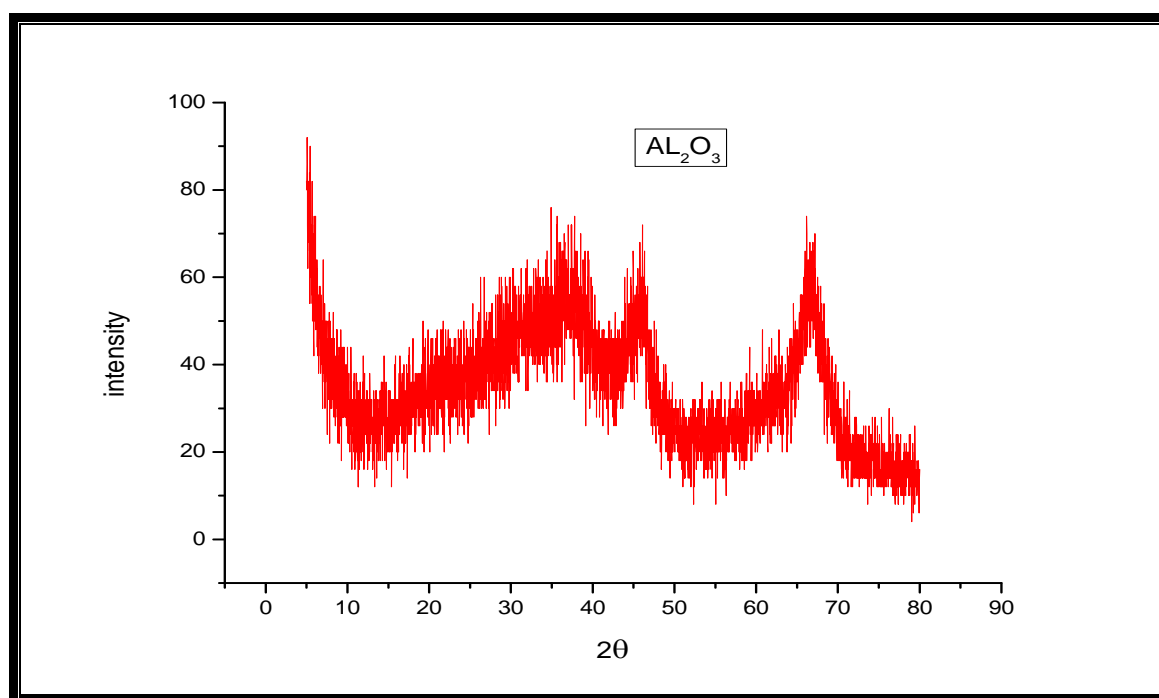


Figure (4.2) :X-ray diffraction of prepared ( $\gamma$  - $\text{Al}_2\text{O}_3$ ) .

#### 4.1.1.3. X-ray diffraction of NiO/ $\gamma$ - $\text{Al}_2\text{O}_3$ catalyst

XRD pattern of as prepared NiO/  $\gamma$  - $\text{Al}_2\text{O}_3$  nanoparticles is shown in Figure (4.3) with the data of strongest three peaks shown in (Table 4.3). The peaks position of the samples exhibited the monoclinic structure and single phase of

NiO/  $\gamma$ -Al<sub>2</sub>O<sub>3</sub> nanoparticles. The broadening of the diffraction peaks indicates that the crystal size is small. The calculated particle size is (5.04 nm) with the presence of sharp peaks in the XRD and particle size being less than 100 nm refers to the Nano-crystalline nature.

**Table ( 4.3).** The strongest three peaks in XRD spectrum of prepared NiO/  $\gamma$  Al<sub>2</sub>O<sub>3</sub> catalyst.

No.	2 $\theta$ (deg)	d ( $\text{\AA}$ )	FWHM (deg)	Intensity (counts)
1	38.5149	2.33556	1.68000	26
2	37.6756	2.38564	0.84000	25
3	33.1897	2.69711	0.70000	20

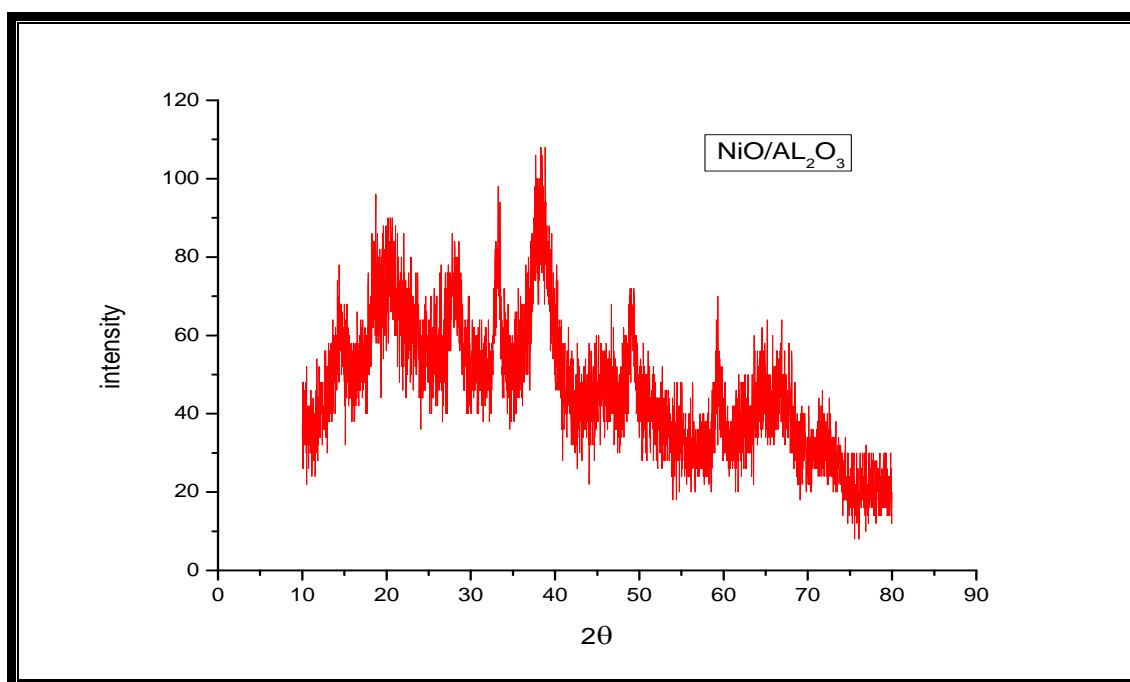


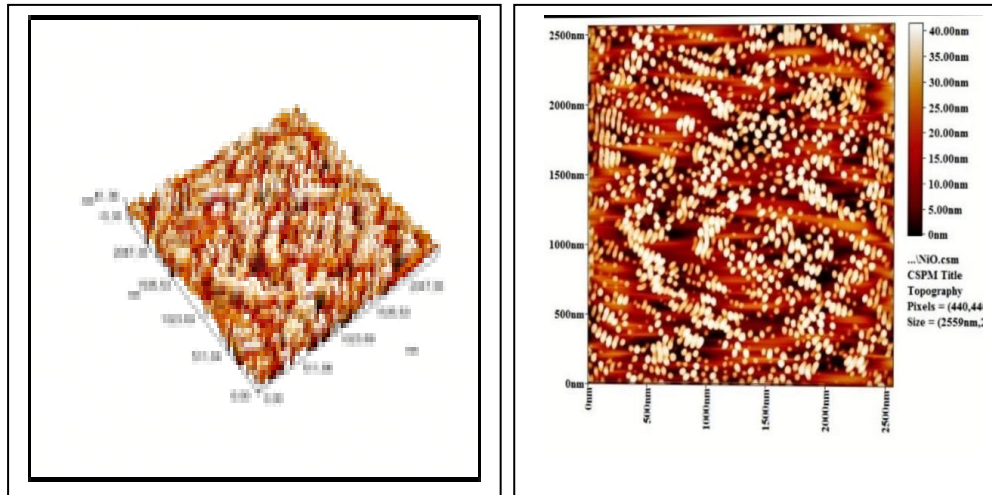
Figure (4.3) :X-ray diffraction of prepared ( NiO/  $\gamma$  Al<sub>2</sub>O<sub>3</sub>) nano catalyst.

## 4.1.2 Atomic force microscope

### 4.1.2.1. AFM of NiO nanoparticle

The AFM analysis is used to provide information about the morphology of surface and average grain size<sup>(123)</sup>. Figures (4.4) show typical AFM images of

the (prepared NiO). its explains images of AFM for catalyst with (size = 2559, 2559 nm) and ability analytical (pixel =440,440) . Figure (4.4.A) is AFM images in three dimensions (3D), it explains structure shape for grain, and Figure (4.4.B) is AFM images in two dimensions (2D), it found that average roughness is (10.4) nm and the root mean square (RMS) is (12) nm.



( A )

( B )

Figure (4.4): AFM images of the NiO nanoparticle

Table (4.4) and figure (4.5) explained the cumulating distribution and average diameter of prepared NiO nanoparticle where the average diameter of NiO is (43.13) nm ,and the particle size of less than 10 % of the total particles is 34 nm, less than 50 % is 44 nm and less than 90% is 48 nm.

**Table (4.4): Granularity cumulating distribution and average diameter of NiO nano-particle.**

Diameter(nm) <	Volume(% )	Cumulation (%)	Diameter( nm)<	Volume (%)	Cumulati on(%)	Diameter( nm)<	Volume (%)	Cumulation(% )
34.00	3.41	3.41	42.00	7.10	38.92	50.00	15.06	95.45
36.00	10.51	13.92	44.00	8.81	47.73	52.00	4.55	100.00
38.00	7.10	21.02	46.00	18.75	66.48			
40.00	10.80	31.82	48.00	13.92	80.40			



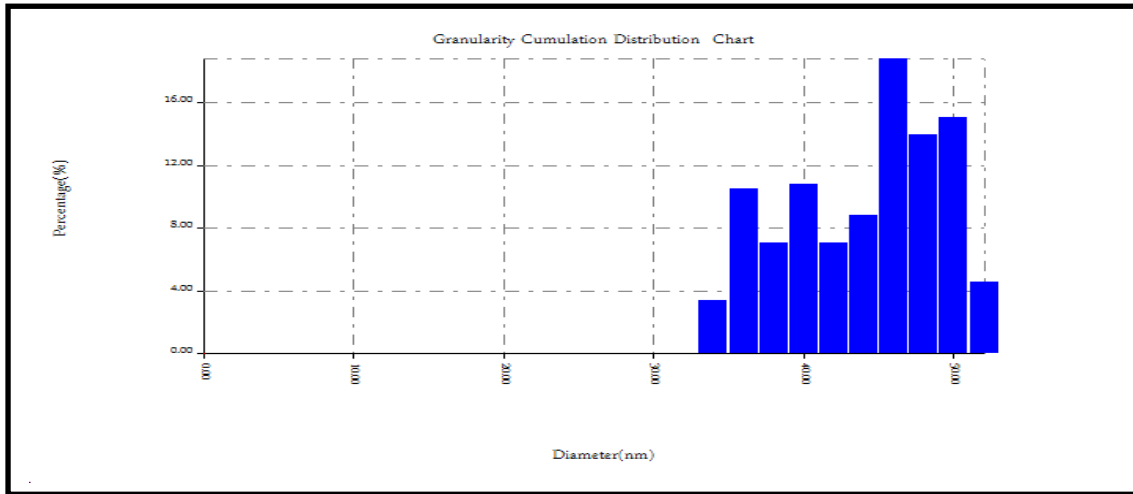


Figure (4.5): Granularity cumulating distribution of NiO/ nanoparticle.

#### 4.1.2.2. AFM of $\gamma\text{-Al}_2\text{O}_3$ nanoparticle

The AFM analysis is used to provide information about the average grain size<sup>(123)</sup>. Figures (4.6) show typical AFM images of the (prepared  $\gamma\text{-Al}_2\text{O}_3$ ). Its explain images of AFM with (size = 2547, 2547 nm) and ability analytical (pixel = 472,472). Figure (4.6A) is AFM images in three dimensions (3D), it explain structure shape for grain, and Figure (4.6.B) is AFM images in two dimensions (2D), it found that average roughness is (6.72) nm and the root mean square (RMS) is (7.76) nm .

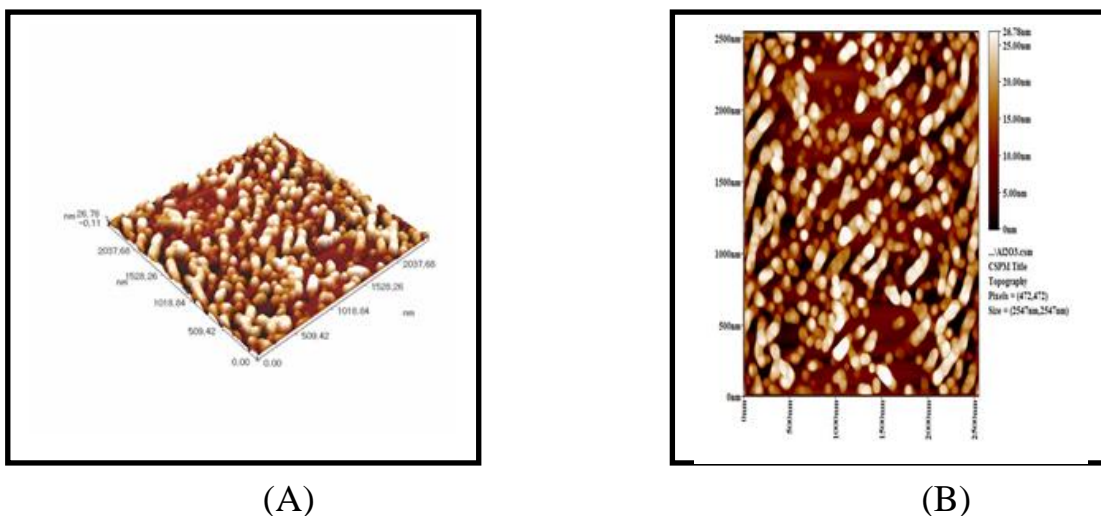


Figure (4.6): AFM images of nano  $\gamma\text{-Al}_2\text{O}_3$  .

Table (4.5) and figure (4.6) explain the cumulating distribution and average diameter of prepared  $\gamma$ - $\text{Al}_2\text{O}_3$  nanoparticle where the average diameter of  $\gamma$ - $\text{Al}_2\text{O}_3$  is (71.84) nm ,and the particle size of less than 10 % of the total particles is 45 nm, less than 50 % is 70 nm and less than 90% is 95 nm.

**Table (4.5): Granularity cumulating distribution and average diameter of nano  $\gamma$ - $\text{Al}_2\text{O}_3$  .**

Diameter( nm)<	Volum e(%)	Cumulati on(%)	Diameter( nm)<	Volum e(%)	Cumulati on(%)	Diameter( nm)<	Volum e(%)	Cumulati on(%)
15.00	0.38	0.38	50.00	4.53	11.70	85.00	10.94	72.83
20.00	0.38	0.75	55.00	8.30	20.00	90.00	5.66	78.49
25.00	0.38	1.13	60.00	7.55	27.55	95.00	8.68	87.17
30.00	0.38	1.51	65.00	9.06	36.60	100.00	7.55	94.72
35.00	1.13	2.64	70.00	9.06	45.66	105.00	5.28	100.00
40.00	2.64	5.28	75.00	7.92	53.58			
45.00	1.89	7.17	80.00	8.30	61.89			

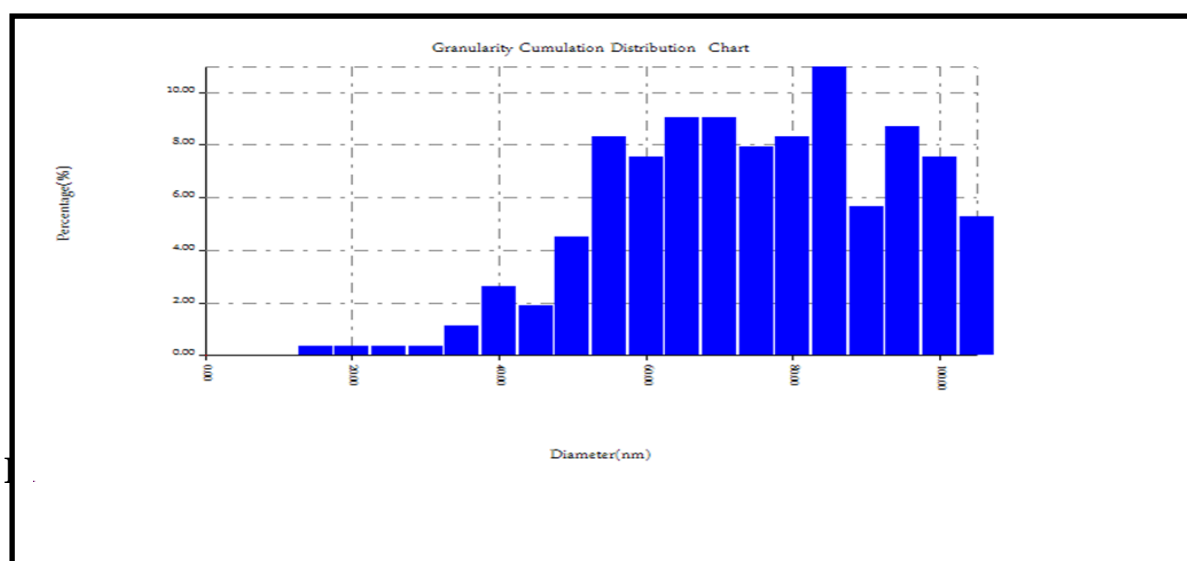
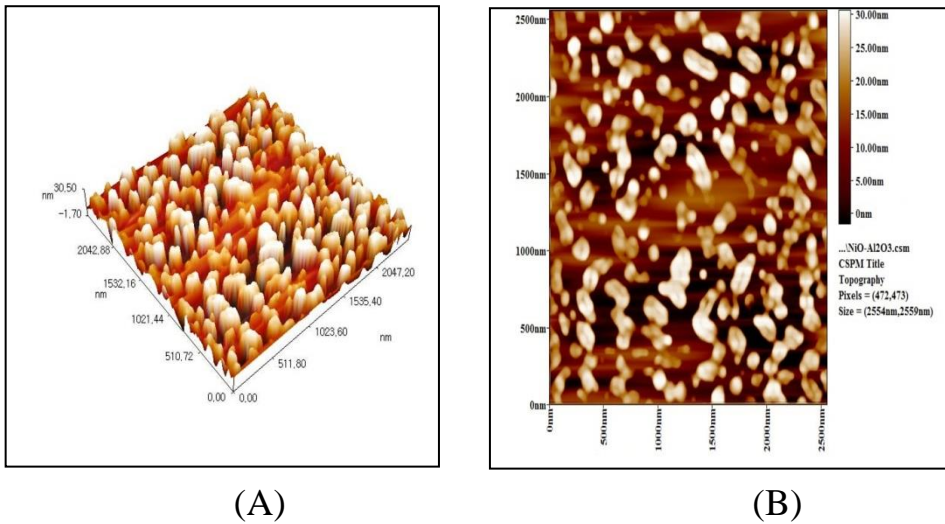


Figure (4.7): Granularity cumulating distribution of  $\gamma$ - $\text{Al}_2\text{O}_3$  nanoparticle.

#### 4.1.2.3. AFM of $\text{NiO}/\gamma$ - $\text{Al}_2\text{O}_3$ nano catalyst

The AFM analysis is used to provide information about the average grain size. Figures (4.8) show typical AFM images of the (prepared  $\text{NiO}/\gamma$ - $\text{Al}_2\text{O}_3$ ). It explains images of AFM for catalyst with (size = 2554, 2559 nm) and ability analytical (pixel = 472,473). Figure (4.8.A) is AFM images in three dimensions

(3D), it explain structure shape for grain, and Figure (4.8.B) is AFM images in two dimensions (2D), it found that average roughness is (8.05) nm and the root mean square (RMS) is (9.3) nm .



**Figure (4.8): AFM images of the NiO/ $\gamma$ -Al<sub>2</sub>O<sub>3</sub> nano catalyst.**

Table (4.6) and figure (4.7) explained the cumulating distribution and average diameter of prepared NiO/  $\gamma$ -Al<sub>2</sub>O<sub>3</sub> nanoparticle where the average diameter of nano NiO/  $\gamma$ -Al<sub>2</sub>O<sub>3</sub> is (69.37) nm ,and the particle size of less than 10 % of the total particles is 40 nm, less than 50 % is 70 nm and less than 90% is 85 nm.

Table (4.6): Granularity cumulating distribution and average diameter of NiO/  $\gamma$ -Al<sub>2</sub>O<sub>3</sub> nanocatalyst .

Diameter( nm)<	Volum e(%)	Cumulati on(%)	Diameter( nm)<	Volum e(%)	Cumulati on(%)	Diameter( nm)<	Volum e(%)	Cumulati on(%)
20.00	1.08	1.08	50.00	3.78	16.22	75.00	13.51	53.51
30.00	2.16	3.24	55.00	1.62	17.84	80.00	16.22	69.73
35.00	2.16	5.41	60.00	4.86	22.70	85.00	14.59	84.32
40.00	1.62	7.03	65.00	7.57	30.27	90.00	14.59	98.92
45.00	5.41	12.43	70.00	9.73	40.00	95.00	1.08	100.00

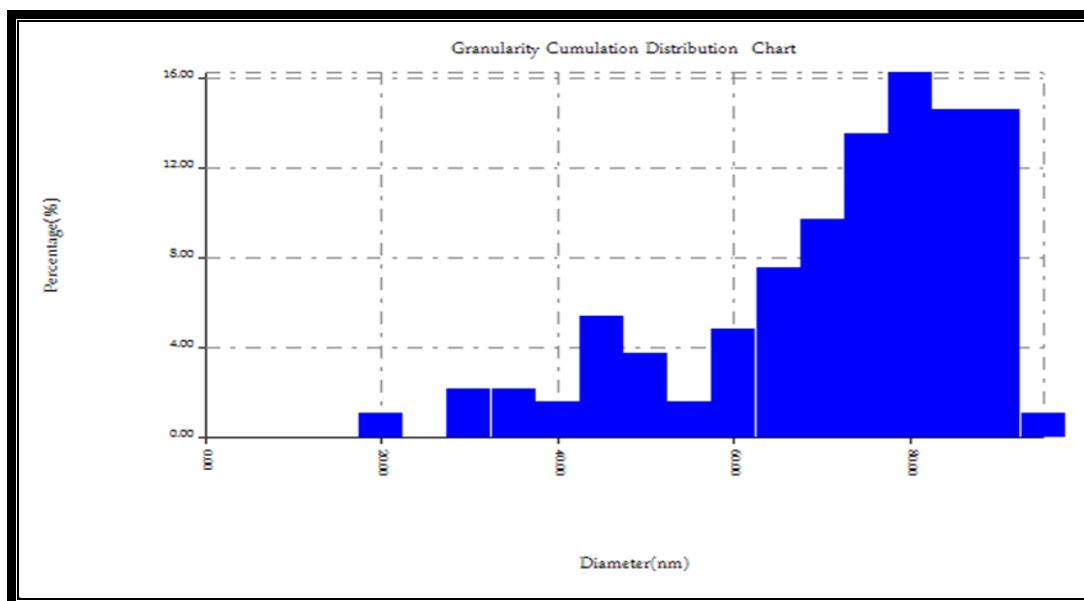


Figure (4.9): Granularity cumulating distribution of NiO/  $\gamma$ -Al<sub>2</sub>O<sub>3</sub> nano catalyst.

### 4.1.3. Fourier Transform Infrared ( FTIR ) Spectra Analysis

#### 4.1.3.1. FTIR spectrum of NiO nanoparticle

FTIR spectroscopy was used in the range of (400-4000)  $\text{cm}^{-1}$ . In figure (4.10) is the FTIR spectra of NiO nanoparticles, which show several significant absorption peaks. The broad absorption band in the region of 600–700  $\text{cm}^{-1}$  is assigned to Ni–O stretching vibration mode <sup>(124-26)</sup>. The broadness of the absorption band indicates that the NiO powders are nanocrystals. The size of samples used in this study was much less than the bulks form NiO, so that NiO nanoparticles had its IR peak of Ni–O stretching vibration and shifted to blue direction. Due to their quantum size effect and spherical nanostructures, the FTIR absorption of NiO nanoparticles is blue-shifted compared to that of the bulk form.

It can be seen also that the FTIR spectra of NiO nanoparticles showed broad absorption band centered at 3440  $\text{cm}^{-1}$  which is attributable to the band O–H stretching vibrations. The weak band near 1635  $\text{cm}^{-1}$  being assigned to H–O–H bending vibrations mode were due to the adsorption of water in air when FTIR sample disks were prepared in an open air. These observations provided the evidence to the effect of hydration in the structure. It implied the presence of

hydroxyl in the precursor, and the broad absorption at around  $767\text{ cm}^{-1}$  is assigned to the bond C=O stretching vibrations. The absorption bands in the region of  $1000\text{--}1500\text{ cm}^{-1}$  are assigned to the O–C=O symmetric and asymmetric stretching vibrations and the C–O stretching vibration <sup>(124-26)</sup>.

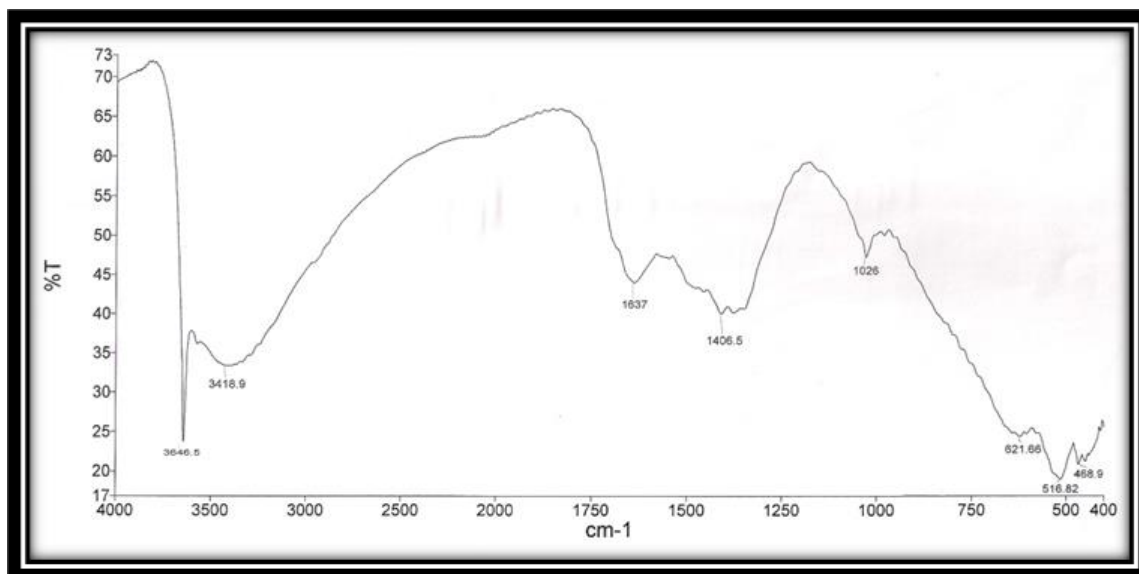


Figure (4.10) FTIR spectrum of prepared nickel (II) oxide nanoparticles.

#### 4.1.3.2. FTIR spectrum of $\gamma$ -Al<sub>2</sub>O<sub>3</sub> nanoparticle

FTIR technique was used in the range of (400-4000) cm<sup>-1</sup>. The spectrum in Figure (4.11) of the alumina powder ( $\gamma$ -Al<sub>2</sub>O<sub>3</sub>) show two broad bands. The absorption bands assigned to vibrations Al-O octahedral (590.15 cm<sup>-1</sup>) and tetrahedral (751.05 cm<sup>-1</sup>) represent aluminum ions. These values found in fingerprint region under 1000 cm<sup>-1</sup> arising from inter-atomic vibrations. The broad band of OH stretching appeared around 3510 cm<sup>-1</sup> reveals the presence of hydroxyl groups (O-H). These results are in agreement with the reported FTIR spectrum of  $\gamma$ -Al<sub>2</sub>O<sub>3</sub> <sup>(125)</sup>.

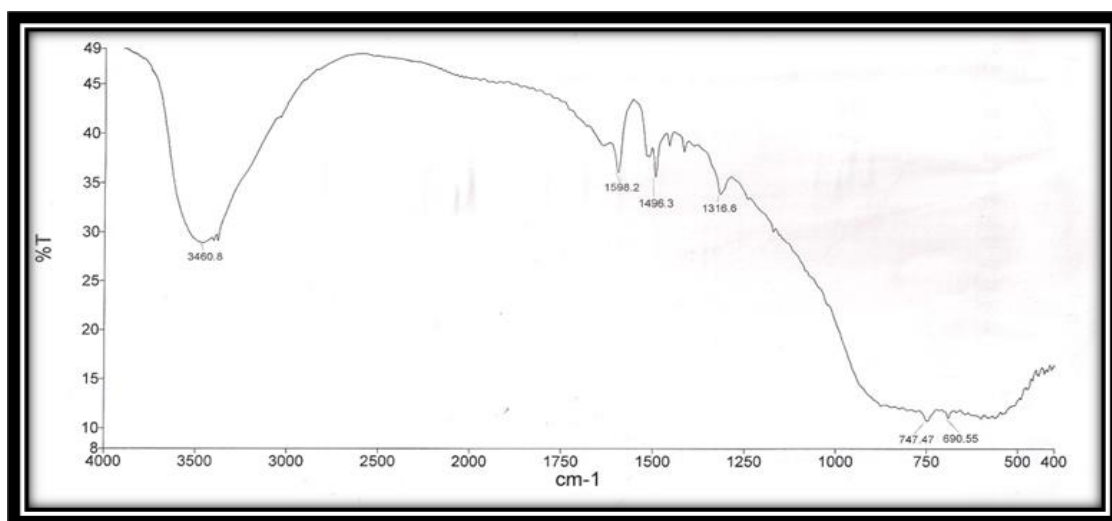


Figure (4.11): FTIR of prepared  $\gamma$ -Al<sub>2</sub>O<sub>3</sub> nanoparticle.

#### 4.1.3.3. FTIR spectrum of NiO/ $\gamma$ -Al<sub>2</sub>O<sub>3</sub> nano catalyst

The spectrum in Figure (4.12) of NiO/  $\gamma$ -Al<sub>2</sub>O<sub>3</sub> show two broad bands. The absorption bands assigned to vibrations Al-O (475.06cm<sup>-1</sup>) and tetrahedral (703.23 cm<sup>-1</sup>) represent aluminum ions. These values found in fingerprint region under 1000 cm<sup>-1</sup> arising from inter-atomic vibrations. The broad band of O-H stretching appeared around 3405.5 cm<sup>-1</sup> reveals the presence of hydroxyl groups (O-H). These results are in agreement with the FTIR spectrum of  $\gamma$ -Al<sub>2</sub>O<sub>3</sub> reported before <sup>(125)</sup>.

The broad absorption band in the region of 600–700 cm<sup>-1</sup> is assigned for Ni–O stretching vibration mode. Weak band near 1635 cm<sup>-1</sup> being assigned to H–O–H

bending vibrations mode were due to the adsorption of water in air when FTIR sample disks were prepared in an open air.

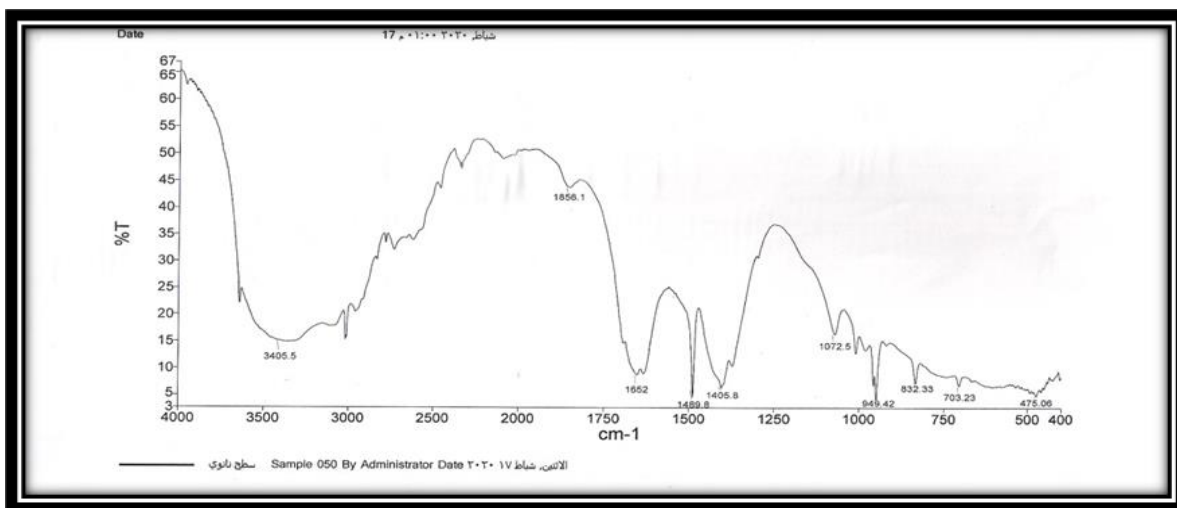


Figure (4.12): FTIR of prepared NiO/  $\gamma$ -Al<sub>2</sub>O<sub>3</sub> nano catalyst.

## 4.2. Adsorption of Cu(II) and Co(II) ions on NiO/ $\gamma$ -Al<sub>2</sub>O<sub>3</sub> nano catalyst.

### 4.2.1. Effect of contact time on adsorption

The effect of the contact time on the adsorption of Cu (II) and Co(II) ion on (NiO/  $\gamma$ -Al<sub>2</sub>O<sub>3</sub>) was studied at (10, 20, 30, 40 and 50) min at (298) K, concentration (100) mg/L of each metal ions. Tables (4.7) and (4.8) explain the change of the percentage removal with contact time of Cu (II) and Co (II) ions respectively. As seen from them that equilibrium time required for the adsorption of both ions on the (NiO/  $\gamma$ -Al<sub>2</sub>O<sub>3</sub>) are almost (50) min.

The effect of contact time on the adsorption of Cu (II) and Co(II) ions on (NiO/  $\gamma$ -Al<sub>2</sub>O<sub>3</sub>) surfaces are also explain in figures (4.13) and (4.14) where a decreasing in the percent removal at the beginning of contact time with both ions, followed by a gradual increase in the percentage removal of Cu <sup>+2</sup> and Cu<sup>+2</sup> ions for surfaces because the rapid initial rate increase followed by a slow rate at later period could be

due to availability of excess adsorption sites on the adsorbent <sup>(126)</sup>. The initial high adsorption rate might possibly be due to ion exchange followed by a slow chemical reaction of the metal ions active groups on the sample <sup>(127)</sup>, and the remaining vacant surface sites are difficult to be occupied due to repulsive force. The metal ions have to traverse further and deeper into the pores encountering much larger resistance <sup>(128)</sup>.

Table (4.7): Effect of contact time on the adsorption of Cu (II) ion by (NiO/  $\gamma$ -Al<sub>2</sub>O<sub>3</sub>) nano catalyst at 298 K

Time (min)	Cu(II)		
	C <sub>o</sub> (mg/L)	C <sub>t</sub> (mg/L)	R%
10	100	5.50	94.5
20	100	3.39	96.61
30	100	3.00	97
40	100	2.5	97.5
50	100	2.00	98



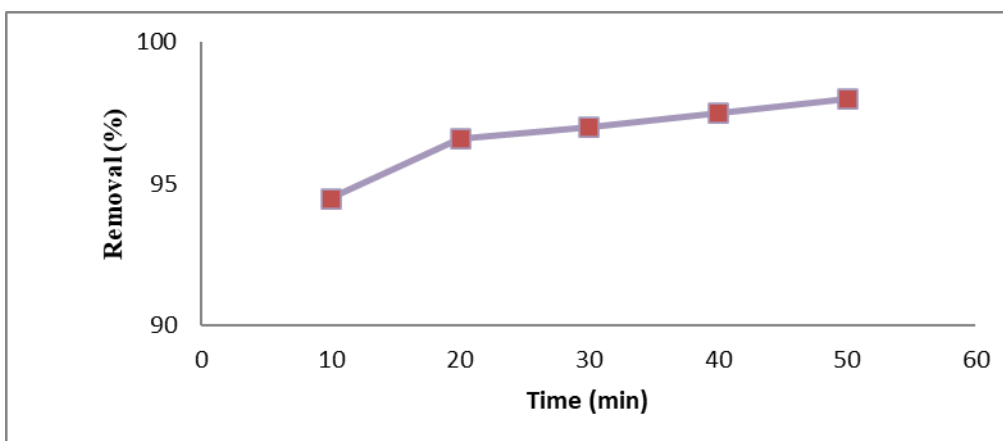


Figure (4.13): Effect of contact time on removal (%) of Cu (II) ion on NiO/ $\gamma$ -Al<sub>2</sub>O<sub>3</sub> nanocatalyst at 298 K.

Table (4.8): Effect of contact time on the adsorption of Co (II) ion by (NiO/  $\gamma$ -Al<sub>2</sub>O<sub>3</sub>) nanocatalyst at 298 K .

Time (min)	Co(II)		
	C <sub>0</sub> (mg/L)	C <sub>t</sub> (mg/L)	R%
10	100	9.95	90.05
20	100	9.23	90.77
30	100	8.1	91.9
40	100	7.89	92.11
50	100	4.87	95.13

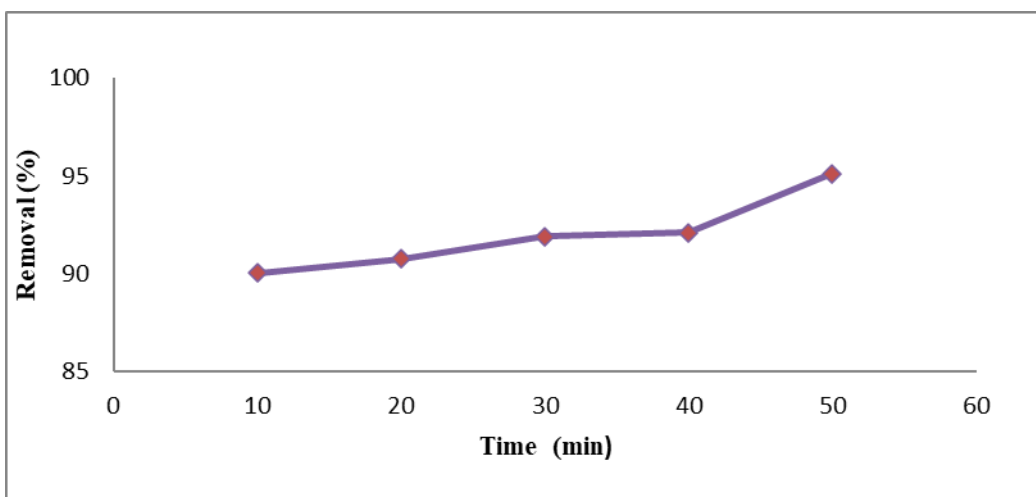


Figure (4.14): Effect of contact time on removal (%) of Co (II) ion on NiO/ $\gamma$ -Al<sub>2</sub>O<sub>3</sub> nano-catalyst at 298 K.

#### 4.2.2. Effect of adsorbent quantity on adsorption

The effect of the adsorbent quantity of Cu (II) and Co (II) ions removal on the (NiO/  $\gamma$ -Al<sub>2</sub>O<sub>3</sub>) surfaces, was studied using different quantity of the adsorbent (0.06, 0.08, 0.1, 0.12 and 0.15) g at (298) K, fixed concentration of Cu (II) and Co (II) ions (100) mg/L, contact time for (NiO/  $\gamma$ -Al<sub>2</sub>O<sub>3</sub>) are being (50) min for both ions.

The influence of adsorbent quantity on the uptake of the metals Cu (II) and Co (II) ions onto (NiO/  $\gamma$ -Al<sub>2</sub>O<sub>3</sub>) are shown in Tables (4.9) and (4.10), and in figures (4.15) and (4.16) with increasing the quantity of NiO/  $\gamma$ -Al<sub>2</sub>O<sub>3</sub> which prepared by Arundo Leaves Extract method, the metals removal will increases too, this means that the increase the amount of oxide nanoparticles increases the percentage removal for metals. The increase in the percentage removal can be explained by the increasing surface area.

Table (4.9): Effect of adsorbent quantity on the adsorption of Cu (II) ion by(NiO/  $\gamma$ - $\text{Al}_2\text{O}_3$ ) nano catalyst at 298 K.

Adsorbent quantity (g)	Cu(II)		
	$C_o$ (mg/L)	$C_t$ (mg/L)	R%
0.06	100	22.99	77.01
0.08	100	15.4	84.60
0.1	100	13.65	86.35
0.12	100	10.21	89.79
0.15	100	9.88	90.12

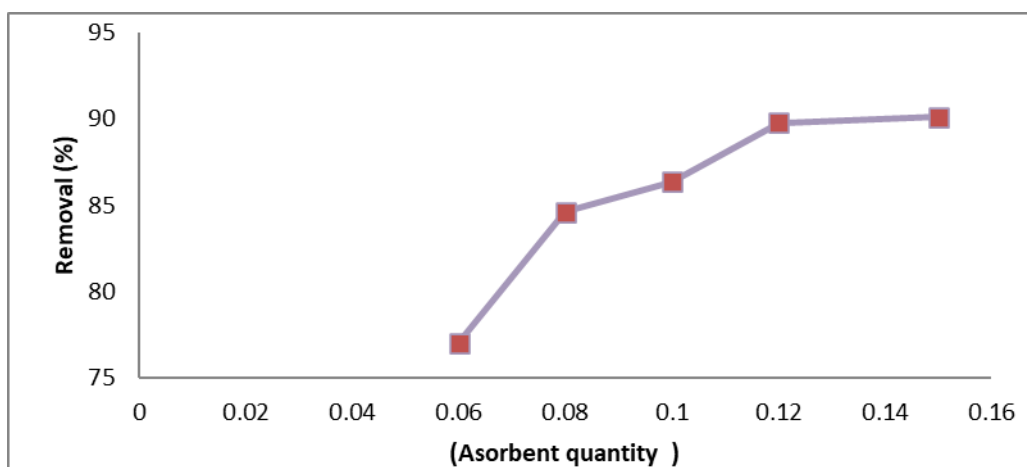


Figure (4.15): Effect of adsorbent quantity on removal (%) of Cu (II) ion on NiO/ $\gamma$ - $\text{Al}_2\text{O}_3$  nano catalyst at 298 K.

Table (4.10): Effect of adsorbent quantity on the adsorption of Co(II) ion by (NiO/ $\gamma$ -Al<sub>2</sub>O<sub>3</sub>) catalyst at 298 K.

Adsorbent quantity (g)	Co(II)		
	C <sub>o</sub> (mg/L)	C <sub>t</sub> (mg/L)	R%
0.06	100	31.85	68.15
0.08	100	29.6	70.40
0.1	100	20.1	79.90
0.12	100	14.05	85.95
0.15	100	9.18	90.82

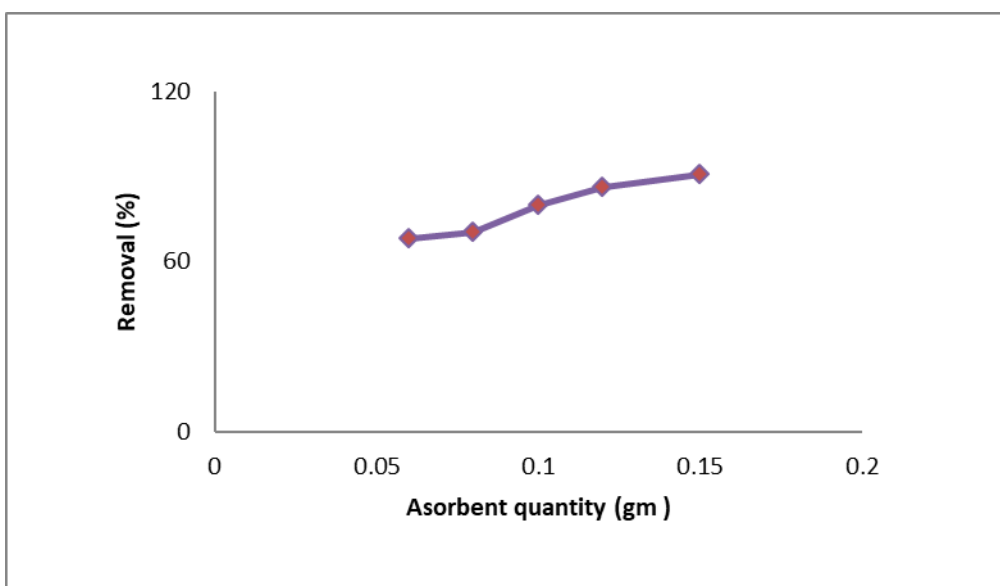


Figure (4.16): Effect of adsorbent quantity on removal (%) of Co (II) ion on NiO/ $\gamma$ -Al<sub>2</sub>O<sub>3</sub> nano-catalyst at 298 K.

### 4.2. 3. Effect of initial adsorbate concentration on adsorption

Adsorption of the metals Cu (II) and Co (II) ions from an aqueous solution on the NiO/ $\gamma$ -Al<sub>2</sub>O<sub>3</sub> was studied first at optimum conditions, using different initial concentration of aqueous solution of (50, 100, 150, 200 and 250) mg/L for each metal ions.

The results shown in Tables (4.11) and (4.12) and Figures (4.17)and (4.18) for Cu (II) and Co (II) ions respectively .The impact of the initial concentration indicate decrease in the removal when increasing the initial concentration of Cu (II) and Co (II) ions on NiO/ $\gamma$ -Al<sub>2</sub>O<sub>3</sub>. This decreasing in the percentage of the removal at higher concentration could be attributed to the a lot of number of active sites of the nanoparticles adsorbents, and because of the small nanoparticles size and high surface area that contains a lot of active adsorption sites which will be available for adsorption to take place<sup>(129)</sup> .

Table (4.11): Effect of initial concentration on the adsorption of Cu (II) on NiO/ $\gamma$ -Al<sub>2</sub>O<sub>3</sub> nano catalyst at 298 K.

Initial concentration(mg/L)	Cu(II)	
	C <sub>t</sub> (mg/L)	R%
50	3.275	93.45
100	8.14	91.86
150	22.14	85.24
200	35.6	82.20
250	54.625	78.15

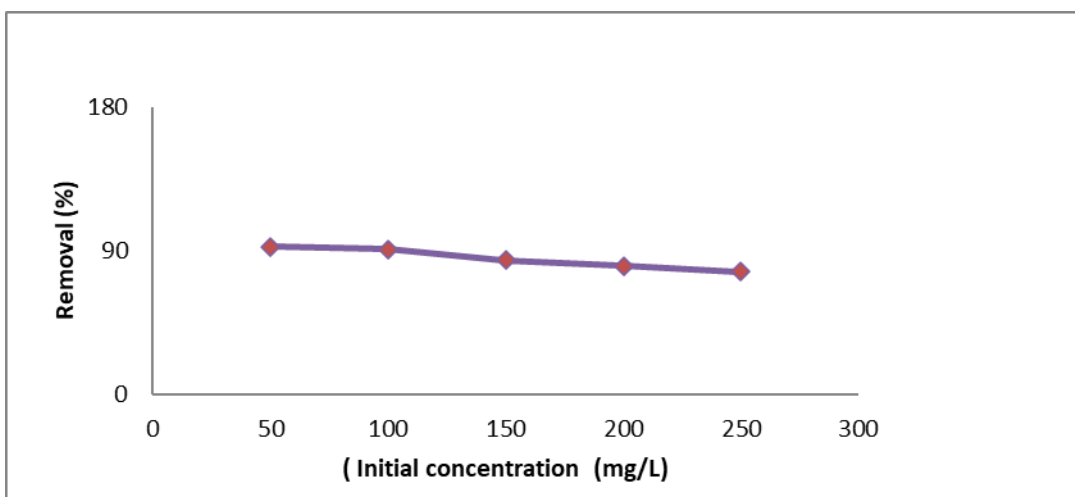


Figure (4.17): Effect of initial concentration on removal (%) of Cu (II) ion on NiO/ $\gamma$ -Al<sub>2</sub>O<sub>3</sub> nano catalyst at 298 K.

Table (4.12): Effect of initial concentration on the adsorption of Co(II) on NiO/ $\gamma$ -Al<sub>2</sub>O<sub>3</sub> at 298 K.

Initial concentration(mg/L)	Co(II)	
	C <sub>t</sub> (mg/L)	R%
50	1.74	96.52
100	6.98	93.02
150	16.29	89.14
200	26.42	86.79
250	49.375	80.25

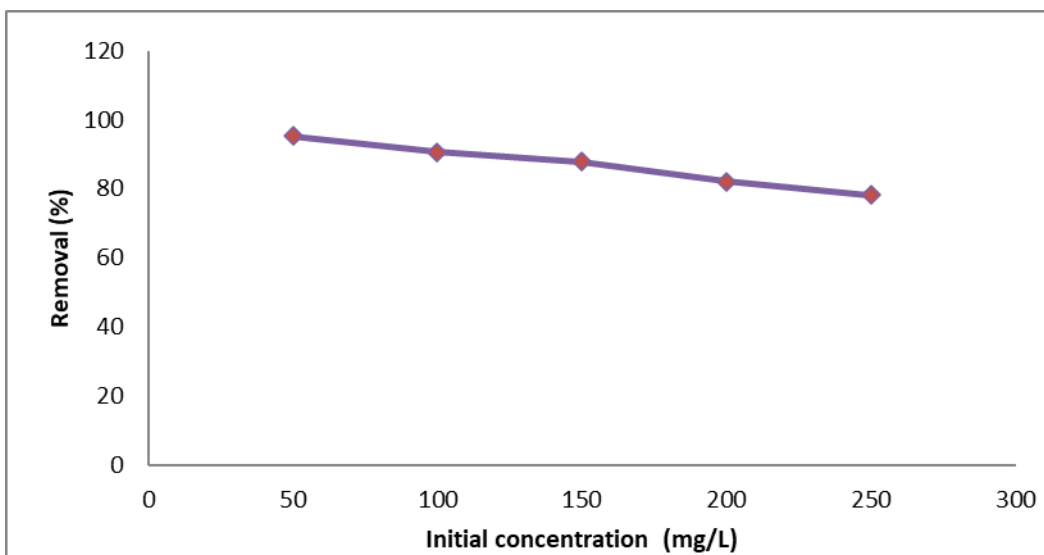


Figure (4.18): Effect of initial concentration on removal (%) of Co(II) ion on NiO/ $\gamma$ -Al<sub>2</sub>O<sub>3</sub> catalyst at 298 K.

#### 4.2.4. Effect of temperature on adsorption

The effect of temperature on the extent of adsorption of the Cu(II) and Co(II) ions on NiO/ $\gamma$ -Al<sub>2</sub>O<sub>3</sub> has been studied at five different temperatures (293, 303, 313, 323 and 333) K, initial concentration (100) mg/L of each metal ions, quantity of adsorbent (0.1) g, the contact time was constant at (50) min. The experimental data and the general shapes of the Cu(II) and Co(II) adsorption on NiO/ $\gamma$ -Al<sub>2</sub>O<sub>3</sub> are given in Tables (4.13) and (4.14), and Figures (4.19) and (4.20) of Cu(II) and Co (II) ions respectively.

The data shows that the percentage removal decrease with increase in temperature. From these data it can be observed that adsorption are exothermic in all cases, the reduction in the rate of adsorption with increase in the temperature, may be backing weakening of interaction force between the active sites of the adsorption surface and the metals ions<sup>(130)</sup>.

Table (4.13): Effect of temperature on the adsorption of Cu (II) on NiO/ $\gamma$ Al<sub>2</sub>O<sub>3</sub> nano catalyst.

Temperature(K)	Cu(II)		
	C <sub>0</sub> (mg/L)	C <sub>t</sub> (mg/L)	R%
293	100	0.6	99.4
303	100	5.9	94.10
313	100	10.1	89.90
323	100	15.99	84.01
333	100	21	79

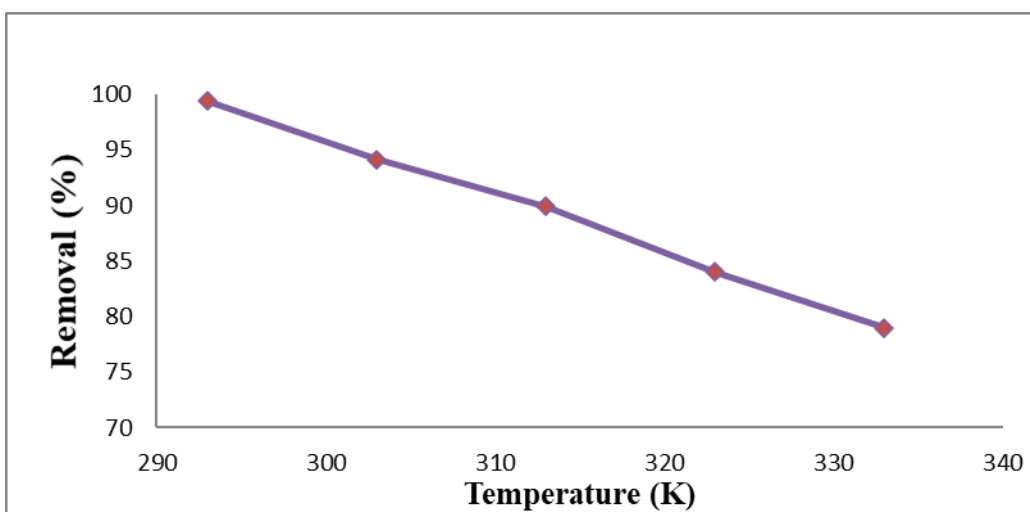
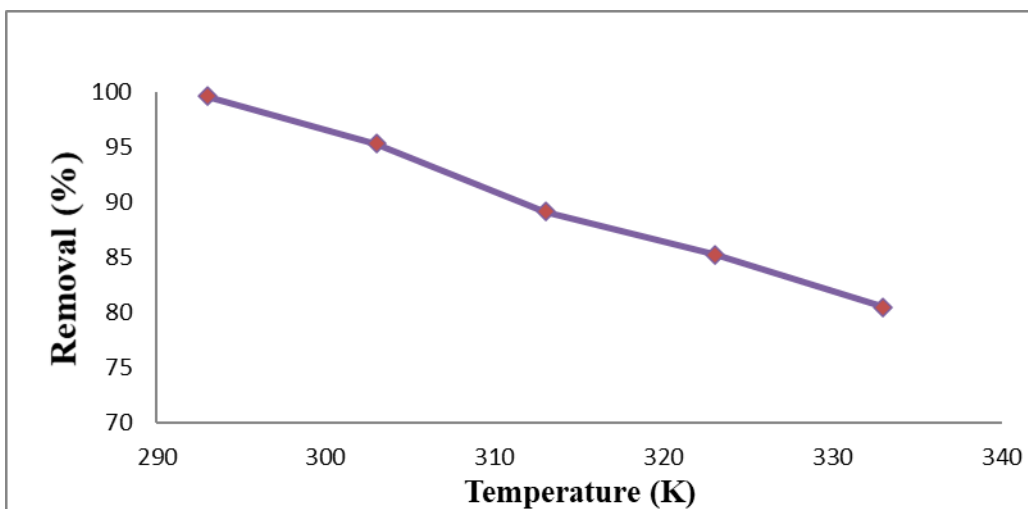


Figure (4.19): Effect of temperature on removal (%) of Cu (II) ion on NiO/ $\gamma$ -Al<sub>2</sub>O<sub>3</sub> nano catalyst.



Table (4.14): Effect of temperature on the adsorption of Co(II) on NiO/ $\gamma$ -Al<sub>2</sub>O<sub>3</sub>.

Temperature(K)	Co(II)		
	C <sub>o</sub> (mg/L)	C <sub>t</sub> (mg/L)	R%
293	100	0.38	99.62
303	100	4.65	95.35
313	100	10.84	89.16
323	100	14.75	85.25
333	100	19.51	80.49

Figure (4.20): Effect of temperature on removal (%) of Co (II) ion on NiO/  $\gamma$ -Al<sub>2</sub>O<sub>3</sub> nano catalyst.

### 4.3. Kinetics Studies of Adsorption Process for Cu<sup>+2</sup> and Co<sup>+2</sup> ions

The kinetic study of adsorption was carried out of each ions on NiO/ $\gamma$ -Al<sub>2</sub>O<sub>3</sub> catalysts by using experimental conditions of initial concentration (100 mg/L), different temperatures (308, 313, 318 and 323) K, 150 rpm and intervals times (5, 15,

25,35 and 45) minutes. The value of  $C_e$  is the concentration of metal ion after adsorption at any time (mg /L),  $q_t$  is the amount adsorbed at any time, (mg/g),  $q_e$  which is the amount adsorbed at equilibrium (mg/g),  $q_e - q_t$ ,  $\ln(q_e - q_t)$ ,  $t$  which is the time (min),  $t^{1/2}$  the square root of the time ( $\text{min}^{1/2}$ ), are given in tables (4.15), (4.16), (4.17) ,(4.18)of Cu(II) and (4.19), (4.20), (4.21) and (4.22) of Co(II) for the adsorption respectively .

These data was applied for four model expressed by its equations to calculate the value of  $k$  as shown in figures (4.21),(4.22),(4.23),(4.24) of Cu(II) and(4.25),(4.26),(4.27),(4.28) of Co(II) for the adsorption of Cu (II) and Co(II) ions on NiO/ $\gamma$ -Al<sub>2</sub>O<sub>3</sub> respectively.

Table (4.15)The adsorption data for Cu (II) ions on removal with (NiO/ $\gamma$ -Al<sub>2</sub>O<sub>3</sub>) nano catalyst at 308K.

	Time	$\sqrt{t}$	$C_e$	$Q_t$	$Q_e - Q_t$	$\ln (Q_e - Q_t)$	$\ln t$	$t/Q_t$
	5	2.236	8.514	45.743	3.1965	1.162	1.6094	0.1093
	15	3.8729	7.619	46.1905	2.749	1.0112	2.708	0.3247
308 K	25	5	5.483	47.2585	1.681	0.5193	3.2188	0.529
	35	5.916	5.001	47.4995	1.44	0.3646	3.5553	0.7368
	45	6.7082	2.121	48.9395	0		3.8066	0.9195

Table(4.16)The adsorption data for Cu (II) ions on removal with (NiO/ $\gamma$ -Al<sub>2</sub>O<sub>3</sub>) nano catalyst at 313K.

	Time	$\sqrt{t}$	C <sub>e</sub>	Q <sub>t</sub>	Q <sub>e</sub> - Q <sub>t</sub>	ln (Q <sub>e</sub> - Q <sub>t</sub> )	ln t	t/Q <sub>t</sub>
	5	2.236	10.789	44.6055	3.5165	1.2574	1.6094	0.112
	15	3.8729	8.556	45.722	2.4	0.8754	2.708	0.328
313 K	25	5	7.405	46.2975	1.8245	0.6013	3.2188	0.5399
	35	5.916	5.78	47.11	1.012	0.0119	3.5553	0.7429
	45	6.7082	3.756	48.122	0		3.8066	0.9351

Table (4.17)The adsorption data for Cu (II) ions removal with (NiO/ $\gamma$ -Al<sub>2</sub>O<sub>3</sub>)nano catalyst at 318K.

	Time	$\sqrt{t}$	C <sub>e</sub>	Q <sub>t</sub>	Q <sub>e</sub> - Q <sub>t</sub>	ln (Q <sub>e</sub> - Q <sub>t</sub> )	ln t	t/Q <sub>t</sub>
	5	2.236	11.925	44.0375	3.9565	1.3753	1.6094	0.1135
	15	3.8729	9.476	45.262	2.732	1.005	2.708	0.331
318 K	25	5	8.971	45.5145	2.4795	0.908	3.2188	0.5492
	35	5.916	6.247	46.8765	1.1175	0.111	3.5553	0.7466
	45	6.7082	4.012	47.994	0		3.8066	0.9376

Table(4.18)The adsorption data for Cu (II) ions on removal with (NiO/ $\gamma$ -Al<sub>2</sub>O<sub>3</sub>) nano catalyst at 323K.

	Time	$\sqrt{t}$	C <sub>e</sub>	Q <sub>t</sub>	Q <sub>e</sub> - Q <sub>t</sub>	ln (Q <sub>e</sub> - Q <sub>t</sub> )	ln t	t/Q <sub>t</sub>
	5	2.236	14.398	42.801	3.9215	1.3664	1.6094	0.1168
	15	3.8729	10.986	44.507	2.2155	0.7954	2.708	0.337
323 K	25	5	9.99	45.005	1.7175	0.5408	3.2188	0.5554
	35	5.916	8.998	45.501	1.2215	0.20007	3.5553	0.7692
	45	6.7082	6.555	46.7225	0		3.8066	0.9631

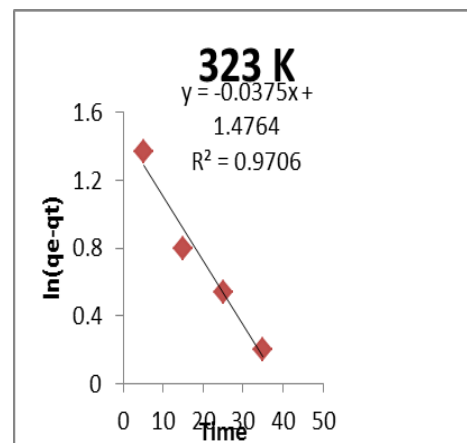
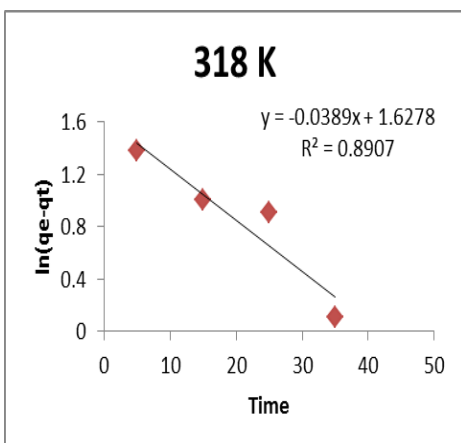
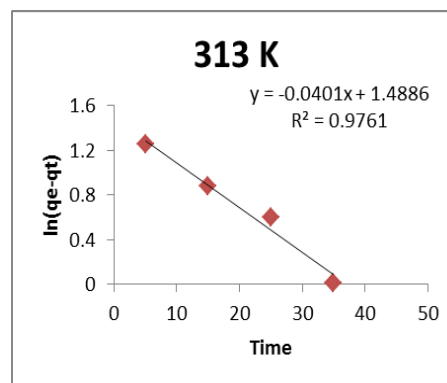
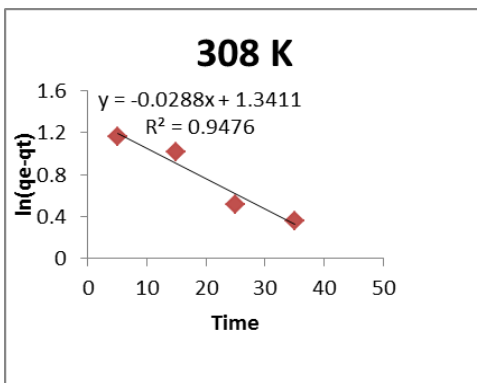


Figure (4.21) The Pseudo First – Order Kinetic Model for Cu<sup>+2</sup> ions adsorption on NiO/ $\gamma$ -Al<sub>2</sub>O<sub>3</sub> nano catalyst

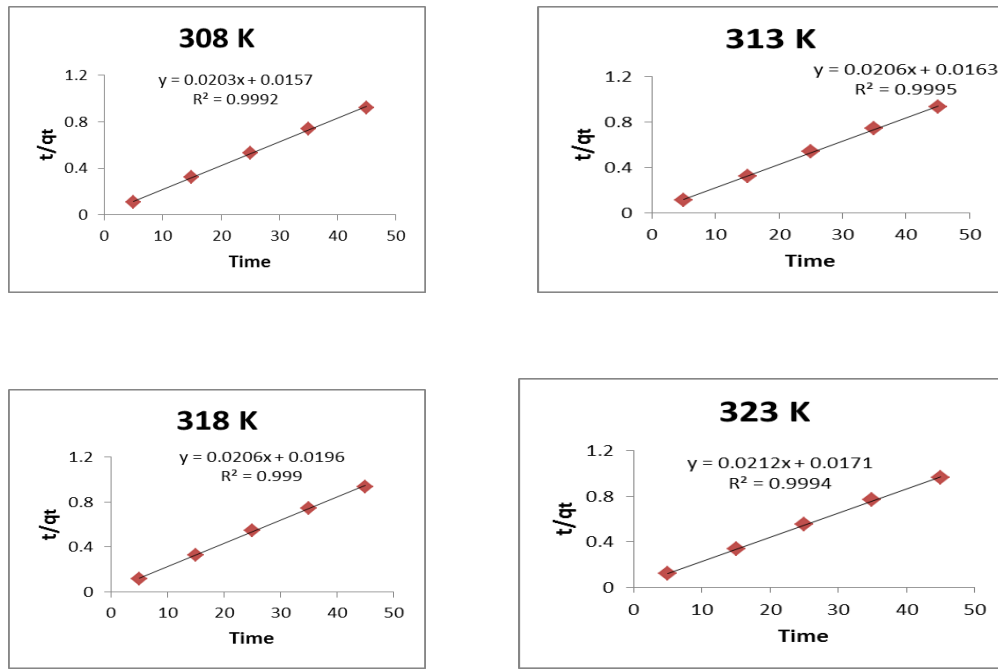


Figure (4.22) The Pseudo Second – Order Kinetic Model for Cu<sup>+2</sup> ions adsorption on NiO/γ-Al<sub>2</sub>O<sub>3</sub> nano catalyst

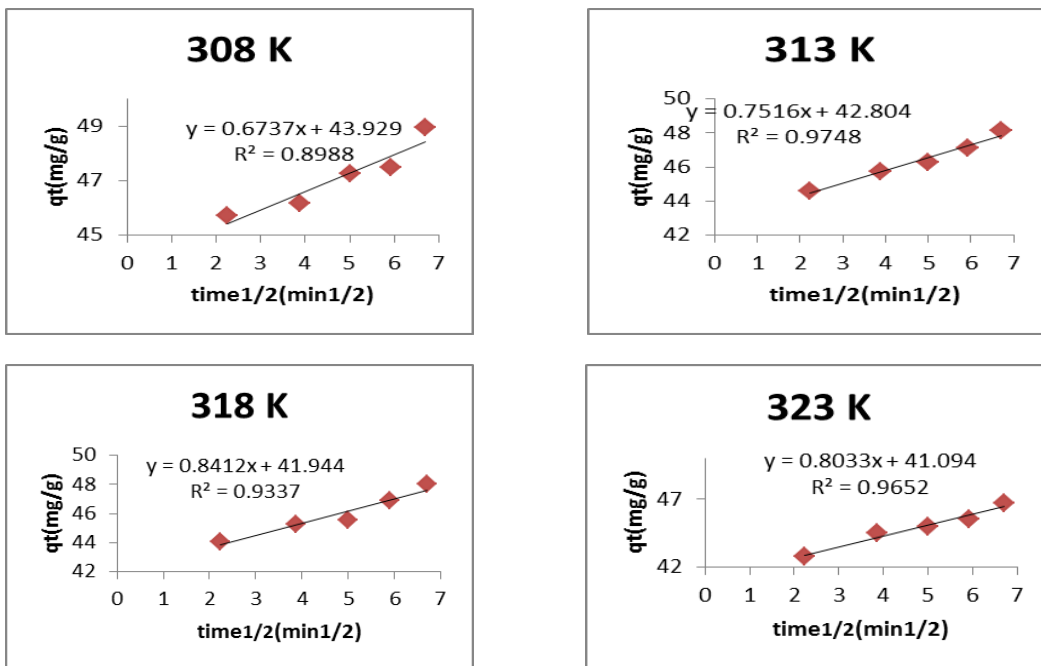


Figure (4.23) The Intraparticle Diffusion Model for Cu<sup>+2</sup> ions adsorption on NiO/γ-Al<sub>2</sub>O<sub>3</sub> nano catalyst

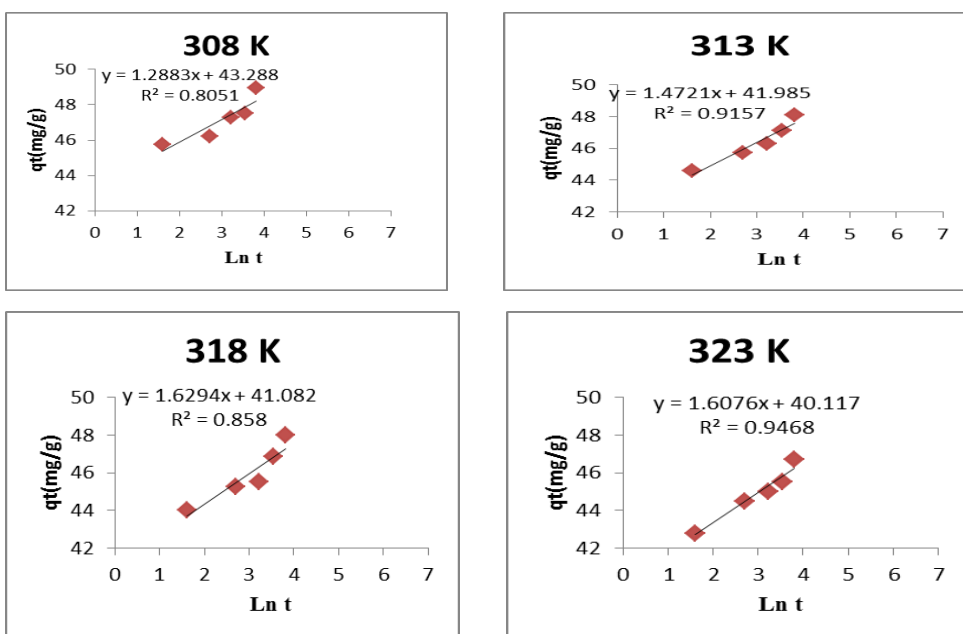


Figure (4.24) The Elovich Model for Cu<sup>2+</sup> ion adsorption on NiO/γ-Al<sub>2</sub>O<sub>3</sub> nano catalyst

Table (4.19) The adsorption data for Co (II) ions removal with (NiO/γ-Al<sub>2</sub>O<sub>3</sub>) nano catalyst at 308K

	Time	$\sqrt{t}$	C <sub>e</sub>	Q <sub>t</sub>	Q <sub>e</sub> - Q <sub>t</sub>	ln (Q <sub>e</sub> - Q <sub>t</sub> )	ln t	t/Q <sub>t</sub>
	5	2.236	8.7	45.65	3.295	1.1924	1.6094	0.1095
	15	3.8729	7.025	46.4875	2.4575	0.8991	2.708	0.3226
308 K	25	5	5.91	47.045	1.9	0.6418	3.2188	0.5314
	35	5.916	4.2	47.9	1.045	0.044	3.5553	0.7231
	45	6.7082	2.11	48.945	0		3.8066	0.9193

Table(4.20)The adsorption data for Co (II) ions removal with (NiO/ $\gamma$ -Al<sub>2</sub>O<sub>3</sub>) nano catalyst at 313K.

	Time	$\sqrt{t}$	C <sub>e</sub>	Q <sub>t</sub>	Q <sub>e</sub> -Q <sub>t</sub>	ln (Q <sub>e</sub> - Q <sub>t</sub> )	ln t	t/Q <sub>t</sub>
	5	2.236	12.841	43.5795	3.972	1.3792	1.6094	0.1147
	15	3.8729	10.64	44.68	2.8715	1.0548	2.708	0.3357
313 k	25	5	9.082	45.459	2.0925	0.7383	3.2188	0.5499
	35	5.916	7.4	46.3	1.2515	0.2241	3.5553	0.7559
	45	6.7082	4.897	47.5515	0		3.8066	0.9463

Table(4.21)The adsorption data for Co (II) ions removal with (NiO/ $\gamma$ -Al<sub>2</sub>O<sub>3</sub>) nano catalyst at 318K.

	Time	$\sqrt{t}$	C <sub>e</sub>	Q <sub>t</sub>	Q <sub>e</sub> -Q <sub>t</sub>	ln (Q <sub>e</sub> - Q <sub>t</sub> )	ln t	t/Q <sub>t</sub>
	5	2.236	13.66	43.17	3.5195	1.2583	1.6094	0.1158
	15	3.8729	11.7	44.15	2.5395	0.9319	2.708	0.3397
318 K	25	5	10.934	44.533	2.1565	0.7684	3.2188	0.5613
	35	5.916	8.998	45.501	1.1885	0.1726	3.5553	0.7692
	45	6.7082	6.621	46.6895	0		3.8066	0.9638

Table(4.22)The adsorption data for Co (II) ion removal with (NiO/ $\gamma$ -Al<sub>2</sub>O<sub>3</sub>) nano catalyst at 323K.

	Time	$\sqrt{t}$	C <sub>e</sub>	Q <sub>t</sub>	Q <sub>e</sub> -Q <sub>t</sub>	ln (Q <sub>e</sub> -Q <sub>t</sub> )	ln t	t/Q <sub>t</sub>
	5	2.236	13.97	43.015	3.215	1.1678	1.6094	0.1162
	15	3.8729	12.908	43.546	2.684	0.9873	2.708	0.3444
323 K	25	5	11.8	44.1	2.13	0.7561	3.2188	0.5668
	35	5.916	9.746	45.127	1.103	0.098	3.5553	0.7755
	45	6.7082	7.54	46.23	0		3.8066	0.9733

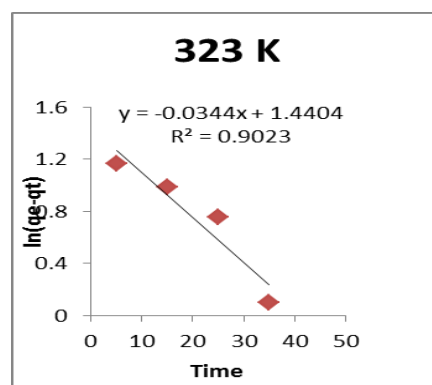
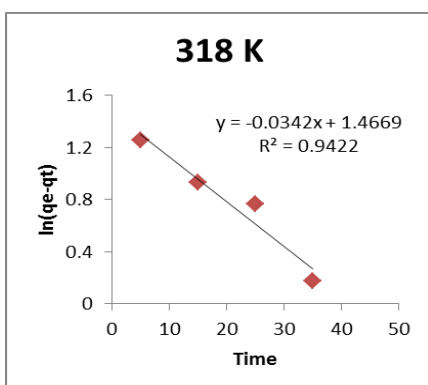
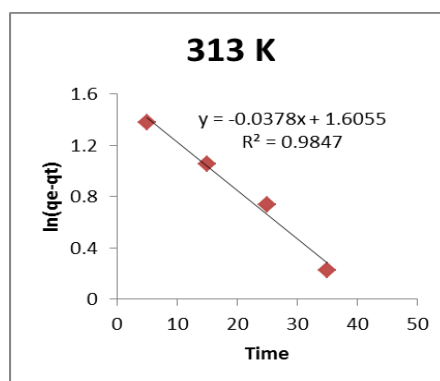
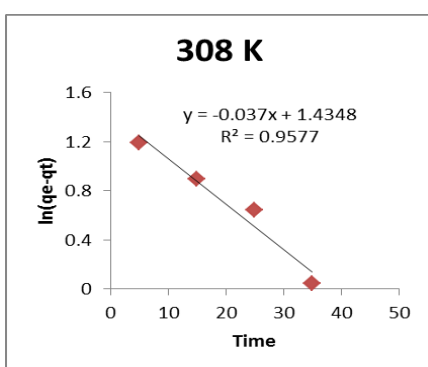


Figure (4.25) The Pseudo First – Order Kinetic Model for Co<sup>+2</sup> ion adsorption on NiO/ $\gamma$ -Al<sub>2</sub>O<sub>3</sub> nano catalyst



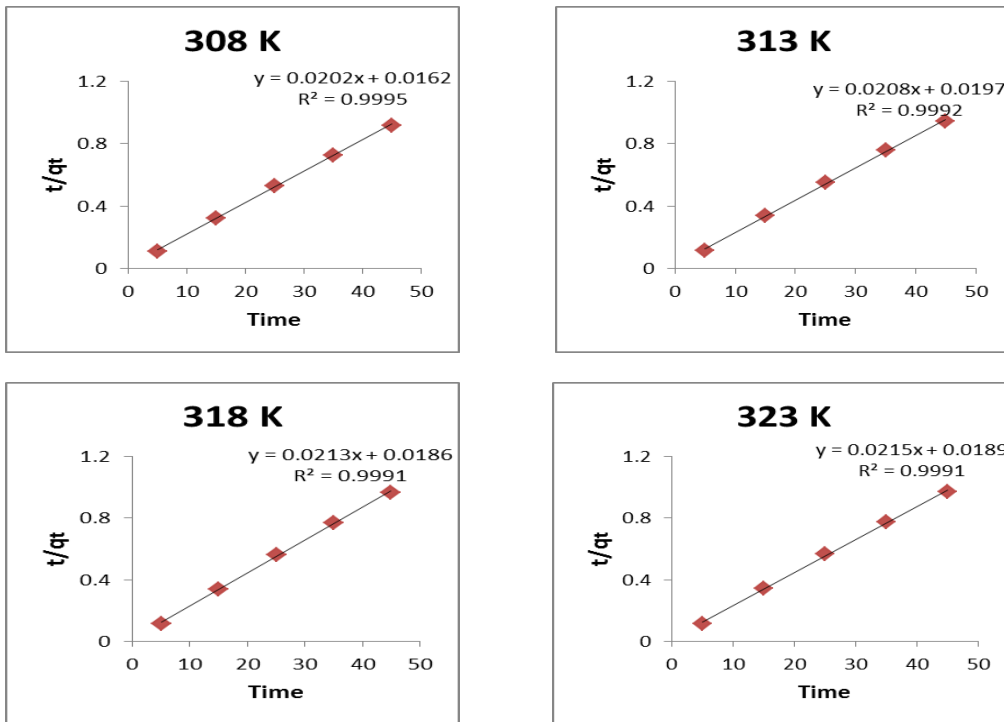


Figure (4.26) The Pseudo Second – Order Kinetic Model for  $Co^{+2}$  ions adsorption on  $NiO/\gamma-Al_2O_3$  nano catalyst

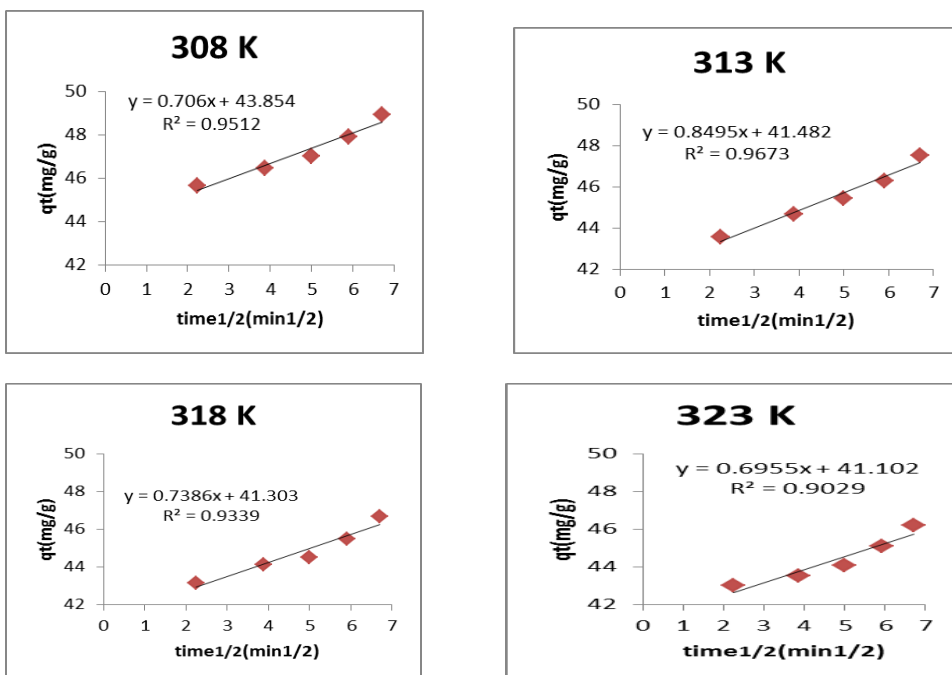


Figure (4.27) The Intraparticle Diffusion Model for  $Co^{+2}$  ions adsorption on  $NiO/\gamma-Al_2O_3$  nano catalyst.

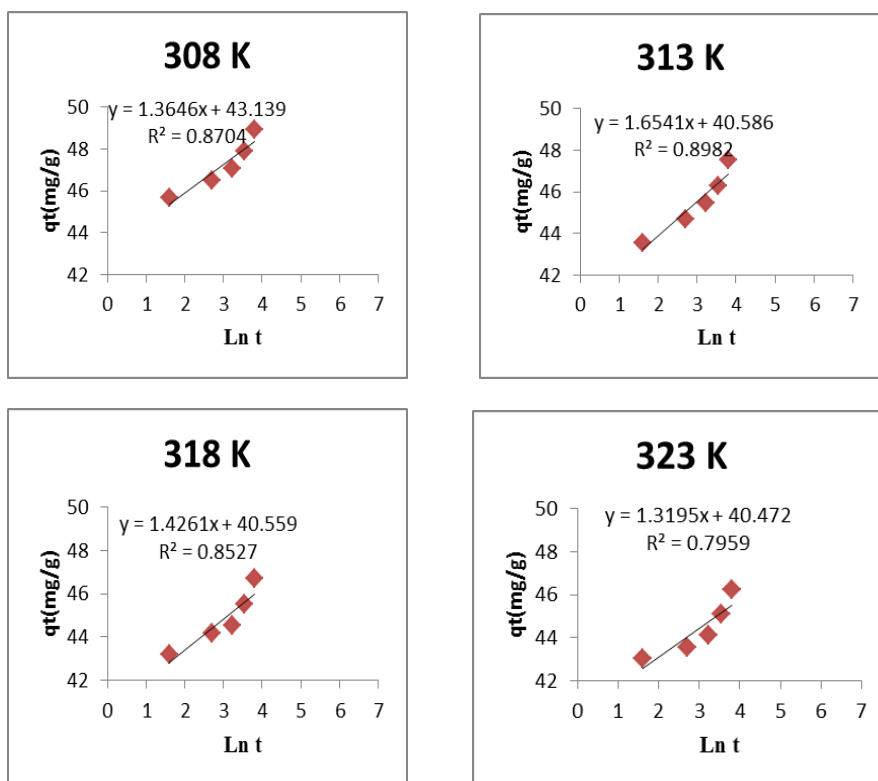


Figure (4.28) The Elovich Model for  $\text{Co}^{2+}$  ion adsorption on  $\text{NiO}/\gamma\text{-Al}_2\text{O}_3$  nano catalyst.

The calculated values of  $k_1$ ,  $k_2$ ,  $k_D$  and  $k_{\text{elovich}}$  with their correlation coefficient of adsorption for  $\text{Cu(II)}$  and  $\text{Co(II)}$  ions on  $\text{NiO}/\gamma\text{-Al}_2\text{O}_3$  adsorbents are given in tables (4.23) and (4.24). The results show the correlation coefficient of pseudo-second order is higher than the pseudo-first-order and intraparticle diffusion models and elovich model catalysts.

**Table (4.23): Adsorption kinetics constants for  $\text{Cu}^{+2}$  ions adsorption on NiO/ $\gamma$ - $\text{Al}_2\text{O}_3$  nano catalyst.**

T(K)	$q_e$ (mg/g)	Pseudo-first order		Pseudo-second order		Intraparticle diffusion		Elovich model	
		$K_1 \text{ min}^{-1}$	$R^2$	$K_2$ g/mg.min	$R^2$	$K_D$ mg/g.min <sup>-1</sup>	$R^2$	$k_{\text{elovich}}$ mg/g.s	$R^2$
308	48.9395	-0.0288	0.9476	0.0262	0.9992	0.6736	0.8988	50369	0.8051
313	48.1220	-0.0401	0.9761	0.02600	0.9995	0.7516	0.9748	35822	0.9157
318	47.994	-0.0389	0.8907	0.02169	0.999	0.8411	0.9337	14501	0.858
323	46.7225	-0.0375	0.9706	0.0264	0.9994	0.8032	0.9652	11042	0.9468

**Table (4.24): Adsorption kinetics constants for  $\text{Co}^{+2}$  ions adsorption on NiO/ $\gamma$ - $\text{Al}_2\text{O}_3$  nano catalyst.**

T(K)	$q_e$ (mg/g)	Pseudo-first order		Pseudo-second order		Intraparticle diffusion		Elovich model	
		$K_1 \text{ min}^{-1}$	$R^2$	$K_2$ g/mg.min	$R^2$	$K_D$ mg/g.min <sup>-1</sup>	$R^2$	$k_{\text{elovich}}$ mg/g.s	$R^2$
308	48.9450	-0.0370	0.9577	0.0252	0.9995	0.7059	0.9512	73132	0.8704
313	47.5515	-0.0378	0.9847	0.0220	0.9992	0.8494	0.9673	74733	0.8982
318	46.6895	-0.0342	0.9422	0.0243	0.9991	0.7385	0.9339	32029	0.8527
323	46.2300	-0.0344	0.9023	0.02433	0.9991	0.6955	0.9029	27612	0.7959

#### 4.4. Thermodynamic study of adsorption for NiO/ $\gamma$ -Al<sub>2</sub>O<sub>3</sub> nanocatalyst

The effect of temperature on removal of Cu<sup>+2</sup> and Co<sup>+2</sup> ions by NiO/ $\gamma$ -Al<sub>2</sub>O<sub>3</sub> at different temperature (293, 303, 313, 323 and 333) K was investigated. This study used for evaluation of the basic thermodynamic function change of free energy  $\Delta G$ , enthalpy  $\Delta H$ , and entropy  $\Delta S$  of adsorption processes.

Equilibrium of adsorption constant,  $K$  is explained thermodynamically by Van 't Hoff equation below:

$$\ln K = -\frac{\Delta H}{R} \left(\frac{1}{T}\right) + \frac{\Delta S}{R} \dots\dots\dots (4.1)$$

The equilibrium constant,  $K$  were calculated at any different temperature by equation below<sup>(131)</sup>:

$$k = \frac{Q_e \times m(g)}{C_e \times V(L)} \dots\dots\dots (4.2)$$

Where:

**Q<sub>e</sub>**: The adsorption capacity of metals ion, (**mg/g**).

**m**: The quantity of NiO/ $\gamma$ -Al<sub>2</sub>O<sub>3</sub> catalysts, (**g**).

**C<sub>e</sub>**: The concentration at equilibrium after removal Cu (II) and Co(II), (**mg/L**).

**V**: Volume of aqueous solution containing Cu (II) and Co (II) (**L**).

Table (4.25) illustrates values of ( $k$ ) for adsorption of Cu (II) and Co(II), ions with NiO/ $\gamma$ Al<sub>2</sub>O<sub>3</sub>, catalysts at different temperatures.

The  $\Delta G^\circ$  Gibbs free energy change can be calculated from relationship<sup>(79,132)</sup>:

$$\Delta G^\circ = -RT \ln k \dots\dots\dots (4.3)$$

Which:

$\Delta G^\circ$  is The standard free energy change, (**kJ/mole**),

**R** is the gas constant, (**8.314 kJ/mol.K**),

**T** is the absolute temperature, (**K**)

and **k** is the equilibrium constant .

Finally, the values of ( $\Delta H$ ) and ( $\Delta S$ ) can be calculated from the slope and intercept of plot (**lnk**) versus ( $1/T$ )<sup>(90,133)</sup> as explained by equations:

$$\text{Slope} = - \Delta H/R \dots\dots (4.4)$$

$$\text{Intercept} = \Delta S /R \dots\dots (4.5)$$

Figures (4.29) and (4.30) shows the Van 't Hoff plot for adsorption of NiO/ $\gamma$ -Al<sub>2</sub>O<sub>3</sub>, and table (4.27) display the thermodynamic value of Cu(II) and Co(II) ions removal on the adsorbent.

Table (4.25): Effect of temperature on equilibrium constant for the adsorption of Cu(II) ions on NiO/ $\gamma$ -Al<sub>2</sub>O<sub>3</sub> nano catalyst.

<b>T(K)</b>	<b>1/T(K<sup>-1</sup>)</b>	<b>C<sub>e</sub>(mg/L)</b>	<b>Q<sub>e</sub>(mg/g)</b>	<b>K</b>	<b>ln k</b>
<b>293</b>	<b>0.003355</b>	<b>0.6</b>	<b>49.7</b>	<b>165.6666</b>	<b>5.1099</b>
<b>303</b>	<b>0.0033</b>	<b>5.9</b>	<b>47.05</b>	<b>15.9491</b>	<b>2.7694</b>
<b>313</b>	<b>0.003194</b>	<b>10.1</b>	<b>44.95</b>	<b>8.9009</b>	<b>2.1861</b>
<b>323</b>	<b>0.003095</b>	<b>15.99</b>	<b>42.005</b>	<b>5.2539</b>	<b>1.6589</b>
<b>333</b>	<b>0.003003</b>	<b>21</b>	<b>39.5</b>	<b>3.7619</b>	<b>1.3249</b>

Table (4.26): Effect of temperature on equilibrium constant for the adsorption of Co(II) ions on NiO/ $\gamma$ -Al<sub>2</sub>O<sub>3</sub> nano catalyst.

T(K)	1/T(K <sup>-1</sup> )	C <sub>e</sub> (mg/)	Q <sub>e</sub> (mg/g)	K	ln k
293	0.003355	0.38	49.81	262.1578	5.5689
303	0.0033	4.65	47.675	20.5053	3.0206
313	0.003194	10.84	44.58	8.225	2.1071
323	0.003095	14.75	42.625	5.7796	1.7543
333	0.003003	19.51	40.245	4.1255	1.4171

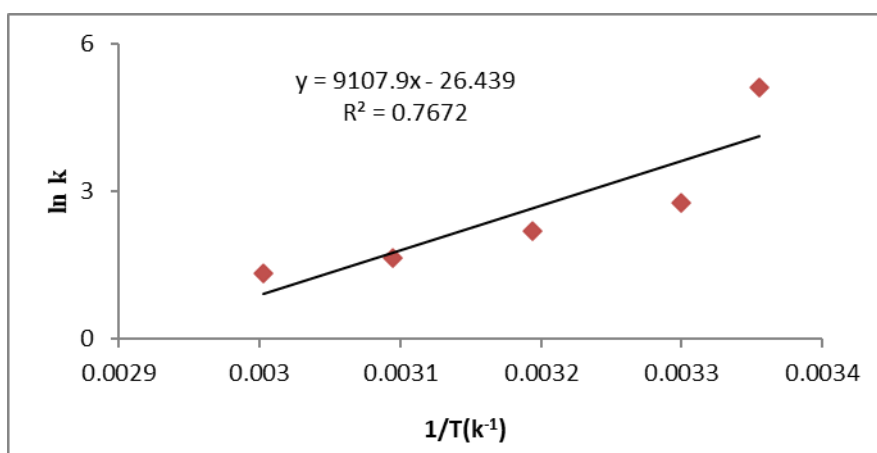
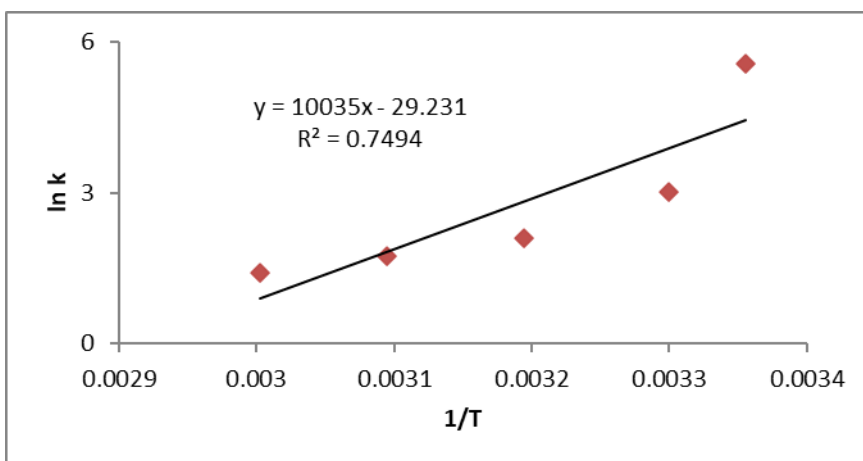


Figure (4.29): Van 't Hoff plot for adsorption of Cu (II) ions on NiO/ $\gamma$ Al<sub>2</sub>O<sub>3</sub> nano catalyst.



**Figure (4.30): Van 't Hoff plot for adsorption of Co (II) ions on NiO/ $\gamma$ Al<sub>2</sub>O<sub>3</sub> catalyst.**

The free energy ( $\Delta G$ ), enthalpy ( $\Delta H$ ), and entropy ( $\Delta S$ ) changes were mentioned in table (4.27). For NiO/ $\gamma$ -Al<sub>2</sub>O<sub>3</sub>, the negative  $\Delta G$  values at different temperature confirm the feasibility of the process and the spontaneous nature of the adsorption<sup>(80)</sup>. The negative  $\Delta H$  values indicates that the adsorption of two ions onto NiO/ $\gamma$ Al<sub>2</sub>O<sub>3</sub> catalysts was an exothermic process and negative  $\Delta S$  indicates decreases in randomness at (solid - solution) interface through adsorption of ions on NiO/ $\gamma$ Al<sub>2</sub>O<sub>3</sub> catalysts .

Table (4.27): Values of thermodynamic function for the adsorption of Cu (II) and Co (II) on NiO/ $\gamma$ -Al<sub>2</sub>O<sub>3</sub> nano catalysts at different temperatures.

Ions	Temperature (K)	$\Delta G$ (KJ/mol)	$\Delta H$ (KJ/mol)	$\Delta S$ (J/mol.K)
Cu <sup>+2</sup>	293	-12447.726	-75722.997	-219.8126
	303	-6976.5118		
	313	-5688.8486		
	323	-4454.8465		
	333	-3668.0677		
Co <sup>+2</sup>	293	-13565.851	-83428.87	-243.0282
	303	-7609.3203		
	313	-5483.2684		
	323	-4711.0358		
	333	-3923.3292		

#### 4.5. The adsorption isotherm

The adsorption of Cu(II) and Co (II) ions on NiO/ $\gamma$ -Al<sub>2</sub>O<sub>3</sub> nano catalyst at ideal condition, are shown in Table (4.28)

Table (4.28) The Ideal condition of The adsorption of Cu (II) and Co (II) ions on NiO/ $\gamma$ -Al<sub>2</sub>O<sub>3</sub> nano catalyst

No.	Conditions of adsorption	Value	
		Cu (II) ion	Co (II) ion
1	Temperature	298 K	298 K
2	Volume of metals Solution	100mL	100mL
3	Contact time	50 (min)	50 (min)
4	Quantity of adsorbents	0.1 (g)	0.1 (g)
5	Stirring speed	150 (rpm)	150 (rpm)



The adsorption isotherms were studied for Cu (II) and Co (II) from an aqueous solution on NiO/  $\gamma$ -Al<sub>2</sub>O<sub>3</sub> surfaces at ideal condition data are listed in Table (4.28). The results are represented by the initial concentration ( $C^0$ ) of ions, and the equilibrium concentration ( $C_e$ ) measured at equilibrium state and the adsorption capacity ( $Q_e$ ) values are calculated from the experimental data by using equation (2.2). The adsorption capacity ( $Q_e$ ) are plotted versus equilibrium concentration ( $C_e$ ) to obtain general adsorption isotherm of Cu (II) ion removal which are described in Table (4.29) and also adsorption isotherm of Co(II) ion removal which are explained in Table (4.30).

Table (4.29): Adsorption parameters values for Cu(II) ion on NiO/  $\gamma$ -Al<sub>2</sub>O<sub>3</sub> nano catalyst at ideal condition.

$C_o$ (mg/L)	$C_e$ (mg/L)	$Q_e$ (mg/g)	Log $C_e$	Log $Q_e$	Ln $C_e$	$C_e/Q_e$
50	3.275	23.3625	0.5152	1.3685	1.1863	0.0856
100	8.14	45.93	0.9106	1.6620	2.0967	0.1772
150	22.14	63.93	1.345	1.8057	3.0973	0.3463
200	35.6	82.2	1.5514	1.9148	3.5723	0.4330
250	54.625	97.6875	1.7373	1.9898	4.0004	0.5591

Table (4.30): Adsorption parameters values for Co(II) ion on NiO/  $\gamma$ -Al<sub>2</sub>O<sub>3</sub> at ideal conditions.

C <sub>o</sub> (mg/L)	C <sub>e</sub> (mg/L)	Q <sub>e</sub> (mg/g)	LogC <sub>e</sub>	LogQ <sub>e</sub>	Ln C <sub>e</sub>	C <sub>e</sub> /Q <sub>e</sub>
50	1.74	24.13	0.2405	1.3825	0.5538	0.0721
100	6.98	46.51	0.8438	1.6675	1.9430	0.1500
150	16.29	66.855	1.2119	1.8251	2.7905	0.2436
200	26.42	86.79	1.4219	1.9384	3.2741	0.3044
250	49.375	100.3125	1.6935	2.001	3.8994	0.4922

#### 4.5.1. Langmuir adsorption isotherm:

Langmuir isotherm equation (2.3) was applied for adsorption of Cu (II) and Co (II) on NiO/  $\gamma$ -Al<sub>2</sub>O<sub>3</sub> nanoparticles by plotting of C<sub>e</sub>/q<sub>e</sub> against C<sub>e</sub> and The values of the Langmuir isotherm constant (a) which is the monolayer adsorption capacity and (b) which is a constant related to the energy of adsorption are calculated from the slope and intercept of the plots (C<sub>e</sub> /Q<sub>e</sub>) versus (C<sub>e</sub>) shown in figure (4.31)and (4.32) for Cu<sup>+2</sup> and Co<sup>+2</sup> removal respectively

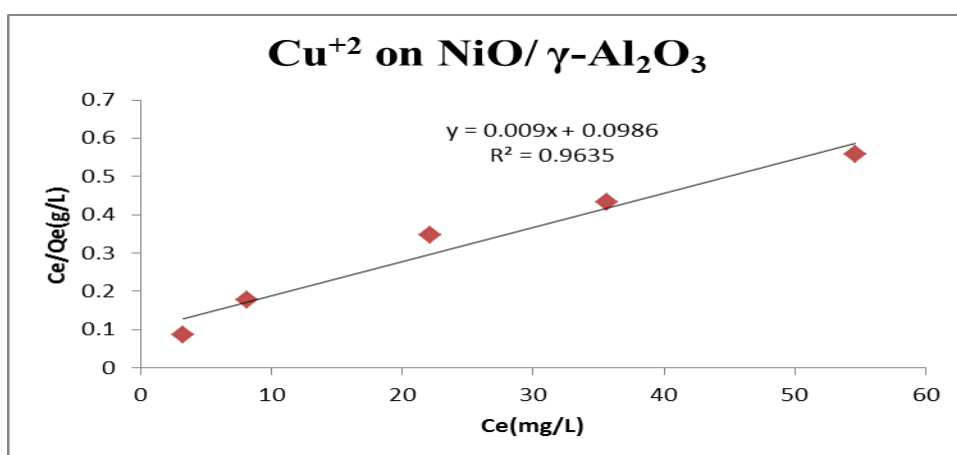


Figure (4.31): Linear Langmuir isotherm of Cu (II) ions removal on NiO/  $\gamma$ -Al<sub>2</sub>O<sub>3</sub> nano catalyst at various initial concentrations.

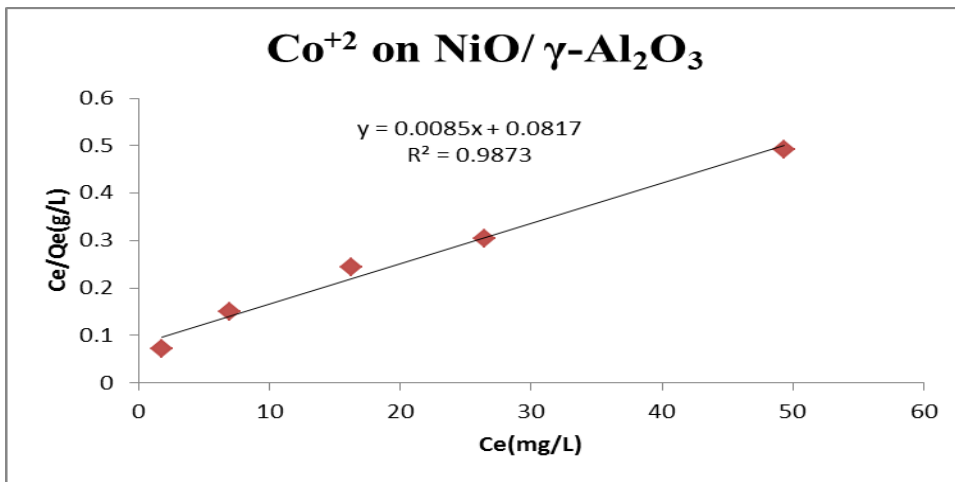


Figure (4.32): Linear Langmuir isotherm of Co (II) ions removal on NiO/  $\gamma$ -Al<sub>2</sub>O<sub>3</sub> at various initial concentrations.

#### 4.5.2. Freundlich adsorption isotherm:

Freundlich isotherm equation (2.4) was applied on adsorption of Cu<sup>+2</sup> and Co<sup>+2</sup> ions on NiO/  $\gamma$ -Al<sub>2</sub>O<sub>3</sub> by plotting of log Q<sub>e</sub> against log C<sub>e</sub>. The Freundlich isotherm constants (K<sub>f</sub>) which is the adsorption capacity of the adsorbent, and (n) which is the adsorption intensity being calculated from the slope and intercept of the plot of (log Q<sub>e</sub>) versus (log C<sub>e</sub>).

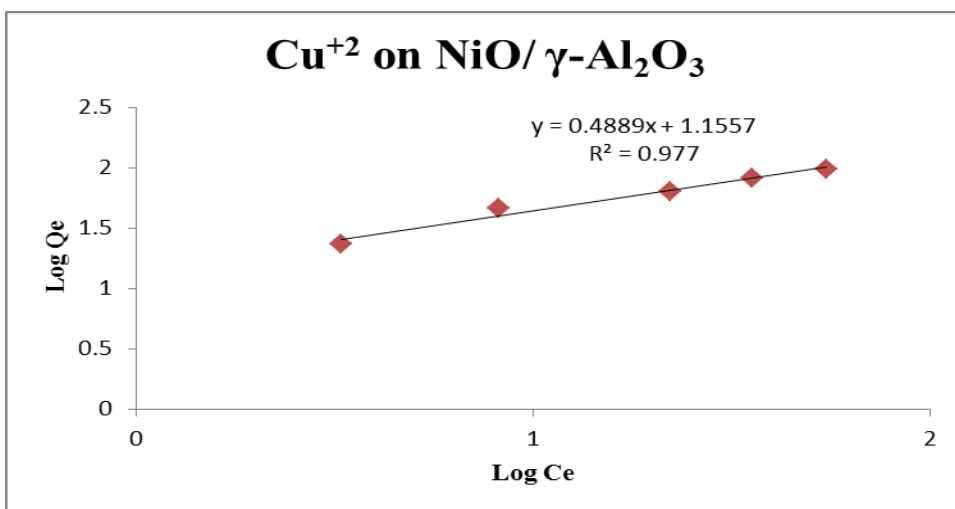


Figure (4.33): Linear Freundlich isotherm of Cu (II) ion removal on NiO/  $\gamma$ -Al<sub>2</sub>O<sub>3</sub> surface at various initial concentrations.

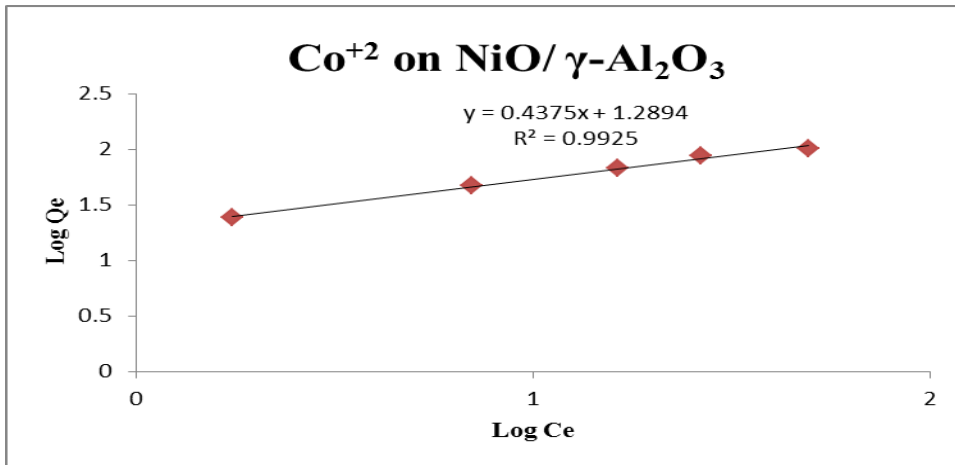


Figure (4.34): Linear Freundlich isotherm of Co (II) ion removal on NiO/  $\gamma$ -Al<sub>2</sub>O<sub>3</sub> surface at various initial concentrations.

#### 4.5.3. Temkin adsorption isotherm

Temkin isotherm equation (2.6) model was applied on the adsorption of Cu (II) and Co (II) ions on NiO/  $\gamma$ -Al<sub>2</sub>O<sub>3</sub> by plotting of  $Q_e$  against  $\ln C_e$ . The Temkin isotherm constants ( $A_T$ ), which is the equilibrium binding constant (L/g) corresponding to the maximum binding energy, and ( $B_T$ ) which is related to heat of adsorption, being calculated from the slope and intercept of the plots of ( $Q_e$ ) versus ( $\ln C_e$ ) shown in figure (4.34) and figure (4.35) for Cu(II) and Co(II) removal respectively.

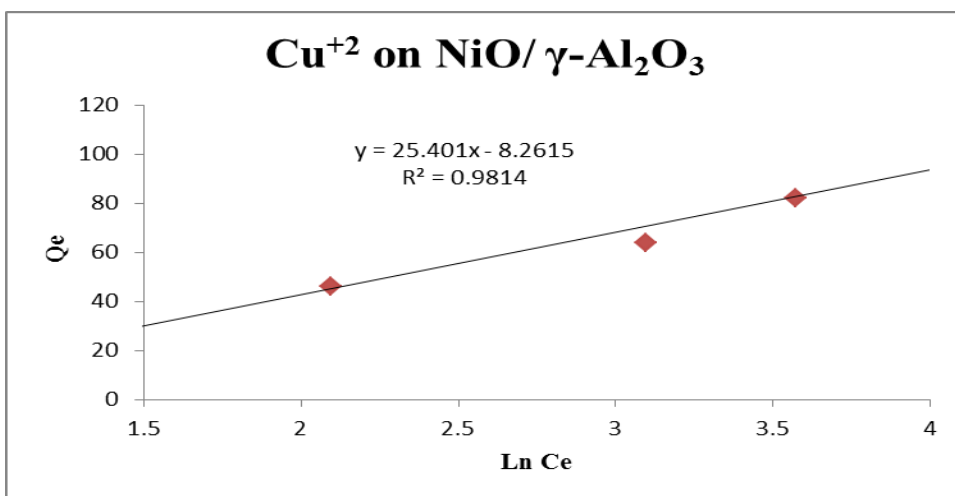


Figure (4.35): Temkin isotherm of Cu (II) ion on removal NiO/  $\gamma$ -Al<sub>2</sub>O<sub>3</sub> surface at various initial concentrations.

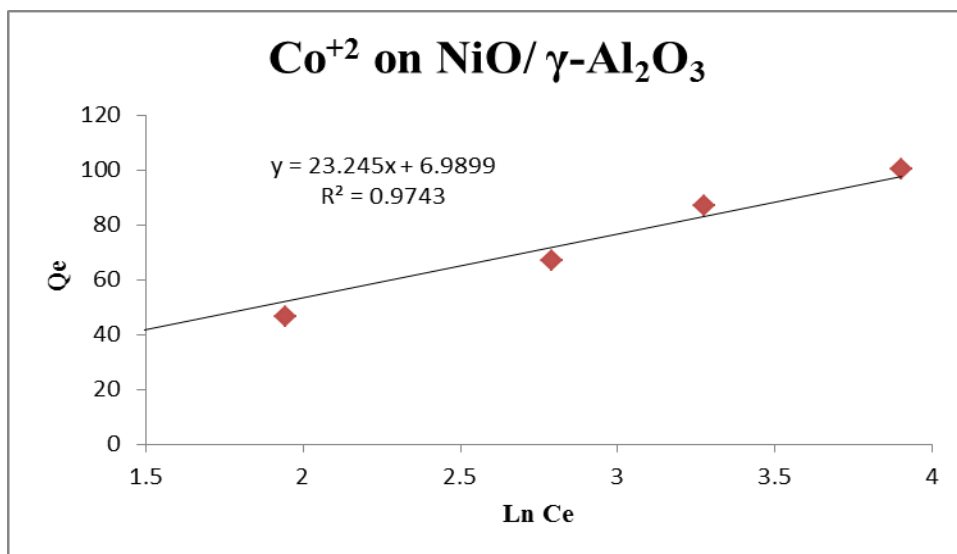


Figure (4.36): Temkin isotherm of Co (II) ions on NiO/  $\gamma$ -Al<sub>2</sub>O<sub>3</sub> surface at various initial concentrations.

Finally temkin isotherm was found to be the best one which can describe removal of Cu<sup>+2</sup>, and freundlich isotherm was the best one which can describe removal Co<sup>+2</sup>

Table (4.31) Langmuir, Freundlich and Temkin constants and the correlation coefficients for the adsorption of Cu<sup>+2</sup> and Co<sup>+2</sup> ions in presence of variable initial ions concentration.

Ions	Langmuir			Freundlich			Temkin		
	a (mg/g)	b (L/g)	R <sup>2</sup>	n	K <sub>f</sub> (mg/g)	R <sup>2</sup>	A <sub>T</sub> (L/g)	B <sub>T</sub> (J/mole)	R <sup>2</sup>
Cu <sup>+2</sup>	112.3595	0.0903	0.9635	2.0458	14.3086	0.977	-22.4570	25.4008	0.9814
Co <sup>+2</sup>	119.0476	0.1029	0.9873	2.2857	19.4670	0.9925	19.0002	23.2447	0.9743

## 4.6. Conclusions

1. The Nickel oxide nanoparticles can be prepared well Arundo donaxi Leaves Extract methods.
2. co-precipitation method is a very good method for synthesis  $\gamma$ -  $\text{Al}_2\text{O}_3$  with nano size particle.
3. X-ray diffraction revealed that particle size obtained is about (12.83) nm for (NiO) and (6.46) nm for ( $\gamma$ - $\text{Al}_2\text{O}_3$ ) and (5.04) for NiO/  $\gamma$ - $\text{Al}_2\text{O}_3$  . Atomic Force Microscopy test found that the average diameter of particles for NiO is 43.13 nm,  $\gamma$ - $\text{Al}_2\text{O}_3$  is 71.84 nm and NiO/ $\gamma$ - $\text{Al}_2\text{O}_3$  is 69.37 nm are in the range of nano type 1-100 nm .
4. The percentage removal of  $\text{Cu}^{+2}$  and  $\text{Co}^{+2}$  ions reaches equilibrium in contact time (50) min for NiO/ $\gamma$ - $\text{Al}_2\text{O}_3$  nano catalysts .
5. The kinetics results conforms the best correlation of the experimental data of adsorption of NiO/ $\gamma$ - $\text{Al}_2\text{O}_3$  by pseudo – second order equation .
6. The negative values of the thermodynamic Functions  $\Delta G$ ,  $\Delta H$  and  $\Delta S$  for the adsorption of  $\text{Cu}^{+2}$  and  $\text{Co}^{+2}$  ion on NiO/ $\gamma$ - $\text{Al}_2\text{O}_3$  indicates that the adsorption processes is spontaneous, exothermic and less randomness at solid– solution interface .

#### 4.7. Future works

1. Using the Nickel (II) oxide nanoparticles prepared by Arundo donaxi Leaves Extract in removal of other various heavy metals such as; Ca,Zn, Cd,Ni,.... etc.
2. Preparation of Nickel (II) oxide nanoparticles using another biomaterial.
3. Studying other adsorbent such as metal oxides, grapheme, clays and zeolites.
4. Experimenting adsorption of other heavy metals such as Zn, Cd, Mo, Hg.....etc.
5. Calculating the removal percentage of  $\text{Cu}^{+2}$  and  $\text{Co}^{+2}$  ions at different pH.
6. Using initial concentration of  $\text{Cu}^{+2}$  and  $\text{Co}^{+2}$  ions less than 50 mg/L.
7. Preparation the  $\gamma\text{-Al}_2\text{O}_3$  by other methods like sol-gel, electrochemical ....etc
8. Using other models in adsorption isotherm such as govanovic model.

# References



## References

---

- 1- Georges, M., Gilbert, Q., & Gailly, B. " The «Living Lab» concept: Exploration and clarification of this a priori catchall term in the innovation landscape.
- 2- Singh, P. (2010). *Environment and ecology*. 1<sup>st</sup> ed. India: New Age International (P) Ltd
- 3- Percival, R.V., Miller, A.S., and Schroeder, C.H. (2014). *Environmental regulation , law, science, and policy*. 6<sup>th</sup> ed. Content Technology Inc.
- 4- Schultz, R.A.,(2014) *.Technology versus ecology: Human superiority and the ongoing conflict with nature*. 1<sup>st</sup> ed. USA. Idea Group Inc.
- 5- Bartram,J. and Balance, R. (1996). *Water quality monitoring: A practical guide to the design and implementation of fresh water quality studies and monitoring programmes*. London. E & FN Spon an imprint of Chapman and Hall.
- 6-Karnib, M., Kabbani, A., Holail, H., and Olama, Z. (2014). Heavy metals removal using activated carbon, silica and silica activated carbon composite. *Energy Procedia*, 50, 113-120.
- 7-Iwahori, K., Watanabe, J., Tani, Y., Seyama, H., and Miyata, N. (2013). Removal of heavy metal cations by biogenic magnetite nanoparticles produced in Fe (III)-reducing microbial enrichment cultures. *Journal of Bioscience and Bioengineering*, 117 (3), 333-335.
- 8-Farghali, A.A., Bahgat, M., Allah, A.E., and Khedr, M.H. (2013). Adsorption of Pb (II) ions from aqueous solutions using copper oxide nanostructures. *Beni-Suef University Journal of Basic and Applied Sciences*, 2 (2), 61-71.
- 9-Al-Joboori, S.K.G. (2016). Adsorption study of some chlorophenols, dyes, heavy metal ions and pesticides onto some adsorbent surfaces. Ph.D. thesis, College of Education Ibn Al- Haitham, University of Baghdad, Iraq.

## References

---

- 10-Contreras, A.R., Garcia, A., Gonzalez, E., Casals, E., Puntos, V., Sanchez, A., Font, X., and Recillas, S. (2012). Potential use of CeO<sub>2</sub>, TiO<sub>2</sub> and Fe<sub>3</sub>O<sub>4</sub> nanoparticles for the removal of cadmium from water. *Desalination and Water Treatment*, 41, 296-300.
- 11-Iravani, S. (2011). Green synthesis of metal nanoparticles using plants. *Green Chemistry*, 13 (10), 2638-2650.
- 12- Saif, S., Tahir, A., Asim, T., and Chen, Y. (2016). Plant mediated green synthesis of CuO nanoparticles: comparison of toxicity of engineered and plant mediated CuO nanoparticles towards daphnia magna. *Nanomaterials*, 6 (11), 1-15.
- 13-Kannan, N., and Sundaram, M.M. (2001). Kinetics and mechanism of removal of methylene blue by adsorption on various carbons—a comparative study. *Dyes and Pigments*, 51 (1), 25-40.
- 14-Yu, Y., Zhuang, Y.Y., and Wang, Z.H. (2001). Adsorption of watersoluble dye onto functionalized resin. *Journal of Colloid and Interface Science*, 242 (2), 288-293.
- 15- Taman, R., Ossman, M.E., Mansour, M.S. and Farag, H.A. (2015). Metal Oxide Nano-particles as an Adsorbent for Removal of Heavy Metals. *Journal of Advanced Chemical Engineering*. 5 (3) : 1- 8.
- 16-Kumar, P. V., Ahamed, A. J., & Karthikeyan, M. (2019). Synthesis and characterization of NiO nanoparticles by chemical as well as green routes and their comparisons with respect to cytotoxic effect and toxicity studies in microbial and MCF-7 cancer cell models. *SN Applied Sciences*, 1(9), 1083.
- 17-Hassan, K. H., Saadi, S. K., Jarullah, A. A., & Harris, P. (2018). Green synthesis and structural characterisation of CuO nanoparticles prepared by

## References

---

- using Fig leaves extract. *Pakistan Journal of Scientific & Industrial Research Series A: Physical Sciences*, 61(2), 59-65.
- 18-Singh, J., Dutta, T., Kim, K. H., Rawat, M., Samddar, P., & Kumar, P. (2018). 'Green'synthesis of metals and their oxide nanoparticles: applications for environmental remediation. *Journal of nanobiotechnology*, 16(1), 84.
- 19-Zafar, U., Bhatti, M. A., and Akram, A. (2018). Kinetics and Thermodynamics Studies of Cobalt (II) Adsorption onto Alumina. *Pakistan Journal of Analytical and Environmental Chemistry*, 19(1) : 53-63.
- 20-Naika, H. R., Lingaraju, K., Manjunath, K., Kumar, D., Nagaraju, G., Suresh, D., & Nagabhushana, H. (2015). Green synthesis of CuO nanoparticles using *Gloriosa superba* L. extract and their antibacterial activity. *Journal of Taibah University for Science*, 9(1), 7-12.
- 21- Tabesh, S., Davar, F., and Loghman-Estarki, M. R. (2017). Preparation of  $\gamma$ - $\text{Al}_2\text{O}_3$  nanoparticles using modified sol-gel method and its use for the adsorption of lead and cadmium ions. *Journal of Alloys and Compounds*, 730 : 441-449.
- 22- Yi, X., Guo, D., Li, P., Lian, X., Xu, Y., Dong, Y., Lai, W. and Fang, W. (2017). One pot synthesis of NiMo- $\text{Al}_2\text{O}_3$  catalysts by solvent-free solid-state method for hydrodesulfurization. *RSC Advances*, 7(86) : 54468-54474.
- 23- Jbara, A. S., Othaman, Z., Ati, A. A., and Saeed, M. A. (2017). Characterization of  $\gamma$ - $\text{Al}_2\text{O}_3$  nanopowders synthesized by Co-precipitation method. *Materials Chemistry and Physics*, 188 : 24-29.
- 24- Mohamed, A. H. A., and Atta, H. H. (2016). Synthesis Of Nano Ni-Mo/ $\gamma$ - $\text{Al}_2\text{O}_3$  Catalyst. *Iraqi Journal of Chemical and Petroleum Engineering*, 17(4) : 11-23.
- 25- Wang, X., Zhao, Z., Zheng, P., Chen, Z., Duan, A., Xu, C., Jiao, J., Zhang, H., Cao, Z and Ge, B. (2016). Synthesis of NiMo catalysts supported on mesoporous  $\text{Al}_2\text{O}_3$  with different crystal forms and superior catalytic performance for the hydrodesulfurization of dibenzothiophene and 4, 6-dimethyldibenzothiophene. *Journal of Catalysis*, 344 : 680-691.

## References

---

- 26- Rahdar, A., Aliahmad, M., & Azizi, Y. (2015). NiO nanoparticles: synthesis and characterization.
- 27- Yuvakkumar, R., Suresh, J., Nathanael, A. J., Sundrarajan, M., & Hong, S. I. (2014). Rambutan (*Nephelium lappaceum* L.) peel extract assisted biomimetic synthesis of nickel oxide nanocrystals. *Materials Letters*, 128, 170-174.
- 28- Garbarino, G., Riani, P., Magistri, L., & Busca, G. (2014). A study of the methanation of carbon dioxide on Ni/Al<sub>2</sub>O<sub>3</sub> catalysts at atmospheric pressure. *International journal of hydrogen energy*, 39(22), 11557-11565.
- 29- Gao, J., Jia, C., Li, J., Zhang, M., Gu, F., Xu, G., ... & Su, F. (2013). Ni/Al<sub>2</sub>O<sub>3</sub> catalysts for CO methanation: Effect of Al<sub>2</sub>O<sub>3</sub> supports calcined at different temperatures. *Journal of energy chemistry*, 22(6), 919-927.
- 30- Rahmanpour, O., Shariati, A., and Nikou, M. R. K. (2012). New Method for Synthesis Nano Size  $\gamma$ -Al<sub>2</sub>O<sub>3</sub> Catalyst for Dehydration of Methanol to Dimethyl Ether. *International journal of chemical engineering and applications*, 3(2), 125.
- 31- Karim, M. R., Rahman, M. A., Miah, M. A. J., Ahmad, H., Yanagisawa, M., and Ito, M. (2011). Synthesis of  $\gamma$ -alumina particles and surface characterization. *Open Colloid Science Journal*, 4 : 32-36.
- 32- Maia, A. O. G., Meneses, C. T., Menezes, A. S., Flores, W. H., Melo, D. M. A., & Sasaki, J. M. (2006). Synthesis and X-ray structural characterization of NiO nanoparticles obtained through gelatin. *Journal of non-crystalline solids*, 352(32-35), 3729-3733.
- 33- Hill, M.K. (2004). *Understanding environmental pollution*. 2<sup>nd</sup> ed., Cambridge University Press, U.K.
- 34- Saravanan, A., Brindha, V., Manimekalai, R., and Krishnan, S. (2009). An evaluation of chromium and zinc biosorption by a sea weed (*Sargassum* sp.) under optimized conditions. *Indian Journal of Science and Technology*, 2(1) : 53-56.

## References

---

- 35-Schwarzenbach, R.P., Egli, T., Hofstetter, T.B., von Gunten, U. and Wehrli, B. (2010). Global water pollution and human health. *Annual Review of Environment and Resources*, 35, 109-136.
- 36-Pradeep, T. (2009). Noble metal nanoparticles for water purification: a critical review. *Thin Solid Films*, 517 (24), 6441-6478.
- 37-Percival, R.V., Christopher, H., Miller, A.S., Schroeder, C.H., and Leape, J.P. (2014). *Environmental regulation, law, science, and policy*. 6th ed., Content Technology Inc.
- 38-Schultz, R.A. (2014). *Technology versus ecology: human superiority and the ongoing conflict with nature*. 1st ed., Idea Group Inc., USA.
- 39-Wang, S., and Peng, Y. (2010). Natural zeolites as effective adsorbents in water and wastewater treatment. *Chemical Engineering Journal*, 156 (1), 11-24.
- 40-(Goel, P. K. (2006). *Water pollution: causes, effects and control*. New Age International.
- 41- Carpenter, S.R., Caraco, N.F., Correll, D.L., Howarth, R.W., Sharpley, A.N. and Smith, V.H. (1998). Non point pollution of surface waters with phosphorus and nitrogen. *Ecological Applications*. 8: 559-568.
- 42- Järup L. (2003). Hazards of heavy metal contamination. *Br Med Bull*68(1): 167–182.
- 43- Jaishankar M, Mathew BB, Shah MS, Gowda KRS. (2014). Biosorption of Few Heavy Metal Ions Using Agricultural Wastes. *Journal of Environment Pollution and Human Health* 2(1): 1–6.
- 44- Nagajyoti PC, Lee KD, Sreekanth TVM. (2010). Heavy metals, occurrence and toxicity for plants: a review. *Environ Chem Lett* 8(3): 199–216.

## References

---

- 45- Lambert M, Leven BA, Green RM. (2000). New methods of cleaning up heavy metal in soils and water. Environmental science and technology briefs for citizens. Kansas State University, Manhattan, KS.
- 46- Morais S, Costa FG, Pereira ML. (2012). Heavy metals and human health, in Environmental health – emerging issues and practice (Oosthuizen J ed), pp. 227–246, InTech.
- 47- Akar, T., Cabuk, A., Tunali, S., and Yamac, M. (2006). Biosorption potential of the macrofungus *ganoderma carnosum* for removal of lead (II) ions from aqueous solutions. *Journal of Environmental Science and Health Part A*, 41(11), 2587-2606.
- 48- Ahmaruzzaman, M. (2011). Industrial wastes as low-cost potential adsorbents for the treatment of wastewater laden with heavy metals. *Advances in Colloid and Interface Science*, 166 (1), 36-59.
- 49- Momodu, M.A., and Anyakora, C.A. (2010). Heavy metal contamination of ground water: the surulere case study. *Research Journal Environmental and Earth Science*, 2 (1), 39-43.
- 50- Amer, H.A.T. (2015). Removal of lead from industrial wastewater using a low-cost waste material. M.Sc. thesis, School of Sciences and Engineering, The American University, Cairo.
- 51- Pérez-Marín, A.B., Zapata, V.M., Ortuno, J.F., Aguilar, M., Sáez, J., and Lloréns, M. (2007). Removal of cadmium from aqueous solutions by adsorption onto orange waste. *Journal of Hazardous Materials*, 139 (1), 122-131.
- 52- Bahadir, T., Bakan, G., Altas, L., and Buyukgungor, H. (2007). The investigation of lead removal by biosorption: an application at storage battery industry wastewaters. *Enzyme and Microbial Technology*, 41 (1), 98-102.

## References

---

- 53- Fu, F., and Wang, Q. (2011). Removal of heavy metal ions from wastewaters: a review. *Journal of Environmental Management*, 92 (3), 407-418.
- 54- Sharma, S.K., Mahiya, S., and Lofrano, G. (2017). Removal of divalent nickel from aqueous solutions using carissa carandas and syzygium aromaticum: isothermal studies and kinetic modelling. *Applied Water Science*, 7 (4), 1855-1868.
- 55- Ku, Y., and Jung, I. L. (2001). Photocatalytic reduction of Cr (VI) in aqueous solutions by UV irradiation with the presence of titanium dioxide. *Water research*, 35(1) : 135-142.
- 56- Özverdi, A., and Erdem, M. (2006).  $\text{Cu}^{2+}$ ,  $\text{Cd}^{2+}$  and  $\text{Pb}^{2+}$  adsorption from aqueous solutions by pyrite and synthetic iron sulphide. *Journal of hazardous materials*, 137(1) : 626-632.
- 57- Kang, S. Y., Lee, J. U., Moon, S. H., and Kim, K. W. (2004). Competitive adsorption characteristics of  $\text{Co}^{2+}$ ,  $\text{Ni}^{2+}$ , and  $\text{Cr}^{3+}$  by IRN-77 cation exchange resin in synthesized wastewater. *Chemosphere*, 56(2) : 141-147.
- 58- Alyüz, B., and Veli, S. (2009). Kinetics and equilibrium studies for the removal of nickel and zinc from aqueous solutions by ion exchange resins. *Journal of Hazardous Materials*, 167(1-3) : 482-488.
- 59- Gode, F., and Pehlivan, E. (2006). Removal of chromium (III) from aqueous solutions using Lewatit S 100: the effect of pH, time, metal concentration and temperature. *Journal of Hazardous Materials*, 136(2) : 330-337.
- 60- Wang, H., Zhou, A., Peng, F., Yu, H., and Yang, J. (2007). *Mechanism study on adsorption of acidified multiwalled carbon nanotubes to Pb (II)*. *Journal of Colloid and Interface Science*, 316(2) : 277-283.

## References

---

- 61- Issabayeva, G., Aroua, M. K., and Sulaiman, N. M. (2006). *Electrodeposition of copper and lead on palm shell activated carbon in a flow-through electrolytic cell*. Desalination, 194(1-3) : 192-201.
- 62- Atkin P.W., “*Physical chemistry*”, 6P th P ed., Oxford university press, Oxford (2001).
- 63- Mohammed, I.S. (2014). *Determination and removal of some organic pollutants from aqueous solution by using Iraqi clays, modified clays and applied semi-empirical program to theoretical adsorption study*. Ph.D. thesis, College of Science for Women, University of Baghdad, Iraq .
- 64- Barakat, M. A. (2011). New trends in removing heavy metals from industrial wastewater. *Arabian Journal of Chemistry*, 4(4) : 361-377.
- 65- Annadurai, G., Juang, R. S., and Lee, D. J. (2003). Adsorption of heavy metals from water using banana and orange peels. *Water science and technology*, 47(1) : 185-190.
- 66- Dąbrowski, A. (2001). Adsorption—from theory to practice. *Advances in colloid and interface science*, 93(1-3) : 135-224.
- 67- Hmad,A.R.(2007). Study of Adsorption process for some Phenolic Compound on the Surface of (Acrylamide-Bisacrylamide) Co polymer. M.Sc.thesis,College of Science,University of Al-Nahrain,Iraq.
- 68- Bellmann, C. (2008). Surface modification by adsorption of polymers and surfactants. Springer, Berlin, Heidelberg : 235-259.
- 69- Ali, M.I. (2015). Adsorption studies of some dyes on different adsorbent surfaces. M.Sc. thesis, College of Science, University of Al- Nahrain, Iraq.
- 70- Sameen, A.S. (2014). Kinetic and thermodynamic studies of adsorption of reactive red and rhodamine 6G dyes from aqueous solution using different



## References

---

adsorbent. M.Sc. thesis, College of Science for Women, University of Baghdad, Iraq.

71- Jarullah, A.A. (2013). Removal of Ni (II) ions from aqueous solutions by adsorption technique using activated carbon as adsorbent. Ph.D. thesis, College of Science for Women, University of Baghdad, Iraq.

72- Mahdi, E.R. (2016). Preparation and characterization of some metal oxides nanoparticles and using them to remove heavy metals from industrial waste water. M.Sc. thesis, College of Science, University of Diyala, Iraq.

73- Silbey, R.J., Alberty, R.A., and Bawendi, M.G. (2005). Physical chemistry. 4<sup>th</sup> ed., John Wiley and Sons, Inc.

74- Adamson, A.W., and Gast, A.P. (2001). Physical chemistry of surfaces. 6<sup>th</sup> ed., John Wiley and Sons, New York.

75- Contreras Rodríguez, A.R. (2015). Removal of cadmium (II), lead (II) and chromium (VI) in water with nanomaterials. Ph.D. thesis, Departament d'Enginyeria Química, Universitat Autònoma de Barcelona, Spain.

76- Ya, Z., Zhou, L., Bao, Z., Gao, P., and Sun, X. (2009). High efficiency of heavy metal removal in mine water by limestone. Chinese Journal of Geochemistry, 28 (3) : 293-298.

77- Laidler, K.J. and Meiser, J.H., (1982). Physical chemistry. 6<sup>th</sup> ed., Benjamin Cummings Publishing Company, California

78- Atkins, P., and Paula, J.D. (2006). Physical Chemistry. 8<sup>th</sup> ed., W. H. Freeman and Company, New York..

79- Suzuki, M. (1990). Adsorption engineering. Tokyo / Amsterdam : Kodansha Ltd., and Elsevier Science Publishers B.V.

## References

---

- 80- Abdulah, F.W. (2010). Removal of chromium(III) Ions from its Aqueous Solution by Adsorbent Surface :Charcoal, Attapulgitte andDate Palm Leaflet Powder (Pinnae).M.Sc.thesis, College ofEducation Ibn-Al-Haitham, University of Baghdad, Iraq.
- 81- Saleh, T. A. (2015). Isotherm, kinetic, and thermodynamic studies on Hg (II) adsorption from aqueous solution by silica-multiwall carbon nanotubes. *Environmental Science and Pollution Research*, 22(21) : 16721-16731..
- 82- Senthilkumar, R., Vijayaraghavan, K., Thilakavathi, M., Iyer, P. V. R., and Velan, M. (2007). *Application of seaweeds for the removal of lead from aqueous solution*. *Biochemical Engineering Journal*, 33(3) : 211-216.
- 83- Al Gohary, O. M. (1997). *In vitro adsorption of mebeverine hydrochloride onto kaolin and its relationship to pharmacological effects of the drug in vivo*. *Pharmaceutica Acta Helvetiae*, 72(1) : 11-21.
- 84- Saadi, S.K. (2017). *Removal of Some Heavy Metal Systems by Adsorption on Metal Oxides Nanoparticles*. M.Sc. thesis, College of Science, University of Diyala, Iraq.
- 85- Taqe, R.M.M. (2015). Removal of some water pollutants using newly synthesised organoclays. M.Sc. thesis, College of Science, University of Al-Mustansiriyah, Iraq.
- 86- Meisslamawy, H.A.J. (2006). Sorption capacity measurement of sulphuric acid in the active mass of Iraq lead acid strong battery. M.Sc. thesis, Collage of Science for Women, University of Baghdad, Iraq.
- 87- Abdeen, Z., and Mohammad, S.G. (2014). Study of the adsorption efficiency of an eco-friendly carbohydrate polymer for contaminated aqueous

## References

---

solution by organophosphorus pesticide. *Open Journal of Organic Polymer Materials*, 4 (1), 16-28.

88- Laidler, K.J. and Meiser, J.H., (1982). *Physical chemistry*. 6th ed., Benjamin Cummings Publishing Company, California.

89- Dada, A.O., Olalekan, A.P., Olatunya, A.M., and Dada, O. (2012). Langmuir, Freundlich, Temkin and Dubinin–Radushkevich isotherms studies of equilibrium sorption of  $Zn^{2+}$  unto phosphoric acid modified rice husk. *IOSR Journal of Applied Chemistry*, 3 (1), 38-45.

90- Shakibabarough, A., Valinejadshoubi, M., and Valinejadshoubi, M. (2014). Useable and precautionary aspects of using nanotechnology and nano-materials in the construction industry. *International Journal of Science , Engineering and Technology Research*, 3 (4), 841- 847.

91- . Qiu, Y., Yu, J., Zhou, X., Tan, C., and Yin, J. (2009). Synthesis of porous NiO and ZnO submicro - and nanofibers from electrospun polymer fiber templates. *Nanoscale Research Letters*, 4, 173-177.

92- Andujar, C.B., Ortega, D., Pankhurst, Q.A., and Thanh, N.T.K. (2012). Elucidating the morphological and structural evolution of iron oxide nanoparticles formed by sodium carbonate in aqueous medium. *Journal of Materials Chemistry*, 22, 12498-12506.

93- Kumar, R., and Chawla, J. (2014). Removal of cadmium ion from water/wastewater by nano-metal oxides: a review. *Water Quality, Exposure and Health*, 5(4), 215-226.

94- Zhao, X., Lv, L., Pan, B., Zhang, W., Zhang, S., and Zhang, Q. (2011). Polymer-supported nanocomposites for environmental application: a review. *Chemical Engineering Journal*, 170 (2), 381- 394.

## References

---

- 95- Geraldes, A.N., Alves, A., Leal, J., Estrada-Villegas, G.M., Lincopan, N., Katti, K.V., and Lugao, A.B. (2016). Green nanotechnology from plant extracts: synthesis and characterization of gold nanoparticles. *Advances in Nanoparticles*, 5, 176-185.
- 96- Nath, D., and Banerjee, P. (2013). Green nanotechnology—a new hope for medical biology. *Environmental Toxicology and Pharmacology*, 36 (3), 997-1014.
- 97- Yuh-Shan, H. (2004). Citation review of Lagergren kinetic rate equation on adsorption reactions. *Scientometrics*, 59(1) : 171-177.
- 98- Ho, Y. S., and McKay, G. (1999). *Pseudo-second order model for sorption processes*. *Process biochemistry*, 34(5) : 451-465.
- 99- Robati, D. (2013). *Pseudo-second-order kinetic equations for modeling adsorption systems for removal of lead ions using multi-walled carbon nanotube*. *Journal of nanostructure in Chemistry*, 3(1), 55.
- 100- Wawrzekiewicz, M., Wiśniewska, M., Gun'ko, V. M., and Zarko, V. I. (2015). *Adsorptive removal of acid, reactive and direct dyes from aqueous solutions and wastewater using mixed silica–alumina oxide*. *Powder Technology*, 278 : 306-315.
- 101- Low, M.J.D. (1960) *Chem. Rev.* 60, 267.
- 102- Chien, S.H. and Clayton, W.R. (1980) *Soil Sci. Soc. Am.*, J. 44, 265.
- 103- Sparks, D.L. (Ed) (1986) *Soil Physical Chemistry*, CRC Press, Boca Raton, FL, pp. 83–145.
- 104- Coulier, L. (2001). *Hydrotreating model catalysts: from characterization to kinetics*. Eindhoven: Technische Universiteit Eindhoven.
- 105- Ahmed, H. S., and Menoufy, M. F. (2012). New trends in hydroprocessing spent catalysts utilization. In *Petrochemicals. In Tech*.
- 106- Richardson, J.T. (1989). *Principles of Catalyst Development*, 1<sup>st</sup> ed., University of Wales, college of Cardiff.

## References

---

- 107- Chen, F., Jiang, X., Zhang, L., Lang, R., and Qiao, B. (2018). Single-atom catalysis: Bridging the homo-and heterogeneous catalysis. *Chinese Journal of Catalysis*, 39(5) : 893-898.
- 108- Boudart, M., and Djéga-Mariadassou, G. (2014). Kinetics of heterogeneous catalytic reactions . Princeton University Press.
- 109- Hummadi, K.K. (1999). Petroleum Residue Hydrotreating-Catalysts Preparation and Activity. Ph.D.thesis, college of Engineering, University of Baghdad, Iraq.
- 110-R. J. F. C. H. Bartholomew, *Fundamentals of Industrial Catalytic Processes*, 2nd edn, 2005.
- 11- T. Ito and J.H. Lunsford, *Nature* 314, 721 (1985).
- 112- T.-C.Liu, M. Forissier, G. Coudurier and J.C. Védrine, *J. Chem. Soc., Faraday Trans.* 85, 1607 (1989).
- 113- Karthik, R., and Meenakshi, S. (2015). Removal of Pb (II) and Cd (II) ions from aqueous solution using polyaniline grafted chitosan. *Chemical Engineering Journal*, 263 : 168-177.
- 114-Onundi, Y. B., Mamun, A. A., Al Khatib, M. F., and Ahmed, Y. M. (2010). Adsorption of copper, nickel and lead ions from synthetic semiconductor industrial wastewater by palm shell activated carbon. *International Journal of Environmental Science & Technology*, 7(4) : 751-758.
- 115- Ahamed, M., Alhadlaq, H. A., Khan, M. A., Karuppiah, P., and Al-Dhabi, N. A. (2014). Synthesis, characterization, and antimicrobial activity of copper oxide nanoparticles. *Journal of Nanomaterials*, 2014. 17.
- 116- Kumar, B. R., and Rao, T. S. (2011). *Effect of Substrate* temperature on structural properties of nanostructure zinc oxide thin films prepared by reactive dc magnetron sputtering. *Digest Journal of Nanomaterials and Biostructures*, 6(3) : 1281-1287.

## References

---

- 117- Akkaya, G., and Güzel, F. (2013). *Optimization of Copper and Lead Removal by a Novel Biosorbent: Cucumber (Cucumis Sativus) Peels—Kinetic, Equilibrium, and Desorption Studies*. Journal of Dispersion Science and Technology, 34(10) : 1295-1307.
- 118- Al-Homaidan, A. A., Al-Abbad, A. F., Al-Hazzani, A. A., Al-Ghanayem, A. A., and Alabdullatif, J. A. (2016). *Lead removal by Spirulina platensis biomass*. International journal of phytoremediation, 18(2) : 184-189.
- 119- Saikrishna, Y.V.S., and Babu, R.R. (2015). *Adsorption of Copper and Lead ions from aqueous solutions using Nickel oxide nanostructure*. International Journal of Engineering Research and General Science. 3(5): 2091-2730.
- 120- Hu, C., Zhu, P., Cai, M., Hu, H., and Fu, Q. (2017). *Comparative adsorption of Pb (II), Cu (II) and Cd (II) on chitosan saturated montmorillonite: Kinetic, thermodynamic and equilibrium studies*. Applied Clay Science, 143: 320-326.
- 121- Abdul-Hussin, E. (2012). *Adsorption studies of Certain Dyes on the Mineral from Aqueous Solution*. M.S.C. Thesis, College of Science for Women, University of Baghdad.
- 122- Ahamed, M., Alhadlaq, H. A., Khan, M. A., Karuppiah, P., and Al-Dhabi, N. A. (2014). *Synthesis, characterization, and antimicrobial activity of copper oxide nanoparticles*. Journal of Nanomaterials, 2014. 17.
- 123- Kumar, B. R., and Rao, T. S. (2011). *Effect of Substrate temperature on structural properties of nanostructure zinc oxide thin films prepared by reactive dc magnetron sputtering*. Digest Journal of Nanomaterials and Biostructures, 6(3) : 1281-1287.
- 124- Qiao, H., Wei, Z., Yang, H., Zhu, L., & Yan, X. (2009). *Preparation and characterization of NiO nanoparticles by anodic arc plasma method*. Journal of Nanomaterials, 2009.
- 125- Karim, M. R., Rahman, M. A., Miah, M. A. J., Ahmad, H., Yanagisawa, M., and Ito, M. (2011). *Synthesis of  $\gamma$ -alumina particles and surface characterization*. Open Colloid Science Journal, 4 : 32-36.

## References

---

- 126- Saeed, A., Akhter, M.W., and Iqbal, M. (2005). Removal and recovery of heavy metals from aqueous solution using papaya wood as a new biosorbent. *Separation and Purification Technology*, 45 (1), 25-31.
- 127- Alfa, Y.M., Hassan, H., and Nda-Umar, U.I. (2012). Agricultural waste materials as potential adsorbent for removal of heavy metals from aqueous solutions. *International Journal of Chemical Research*, 2 (2), 48-54.
- 128- Srivastava, V.C., Mall, I.D., and Mishra, I.M. (2006). Equilibrium modelling of single and binary adsorption of cadmium and nickel onto bagasse fly ash. *Chemical Engineering Journal*, 117 (1), 79-91.
- 129- Onundi, Y.B., Mamun, A.A., Al Khatib, M.F., and Ahmed, Y.M. (2010). Adsorption of copper, nickel and lead ions from synthetic semiconductor industrial wastewater by palm shell activated carbon. *International Journal of Environmental Science and Technology*, 7 (4), 751-758.
- 130- Sheela, T., Nayaka, Y.A., Viswanatha, R., Basavanna, S., and Venkatesha, T.G. (2012). Kinetics and thermodynamics studies on the adsorption of Zn (II), Cd (II) and Hg (II) from aqueous solution using zinc oxide nanoparticles. *Powder Technology*, 217, 163-170.
- 131-Taqe, R.M.M. (2015). Removal of some water pollutants using newly synthesised organoclays. M.Sc. thesis, College of Science, University of Al-Mustansiriyah, Iraq.
- 132-Boparai, H.K., Joseph, M., and O'Carroll, D.M. (2011). Kinetics and thermodynamics of cadmium ion removal by adsorption onto nano zerovalent iron particles. *Journal of Hazardous Materials*, 186 (1), 458-465.
- 133-Shabani, K.S., Ardejani, F.D., Badii, k., and Olya, M.E. (2017). Preparation and characterization of novel nano-mineral for the removal of several heavy metals from aqueous solution: batch and continuous systems. *Arabian Journal of Chemistry*, 10, 3108 - 3127.



وزارة التعليم العالي والبحث العلمي

جامعة ديالى

كلية العلوم

قسم الكيمياء

## امتزاز الايونات السامه الملوثة للماء على محفز نانوي

### ثنائي الاكاسيد

رسالة مقدمة الى

مجلس كلية العلوم / جامعة ديالى

وهي جزء من متطلبات نيل درجة الماجستير في علوم الكيمياء

من قبل الطالبة

**نورس عدنان جواد**

بكالوريوس في علوم الكيمياء 2014

كلية العلوم - جامعة تكريت

بإشراف

**أ.د. كريم هنيكش حسن**



## الملخص

في هذه الدراسة تم تحضير اوكسيد النيكل النانوي وذلك بأستخدام مستخلص اوراق نبات الغاب وايضا تم تحضير اوكسيد الالمنيوم النانوي نوع (كاما) بواسطه طريقه الترسيب المشترك من ملح كلوريد الالمنيوم المائي ثم بعد ذلك يتم كلستته في حراره 550 مئوي .تم تحضير المحفز النانوي ( $\text{NiO}/\text{Al}_2\text{O}_3$ ) باستخدام جهاز (ultrasonic) عن طريق مزج نسب معينه من الاكاسيد النانويه المتمثله ب20% من اوكسيد النيكل النانوي و80% من الالومينا . استخدم طيف حيود الاشعه السينيه (-x ray) وتقنيه طيف الاشعه تحت الحمراء (FTIR) ومجهر القوه الذريه (AFM) لتشخيص هذه الاكاسيد النانويه حيث اظهرت نتائج قياس (XRD) ان حجم الجسيمات كانت (12.83) نانومتر لاوكسيدالنيكل (6.46) نانومتر للالومينا و(5.04) للمحفز النانوي ( $\text{NiO}/\text{Al}_2\text{O}_3$ ) .

ان تلوث الماء بالعديد من المعادن الثقيله يشكل ضرا كبيرا على البيئه لذلك استخدم المحفز النانوي ( $\text{NiO}/\text{Al}_2\text{O}_3$ ) لازاله ايونات النحاس والكوبلت الثنائيه من المحاليل المائيه المخففه .

في هذا البحث تم دراسته عدد من العوامل التي تؤثر على نسبه ازاله المعادن ،حيث وجد ان الزمن اللازم لازاله ايونات النحاس والكوبلت والوصول الى حاله الاتزان هو (50) دقيقه ،لقد تبين ان ازاله ايونات النحاس والكوبلت الثنائيه تقل بزياده تركيز ماده الممتزه وتزداد بزياده وزن السطح الماز. اما تأثير درجه الحراره على امتزاز كل من الايونين فقد اشار بأن نسبه الازاله تقل بزياده درجه الحراره مما اتضح بأن العمليه باعته للحراره وعند حساب قيم الدوال الترموداينميكيه لعمليه الامتزاز ( $\Delta G, \Delta H, \Delta S$ ) تبين ان عمليه الامتزاز هي تلقائيه باعته للحراره واكل عشوائيه عند تداخل ايونات الفلزين مع السطح المحضر .وقد تم مطابقه النتائج باستخدام اربعة معادلات حركيه وهي معادله الدرجه الاولى الكاذبه، معادله الدرجه الثانيه الكاذبه ، معادله الانتشار الداخلي للجزيئات ومعادله ايلوفك وقد اشارت النتائج الى ان عمليه الامتزاز تخضع لمعادله الدرجه الثانيه الكاذبه لان معامل الارتباط ( $R^2$ ) قد اعطى افضل قيمه مقارنة بالنماذج الحركيه الاخرى.قد تبين ايضا بان ايزوثرم لانكماير هو الافضل لوصف عمليه ازاله ايونات النحاس والكوبلت الثنائيه على المحفز النانوي ( $\text{NiO}/\text{Al}_2\text{O}_3$ ) المحضر هذا ما لاحضناه من قيم معامل الارتباط.